

University of Kentucky

UKnowledge

Theses and Dissertations--Neuroscience

Neuroscience

2015

MITOCHONDRIAL AND NEUROPROTECTIVE EFFECTS OF PHENELZINE RELATED TO SCAVENGING OF NEUROTOXIC LIPID PEROXIDATION PRODUCTS

John Cebak

University of Kentucky, jeceba2@uky.edu

[Right click to open a feedback form in a new tab to let us know how this document benefits you.](#)

Recommended Citation

Cebak, John, "MITOCHONDRIAL AND NEUROPROTECTIVE EFFECTS OF PHENELZINE RELATED TO SCAVENGING OF NEUROTOXIC LIPID PEROXIDATION PRODUCTS" (2015). *Theses and Dissertations--Neuroscience*. 12.

https://uknowledge.uky.edu/neurobio_etds/12

This Doctoral Dissertation is brought to you for free and open access by the Neuroscience at UKnowledge. It has been accepted for inclusion in Theses and Dissertations--Neuroscience by an authorized administrator of UKnowledge. For more information, please contact UKnowledge@lsv.uky.edu.

STUDENT AGREEMENT:

I represent that my thesis or dissertation and abstract are my original work. Proper attribution has been given to all outside sources. I understand that I am solely responsible for obtaining any needed copyright permissions. I have obtained needed written permission statement(s) from the owner(s) of each third-party copyrighted matter to be included in my work, allowing electronic distribution (if such use is not permitted by the fair use doctrine) which will be submitted to UKnowledge as Additional File.

I hereby grant to The University of Kentucky and its agents the irrevocable, non-exclusive, and royalty-free license to archive and make accessible my work in whole or in part in all forms of media, now or hereafter known. I agree that the document mentioned above may be made available immediately for worldwide access unless an embargo applies.

I retain all other ownership rights to the copyright of my work. I also retain the right to use in future works (such as articles or books) all or part of my work. I understand that I am free to register the copyright to my work.

REVIEW, APPROVAL AND ACCEPTANCE

The document mentioned above has been reviewed and accepted by the student's advisor, on behalf of the advisory committee, and by the Director of Graduate Studies (DGS), on behalf of the program; we verify that this is the final, approved version of the student's thesis including all changes required by the advisory committee. The undersigned agree to abide by the statements above.

John Cebak, Student

Dr. Edward D. Hall, Major Professor

Dr. Wayne A. Cass, Director of Graduate Studies

MITOCHONDRIAL AND NEUROPROTECTIVE EFFECTS OF PHENELZINE RELATED
TO SCAVENGING OF NEUROTOXIC LIPID PEROXIDATION PRODUCTS

DISSERTATION

A dissertation submitted in partial fulfillment of the
Requirements for the degree of Doctor of Philosophy in the
College of Medicine
at the University of Kentucky

By

John Eric Cebak

Lexington, Kentucky

Director: Dr. Edward D. Hall, Professor of
Anatomy and Neurobiology, Neurology and Neurosurgery

Lexington, Kentucky

2015

Copyright © John Eric Cebak 2015

ABSTRACT OF DISSERTATION

MITOCHONDRIAL AND NEUROPROTECTIVE EFFECTS OF PHENELZINE RELATED TO SCAVENGING OF NEUROTOXIC LIPID PEROXIDATION PRODUCTS

Lipid peroxidation is a key contributor to the pathophysiology of traumatic brain injury (TBI). Traditional antioxidant therapies are intended to scavenge the free radicals responsible for either the initiation or propagation of lipid peroxidation (LP). However, targeting free radicals after TBI is difficult as they rapidly react with other cellular macromolecules, and thus has a limited post-injury time window in which they may be intercepted by a radical scavenging agent. In contrast, our laboratory has begun testing an antioxidant approach that scavenges the final stages of LP i.e. formation of carbonyl-containing breakdown products. By scavenging breakdown products such as the highly reactive and neurotoxic aldehydes (often referred to as “carbonyls”) 4-hydroxynonenal (4-HNE) and acrolein (ACR), we are able to prevent the covalent modification of cellular proteins that are largely responsible for posttraumatic neurodegeneration. Without intervention, carbonyl additions render cellular proteins non-functional which initiates the loss of ionic homeostasis, mitochondrial failure, and subsequent neuronal death. Phenelzine (PZ) is an FDA-approved monoamine oxidase (MAO) inhibitor traditionally used for the treatment of depression. Phenelzine also possesses a hydrazine functional group capable of covalently binding neurotoxic carbonyls. The hypothesis of this dissertation is that carbonyl scavenging with PZ will exert an antioxidant neuroprotective effect in the traumatically injured rat brain mechanistically related to PZ’s hydrazine moiety reacting with the lipid peroxidation (LP)-derived reactive aldehydes 4-hydroxynonenal (4-HNE) and acrolein (ACR). Data from our *ex vivo* experiments demonstrate that the exogenous application of 4-HNE or ACR significantly reduced respiratory function and increased markers of oxidative damage in isolated non-injured rat cortical mitochondria, whereas PZ pre-treatment significantly prevented mitochondrial dysfunction and oxidative modification of mitochondrial proteins in a concentration-related manner. Additionally, PZ’s neuroprotective scavenging mechanism was confirmed to require the presence of a hydrazine moiety based on experiments with a structurally similar MAO inhibitor, pargyline, which lacks the hydrazine group and did not protect the isolated mitochondria from 4-HNE and ACR. Our *in vivo* work demonstrates that subcutaneous injections of PZ following TBI in the rat are able to significantly protect brain mitochondrial respiratory function, decrease markers of oxidative damage, protect mitochondrial calcium buffering capacity, and increase cortical tissue sparing without decreasing neuronal cytoskeletal spectrin degradation. These results confirm that PZ is

capable of protecting mitochondrial function and providing neuroprotection after experimental TBI related to scavenging of neurotoxic LP degradation products.

KEYWORDS: phenelzine, lipid peroxidation, 4-hydroxynonenal, acrolein, brain mitochondria

John E. Cebak
Student's Signature

05 August 2015
Date

MITOCHONDRIAL AND NEUROPROTECTIVE EFFECTS OF PHENELZINE
RELATED TO SCAVENGING OF
NEUROTOXIC LIPID PEROXIDATION PRODUCTS

By

John Eric Cebak

Edward D. Hall, PhD.

Director of Dissertation

Wayne A. Cass, PhD.

Director of Graduate Studies

05 August 2015

For my brother, Tony, the only hero I have ever known. You kept me alive through my darkest times and I love you more than myself. Also, you forgot to pay your half of the phone bill last month.

ACKNOWLEDGEMENTS

You took a chance on me and provided me with the faculties and direction I needed, not to simply survive graduate school, but to flourish professionally and personally. Thank you, Dr. Edward Hall, for giving me the intellectual latitude to academically express myself. I am fairly aware that my methods are idiosyncratic and possibly even “high maintenance,” but so too are Ferraris! Your constant mentorship with regard to my personal and professional life has afforded me innumerable opportunities. Although, I am certain all graduate students have a selfish parasitic relationship with their mentors, I hope that I made you proud. I promise you will not regret the time invested in me. I also will not be returning any of the text books or movies you lent me, for sentimental reasons, of course.

Special admiration and thanks to my esteemed committee members, listed in alphabetical order to obfuscate favoritism: Dr. Greg Gerhardt, Dr. Edmund Rucker, Dr. Kathryn Saatman, and Dr. Patrick Sullivan. Your input has been invaluable and I will be forever appreciative of your tolerance and flexibility, but more importantly, your approval of this dissertation. Dr. Philip Bonner, you have saved my academic career through research. You found me a diamond in the (really) rough. Thank you.

Additional reverence is held for my wonderful laboratory members—OK, to Dr. Hall’s lab members. You have collectively refined my scientific technique and made the rigor of lab delightful. I appreciate that you have, to this date, never told me to stop dancing and singing ‘90s pop songs in lab. Dr. Indrapal Singh, Dr. Juan Wang, and Dr. Rachel Hill, I am forever grateful for your help. Dr. Jeffery Bosken, I hope you enjoyed our Dennis-the-Menace-and-Mr.-Wilson-like relationship. To my fellow graduate students, I wish you the absolute best in your neuroscience careers, unless you are in direct competition with me, in which case I hope I win. You all have been wonderful in your own precious ways.

Lastly, to my friends and family. I appreciate the guilt-trips that were effective in pulling me from lab and my study to enjoy life. Except the times where hanging out with you all led to hospitalization subsequent to a motorcycle wreck, retinal detachment, and that time we went to Iraq. Besides that, it’s been a blast. I regret nothing.

ACKNOWLEDGEMENTS	iii
LIST OF TABLES	ix
LIST OF FIGURES	x
Chapter 1 Introduction and Background	1
1.1 Introduction	1
1.2 Classifications and Models of Traumatic Brain Injury	1
1.3 Initiation of the Secondary Injury Cascade	3
1.4 Calcium Homeostasis & Pathology	4
1.5 Reactive Oxygen Species	7
1.6 Superoxide Radical	9
1.7 Reactions with Superoxide Radical	11
1.8 Lipid peroxidation	15
1.8.1 Treatment of Lipid Peroxidation	19
1.9 Reactive Aldehydes	20
1.9.1 Reactive Aldehydes in Traumatic Brain Injury	24
1.10 Mitochondria	26
1.10.1 Mitochondrial function	27
1.10.2 Mitochondrial States of Respiration	32
1.10.3 Mitochondrial Superoxide Production	34
1.10.4 Mitochondrial Peroxynitrite Formation	35
1.10.5 Role of Mitochondria in Calcium Homeostasis	36
1.10.6 Mitochondrial Dysfunction after TBI	36
1.11 Carbonyl Scavenging	39
1.12 Dissertation Hypothesis	46
Chapter 2 Materials and Methods	47
2.1 Animals	47
2.2 Drug & Substrate Preparation	47
2.2.1 4-HNE and Acrolein	47
2.2.2 Pargyline	48
2.2.3 Phenelzine	48
2.2.4 Mitochondrial Substrates & Inhibitors	48
2.3 Controlled Cortical Impact Surgical Procedures	50

2.4 Ficoll- Purified Mitochondrial Isolation and Protein Assay	51
2.5 Mitochondrial Bioenergetics Analysis	52
2.5.1 Clark-type Electrode for in Vivo Use	52
2.5.2 Preparation of Seahorse Sensor Cartridge and Mitochondrial Substrates/ Inhibitors	54
2.6 Mitochondrial Calcium-Buffering.....	60
2.7 Western Blot Analysis.....	61
2.7.1 Western Blot Analysis of Oxidative Damage Markers	61
2.7.2 Western Blot Analysis of Spectrin Degradation	62
2.8 Mitochondrial Respiratory Control Ratio.....	64
2.9 Tissue Processing and Histology	64
2.10 Statistical Analysis	66
2.10.1 Mitochondrial Respiration	66
2.10.2 Calcium Buffering.....	67
2.10.3 Spectrin Degradation	67
2.10.4 Histology.....	67
Chapter 3 Dissertation Research Approach.....	68
3.1 Hypothesis	68
3.2 Aim 1	68
3.2.1 Aim 1 Rationale	68
3.2.2 Experiment 1, Aim 1	70
3.2.3 Experiment 2, Aim 1	73
3.2.4 Experiment 3, Aim 1	76
3.3. Aim 2	80
3.3.1 Aim 2 Rationale	80
3.3.2 Experiment 1, Aim 2	80
3.3.4 Experiment 2, Aim 2	84
3.3.5 Experiment 3, Aim 2	86
3.4.1 Aim 3	89
3.4.2 Aim 3 Rationale	89
3.4.4 Experiment 1, Aim 3	89
3.4.3 Experiment 2, Aim 3	92

Chapter 4 Phenelzine protects brain mitochondrial respiratory function from oxidative damage by scavenging the lipid peroxidation-derived reactive carbonyls 4-hydroxynonenal and acrolein	96
4.1 <i>Specific Aim</i>	96
4.2 <i>Introduction</i>	96
4.3 <i>Results</i>	98
4.3.1 <i>4-HNE and Acrolein Inhibit Brain Mitochondrial Respiration</i>	98
4.3.2 <i>Phenelzine Protects Against 4-HNE or ACR-Induced Mitochondrial dysfunction in a Concentration -Dependent Fashion</i>	101
4.3.3 <i>Phenelzine, but not Pargyline, Protects Against 4-HNE and ACR-Induced Mitochondrial Dysfunction</i>	103
4.3.4 <i>Phenelzine Prevents Mitochondrial Oxidative Damage Ex Vivo in a Dose-Dependent Fashion</i>	105
4.3.5 <i>Phenelzine, but not Pargyline, Protects against Mitochondrial Oxidative Damage Markers 4-HNE and ACR</i>	107
4.4 <i>Discussion</i>	109
Chapter 5 Phenelzine protects mitochondrial respiratory and calcium buffering functions together with a reduction in mitochondrial oxidative damage after traumatic brain injury	113
5.1 <i>Specific Aim</i>	113
5.2 <i>Introduction</i>	113
5.3 <i>Results</i>	115
5.3.1 <i>Mitochondrial Respiration</i>	115
5.3.2 <i>Respiratory Control Ratio</i>	116
5.3.3 <i>States of Respiration</i>	119
5.3.4 <i>Mitochondrial Oxidative Damage</i>	129
5.3.5 <i>Mitochondrial Calcium Buffering</i>	131
5.4 <i>Discussion</i>	134
5.4.1 <i>Hypothesis 1: Phenelzine-induced Monoamine Oxidase Inhibition Could Have a Greater Proportional Effect on Overall Mitochondrial Oxygen Consumption in Injured Mitochondria</i>	135
5.4.2 <i>Hypothesis 2: Phenelzine-induced MAO Inhibition Leads to Increased levels of Monoamine Neurotransmitters Leading to Autoxidation-induced Free Radical Production</i>	137

5.4.3 Hypothesis 3: Possible Negative Effects of Phenzazine-induced GABA Transaminase Inhibition Exacerbating Post-TBI GABA Excitotoxicity.....	138
Chapter 6 Role of phenzazine in histological sparing of cortical tissue and spectrin degradation.....	143
6.1 Specific Aim 3.....	143
6.2 Introduction.....	143
6.3 Results.....	147
6.3.1 Spectrin Degradation.....	147
6.3.2 Cortical Tissue Sparing.....	152
6.4 Discussion.....	155
6.4.1 Multiple Phenzazine Dosing Protects Cortical Tissue but Does Not Decrease Spectrin Degradation Compared to Sham.....	155
6.4.2 Phenzazine Could Actually Exacerbate Spectrin Degradation.....	156
6.4.3 Phenzazine Could Increase Total Intact Spectrin.....	156
6.4.4 Some Calpain Inhibitors Fail to Prevent Spectrin Degradation but Increase Behavioral Recovery.....	158
Chapter 7 Final Discussion.....	159
7.1 Brief Summary of Results.....	159
7.1.1 Summary of Aim 1 Ex Vivo Experiments.....	159
7.1.2 Summary of Aim 2 In Vivo Experiments.....	161
7.1.3 Summary of Aim 3 Neuroprotection Experiments.....	163
7.2 Expansion of General Discussion.....	165
7.2.1 Mitochondrial Respiration.....	165
7.2.2 Cortical Tissue Sparing without Protection from Spectrin Degradation.....	167
7.3 Experimental Limitations.....	169
7.3.1 Synaptic Mitochondria vs. Non-Synaptic Mitochondria.....	169
7.3.2 Phenzazine Dose Response.....	169
7.4 Technical Considerations.....	170
7.4.1 Previous Experiment Repeatability.....	170
7.4.2 Possibility of Mitochondrial Sampling Bias.....	179
7.4.3 Decreased Respiration of PZ-treated Mitochondria.....	183
7.4.4 Increased Spectrin Degradation and Increased Calcium Buffering Capacity.....	185
7.4.5 Preserving Cortical Lesion Volume.....	185

7.5 Ancillary considerations	189
7.5.1 Profiling.....	189
7.5.2 Aberrant Scavenging and Metabolism	189
7.6 Concluding Remarks	190
APPENDIX.....	192
Appendix A: List of Acronyms and Abbreviations	192
Appendix B: Immunoblotting, No Primary Controls	194
.....	194
REFERENCES	195
VITA.....	207

LIST OF TABLES

Table 2.1 Preparation of Mitochondrial Substrates and Inhibitors	49
Table 2.2 Inducers of Various States of Respiration	53
Table 2.3 Standard Seahorse Protocol	56
Table 3.1 Aim 1, Experiment 1 4-HNE and ACR Dose Response	71
Table 3.2 Aim 1, Experiment 2 Phenzazine Dose Response	74
Table 3.3 Aim 1, Experiment 3 PZ versus PG	77
Table 3.4 Aim 2, Experiment 1 <i>In Vivo</i> Mitochondrial Respiration	82
Table 3.5 Aim 2, Experiment 2 <i>In Vivo</i> Mitochondrial Oxidative Damage	85
Table 3.6 Aim 2, Experiment 3 Mitochondrial Calcium Buffering	87
Table 3.8 Aim 3, Experiment 1 <i>In Vivo</i> Therapeutic Window	91
Table 3.7 Aim 3, Experiment 2 <i>In Vivo</i> Neuroprotection, Tissue Spraying	94

LIST OF FIGURES

Figure 1.1 Reactions of Superoxide Radical	13
Figure 1.2 Lipid Peroxidation of 4-HNE	18
Figure 1.3 Structure of 4-HNE and ACR	22
Figure 1.4 4-HNE Binding to Proteins via Schiff Base and Micheal Addition	23
Figure 1.5 Mitochondrial Electron Transport System	31
Figure 1.6 Structure of Phenelzine	42
Figure 1.7 Phenelzine Scavenging of 4-HNE and ACR	44
Figure 2.1 Typical Oxymetric Trace with Mitochondrial Complexes	59
Figure 3.1 Structural Differences between PZ and PG	79
Figure 4.1 4-HNE and ACR Mitochondrial Dose Response	100
Figure 4.2 Phenelzine Pre-Treatment Dose Response	102
Figure 4.3 Mitochondrial Respiration PZ versus PG	104
Figure 4.4 PZ Dose Response on Mitochondrial Oxidative Damage Markers	106
Figure 4.5 PZ versus PG on Mitochondrial Oxidative Damage Markers	108
Figure 5.1 PZ Treatment after TBI on Mitochondrial RCR	118
Figure 5.2 PZ Treatment after TBI on State II Respiration	120
Figure 5.3 PZ Treatment after TBI on State III Respiration	122
Figure 5.4 PZ Treatment after TBI on State IV Respiration	124
Figure 5.5 PZ Treatment after TBI on State Va Respiration	126
Figure 5.6 PZ Treatment after TBI on State Vb Respiration	128
Figure 5.7 PZ Treatment after TBI on Mitochondrial 4-HNE Accumulation	130
Figure 5.8 PZ Treatment after TBI on Calcium Buffering	132
Figure 5.9 Typical Mitochondrial Buffering Trace	133
Figure 6.1 PZ Treatment on Spectrin Degradation 15 min post-TBI	149
Figure 6.2 PZ Treatment on Spectrin Degradation 3 hr post-TBI	151
Figure 6.3 PZ Treatment on Cortical Tissue Sparing	153
Figure 7.1 Comparison of Previous and Current Tissue Sparing Experiments	175
Figure 7.2 Macroscopic Morphology of Extracted Rat Brains	178
Figure 7.3 Quantification of Cortical Mitochondria Extracted	181
Figure 7.4 High Magnification Images of Vehicle-treated Glial Scar	182
Figure 7.5 High Magnification Penumbra Regions	187

Chapter 1

Introduction and Background

(Portions submitted for publication in Free Radical Biology and Medicine)

1.1 Introduction

Traumatic Brain Injury (TBI) is a condition that presents serious challenges to the health and welfare of civilians, soldiers, and veterans. In the United States alone, 1.7 million persons are diagnosed with TBI each year [1]. 5.3 million persons in the United States are living with permanent or temporary posttraumatic disability [2]. Additionally, the military subset population is realizing an unprecedented shift in TBI occurrence since the onset of the wars in Iraq and Afghanistan. Military TBI diagnoses have almost tripled in 8 years with 30,000 diagnosed soldiers in 2012, from approximately 10,000 soldiers in 2004 [3]. The Center for Disease Control (CDC) has previously advocated TBI as a “major public health epidemic,” calculating an overwhelming economic burden of over \$16 billion a year and \$56 billion overall [4].

1.2 Classifications and Models of Traumatic Brain Injury

There exist two broad classifications of traumatic brain injury (TBI.) The classifications are sequential and describe two sources of damage: primary and secondary damage. Primary damage is characterized by mechanical forces acting externally on the

brain either by rapid changes in acceleration, blunt force trauma, penetrating trauma, or from primary blast waves [5]. This type of damage directly disrupts membranes and their permeability [6].

Unfortunately, primary damage cannot be prevented by surgical or pharmacological intervention and prevention is generally the only true means available to treat primary sources of injury. Secondary damage is, however, a source of injury that is often the target of surgical or pharmacological treatment. Secondary sources of TBI develop within hours to weeks after the primary insult and often exacerbate with time [6, 7]. In fact, 40% of patients admitted to hospitals for TBI continue to deteriorate weeks after the primary mechanical insult [8, 9].

The pathophysiology of the secondary injury cascade is complex and the current clinical classification to describe the severity of injury is the 15-point Glasgow Coma Score (GCS) [10]. However, the GCS is not applicable to rodent models of TBI nor does it communicate much regarding the pathology of TBI [11] which can vary substantially.

Experimental models of TBI are designed to decrease this variability by mimicking a particular type of brain injury (diffuse, focal, mixed diffuse/focal complex) in a controlled and repeatable manner.

The controlled cortical impact (CCI) model of TBI is just one means to experimentally induce a brain injury. The CCI model uses a pneumatically controlled piston to physically contact the brain through a craniotomy in the skull and deform/displace the tissue to pre-specified distance with a controlled velocity and dwell time. The model

was first employed in ferrets [12] but was adapted and validated in mice [13, 14] and rats [15].

It is important to recognize that the CCI-TBI model is considered a focal model of TBI; however, reports demonstrate that the contusion is not entirely focal. These experiments were able to show diffuse neuronal damage in the cortex, hippocampus, and corpus callosum of the ipsilateral (insulted) and contralateral (non-insulted) hemisphere. Furthermore, it was concluded to be mediated primarily by retrograde and anterograde e.g. Wallerian degeneration [13]. Therefore, special consideration should be made when designing experiments to account for this observation as to not unintentionally obfuscate the interpretation of data as in the instance when ipsilateral treatment groups are compared internally to their “control” contralateral counterparts.

Our lab uses the CCI-TBI model to induce a severe brain injury in rats. Accordingly, this model is intended to represent the respective severe-TBI population in humans. It is our intention to measure the efficacy of pharmacological treatments following severe TBI first, then to assess the treatment potential of a “less severe” TBI.

1.3 Initiation of the Secondary Injury Cascade

Following the primary mechanical insult, neuronal membrane integrity is compromised and excessive excitatory neurotransmitters such as glutamate are released from the presynaptic neuron. Glutamate under normal physiological conditions will bind to NMDA (N-methyl-D-aspartate) and AMPA (α -amino-3-hydroxy-5-methyl-4-isoxazolepropionic acid) receptors to facilitate the influx of sodium (Na^+) and calcium

(Ca²⁺). Perpetual activation of NMDA and AMPA receptors by excitatory neurotransmitters facilitates excessive influx of sodium and calcium ions and efflux of potassium (K⁺) ions. [16-18]. The influx of Ca²⁺ can have dire consequences that effect a multitude of cellular and physiologic processes which will be considered individually later in this chapter.

Though described broadly, this excitotoxic environment exacerbates the disruption of ionic homeostasis, increases formation of reactive oxygen species (ROS), decreases mitochondrial function, increases peroxidation of membrane and organellar lipids, and increases the formation of deleterious reactive aldehydes otherwise known as cytotoxic carbonyls.

Evidence for glutamate as a facilitator of excitotoxicity was gained from experimental animal TBI models in which a dose-dependent relationship was found to exist between glutamate levels and severity of brain injury [19].

1.4 Calcium Homeostasis & Pathology

The physiologic role of calcium is widespread and is involved in multiple processes regarding membrane excitability, synaptic plasticity, modulation of cytoskeletal structure, enzymatic activation and subsequent signal transduction, as well as calcium-regulated gene expression.

Many of these cellular processes are manipulated by controlling the concentration, movement, or localization of Ca²⁺ within the neuron. Typical intracellular calcium (Ca²⁺_i)

concentration is approximately 100 nM, whereas the extracellular calcium (Ca^{2+}_e) concentration is on the order of 1-2 mM. This concentration gradient facilitates the natural influx of Ca^{2+} through voltage-operated channels (VOCs). Ca^{2+} -ATPase pumps on the plasma membrane (PM) and the endoplasmic reticulum (ER) and the $\text{Ca}^{2+}/\text{Na}^+$ exchanger also contribute to Ca^{2+}_i regulation.

Ionotropic channels on the PM such as NMDA and AMPA receptors respond to glutamate and mediate the influx of Ca^{2+} . Whereas, metabotropic receptors generally localized to the (ER) facilitate the efflux of Ca^{2+} into the cytosol. The cell is additionally equipped with the ability to buffer Ca^{2+} through Ca^{2+} -binding proteins and more powerfully through the sequestration by the mitochondria. Despite the expansive array of Ca^{2+} modulating mechanisms traumatic brain injury can overwhelm these systems.

Following mechanical trauma neurons sustain non-specific leaks that facilitate Ca^{2+} influx and depolarization. Excitatory neurotransmitters such as glutamate become elevated in the synaptic cleft following TBI [20]. Excessive stimulation by glutamate prolongs depolarization and activates NMDA and AMPA Ca^{2+} -permeable channels [21]. Support for glutamate mediated increase of Ca^{2+}_i concentration was demonstrated in vitro, wherein high concentrations of exogenously applied glutamate elevated Ca^{2+} influx in neuronal cultures [22]. And, the Ca^{2+} influx was determined to be mediated by activation of the NMDA receptor [17]. Other investigators support these observations by concluding that Ca^{2+}_i can increase transiently from injury as demonstrated in in vitro fluid shear stress injury models [23].

The consequence of intracellular Ca^{2+} accumulation has pathological implications. Two notable pathologies involve the generation of free radicals and mitochondrial dysfunction, both of which will be discussed in later sections. Aside from contributing to free radical formation and mitochondrial dysfunction, intracellular Ca^{2+} can activate phospholipases, kinases, and endonucleases which contribute to aberrant cellular processes and contribute to the depletion of adenosine triphosphate (ATP) energy reserves along with excessive Ca^{2+} -ATPase pump activity. Additional pathological consequences involve that of Ca^{2+} activated proteases such as calpains [24].

Calpains are cytoplasmic cysteine proteases that are activated by Ca^{2+} . Two types of calpains are μ -calpains and m-calpains [25]. The former μ -calpains are activated by μM concentrations of Ca^{2+} (while m-calpains are activated by mM concentrations of Ca^{2+}) and are located in the cytosol near the plasma membrane. Excitotoxic concentrations of Ca^{2+} (5-10 μM) [26] and reactive aldehydes discussed in later sections activate calpains which mediate cytoskeletal breakdown [27]. Calpains target a wide variety of substrates and cleave their targets not based on primary amino acid sequence, rather, on secondary and tertiary structure [25, 28].

Among the variety of calpain targets is spectrin, a scaffolding protein involved in the maintenance of the PM. Calpains are activated to cleave αII -spectrin to influence synaptic remodeling and plasticity [29]. *In vitro* models have demonstrated a link between injury, Ca^{2+} , and calpain activation when various Ca^{2+} chelators prevented the cleavage of fluorescent calpain substrates following stretch injury [30]. Extensive work has demonstrated calpain activation in multiple instances of traumatic axonal injury [31, 32] and in *in vivo* TBI models [33, 34].

While it is apparent that intracellular Ca^{2+} increases after injury, and subsequently calpains are pathological activated, the success of pharmacological intervention by virtue of calpain inhibition has been modest. Compounds such as Calpain Inhibitor 2 and SNJ 1945 reduce spectrin degradation [35, 36]. Other compounds such as AK295 have attenuated motor and cognitive deficits in the rat following TBI [37].

It is important to note that while calpain inhibition is a potential therapeutic strategy, the work of this dissertation aims to pursue a new means of pharmacological intervention, but maintain the spectrin degradation assay as a relevant and capable biomarker for the assessment of drug efficacy in the treatment of TBI.

1.5 Reactive Oxygen Species

Free radicals are essentially molecular fragments that can exist in mono or poly atomic form and contain at least one unpaired electron [38]. Because the outer most atomic or molecular orbital lacks a paired electron then the species is capable of either oxidation or reduction. Gaining the “missing” electron means the species reduces its oxidation state. If the species “loses” its unpaired electron the species is said to oxidize. While the designation “free radical” has an inherently negative connotation, a free radical can function beneficially in a biological system as an anti-oxidant e.g. donates its free electron which stabilizes both compounds in the reaction. Alternatively free radicals can be used to destroy bacterial invasions in many eukaryotic cells. Free radicals have been extensively documented as being either harmful or beneficial [39], and some free radicals discussed in this chapter are relatively stable and do not damage biological tissues.

Free radicals and reactive oxygen species (ROS) are closely related but one species facilitates the other. ROS produce free radicals and some ROS species are examples of free radicals; examples are given below. The exception to the nomenclature involves peroxyntirite which is regarded as a reactive nitrogen species (RNS). ROS-generated free radicals mediate oxidative damage and can be categorized into superoxide ($O_2^{\bullet -}$) and those derived from such. The use of the “•” which precedes or follow an atomic symbol indicates the presence of an unpaired electron on that particular species.

Examples of reactive oxygen species:

- Hydrogen peroxide (H_2O_2)
- Peroxynitrite anion ($ONOO^-$)
- Peroxynitrous acid ($ONOOH$)
- Nitrosoperoxocarbonate ($ONOOCO_2$)

Examples of free radicals:

- Superoxide ($O_2^{\bullet -}$)
- Superoxide-derived:
- Hydroxyl radical ($\bullet OH$)
- Nitrogen dioxide ($\bullet NO_2$)

- Carbonate radical (CO_3^-)
- Peroxyl radical ($\text{LOO}\cdot$)
- Alkoxyl radical ($\text{LO}\cdot$)
- Iron-oxygen complexes

1.6 Superoxide Radical

The superoxide radical ($\text{O}_2^{\cdot-}$) is an aberration of diatomic oxygen (O_2). O_2 is unique in that it is a diradical, wherein each oxygen contains one unpaired electron, as opposed to the molecule containing a pair of electrons in its outer orbitals. Therefore diatomic oxygen (O_2) can serve as an oxidizing agent, meaning it can accept electrons. Normal cellular processes can cause the partial reduction (gain of an electron) of O_2 . Subsequently, the species becomes a free radical: superoxide radical ($\text{O}_2^{\cdot-}$). The generation of superoxide radical is physiologically sequestered by innate cellular antioxidant mechanisms. It is only when free radical production surpasses the ability of endogenous control mechanism that free radicals contribute to a pathological state of “oxidative stress.”

Oxidative stress or nitrosative stress (for nitrogen passed radicals) is defined as the state wherein the production of free radicals has the potential to elicit damage[40]. The term oxidative damage is the state wherein free radicals have irreversibly impaired function.

The largest contributor of oxidative stress and greatest source of oxidative damage is the mitochondria [41]. Specifically Complex I, a major protein complex of the electron

transport system (ETS), is the largest contributor to electron leak and subsequent generation of superoxide radical [42]. However, due to the complex nature of the mitochondria in a pathological state, this and other concepts will be discussed in further detail later.

NADPH Oxidase:

Another major contributor, though indeed apart of mitochondrial complexes, nicotinamide adenine dinucleotide phosphate-oxidase (NADPH oxidase) is utilized in neutrophil phagosomes to reduce O_2 into $O_2^{\cdot-}$ [43, 44]. NADPH oxidase is also utilized by microglia and is a considerable contributor of superoxide radical formation, especially during the later time points following traumatic brain injury (TBI)[45, 46]. *In vivo* support for the role of NADPH oxidase was recently and interestingly demonstrated in Gp91phox (NOX2) knockout mice that sustained a TBI. In these experiments, mice lacking a functional domain of NADPH encoded by the gene NOX2 demonstrated reduced markers of apoptosis, superoxide radical formation, and peroxynitrite formation following a controlled cortical impact (CCI) TBI [47].

Xanthine Oxidase:

Aside from immune-based contributors, other means of superoxide radical generation can be accounted by normal cellular purine metabolism. Xanthine reductase is among such compounds that reside within endothelial cells that facilitates the oxidative metabolism of heterocyclic, aromatic compounds [48]. However, in a pathologic state i.e. abundance of free radicals, xanthine reductase can be oxidized to xanthine oxidase.

Xanthine oxidase will still metabolize substrates; however, the final transfer of electrons will be received by oxygen and hydrogen peroxide creating superoxide radicals.

Heme Proteins:

The iron centers of heme contained within hemoglobin and myoglobin exist in a ferrous state (Fe^{2+}) which facilitates the functionality of the red blood cell to transfer oxygen. Due to the aromatic ring structure electrons are capable of delocalizing which creates a ferric (Fe^{3+}) state that is incapable of binding O_2 . Oxygen is reduced and the molecule released is a superoxide radical. In a pathological state this process further catalyzes free radical formation, discussed later, by the Fenton and Haber-Weiss reactions.

Many sources of superoxide radicals exist that are not elaborated upon in this text; however, typical processes under normal physiologic conditions will create superoxide radicals. And, those process are often exacerbated by central nervous system (CNS) injury. Experiments *in vivo* utilizing the fluid percussion model were able to demonstrate an immediate increase in superoxide radical within brain microvasculature concurrent with auto-regulatory dysfunction that could be ameliorated with superoxide radical scavengers [49].

1.7 Reactions with Superoxide Radical

Typically following the primary injury, a mechanical depolarization of neurons leads to the loss of Ca^{2+} homeostasis and subsequent elevation of intracellular Ca^{2+} . [50] As a result, superoxide ($\text{O}_2^{\bullet-}$) production elevates due to a single electron (e^-) reduction of

molecular oxygen (O_2). $O_2^{\cdot-}$ is capable of stealing an electron (an oxidizing agent) or donating an electron (a reducing agent), this dual nature is the source of $O_2^{\cdot-}$ modest reactivity. However, $O_2^{\cdot-}$ can undergo several fates leading to generation of more prolific and excessively volatile radicals. Should $O_2^{\cdot-}$ undergo either enzyme-mediated (superoxide dismutase, SOD) or spontaneous dismutation to create hydrogen peroxide (H_2O_2), iron from brain tissue hemorrhage can cause iron-catalyzed Fenton reactions which generate excessive hydroxyl radicals ($\cdot OH$) [51]. The other fate of $O_2^{\cdot-}$ is to react with nitric oxide radical ($NO\cdot$). $NO\cdot$ is readily produced in mitochondria upon activation of mitochondrial nitric oxide synthase (mtNOS) [52, 53]. Should $O_2^{\cdot-}$ react with $NO\cdot$, a temporary peroxynitrite anion ($ONOO^-$) is formed, which in the context of TBI pathology leans towards protonation or reaction with CO_2 . In the later circumstance, CO_2 exposure will generate unstable nitrosoperoxocarbonate ($ONOOCO_2$) whose degradation products generate carbonate radical ($CO_3^{\cdot-}$) and nitrogen dioxide radical ($\cdot NO_2$). In the former circumstance of protonation, peroxynitrous acid is formed and degraded into $\cdot OH$ and $\cdot NO_2$. The chemistry of peroxynitrite formation and its generation of highly reactive radicals is shown in **Figure 1.1**.

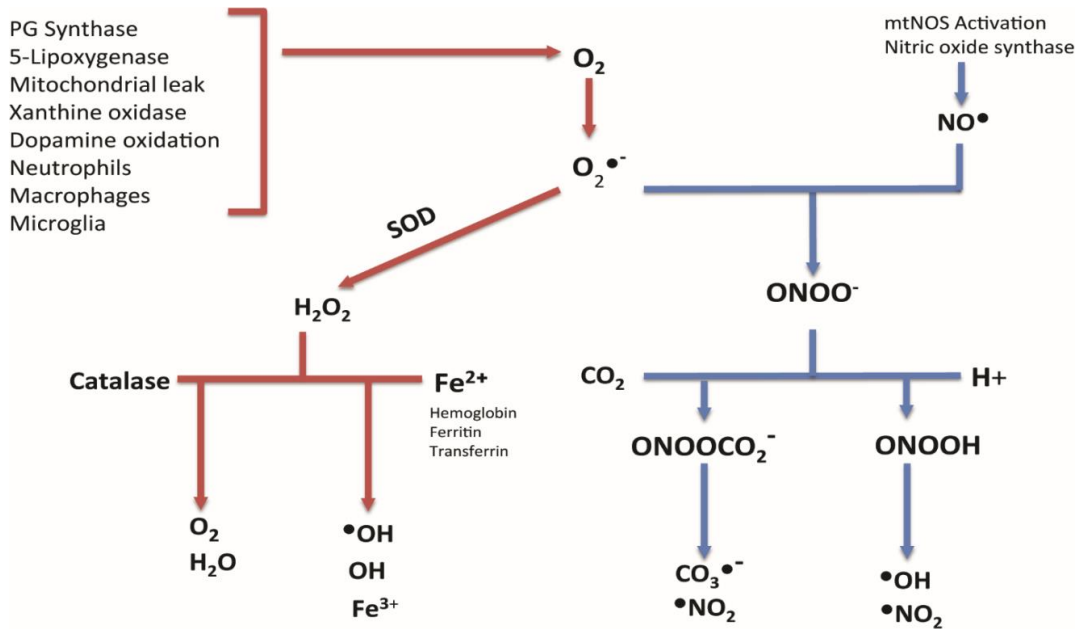


Figure 1.1 Multiple sources contribute to superoxide ($O_2^{\bullet-}$) production. Superoxide can undergo enzymatic or spontaneous dismutation to form hydrogen peroxide (H_2O_2). Subsequent iron catalyzed reactions contribute to the formation of hydroxyl radicals ($\bullet OH$). Superoxide in combination with nitric oxide radical ($\bullet NO$) produces peroxynitrite anion ($ONOO^-$). Peroxynitrite reacts with CO_2 to produce intermediaries that degrade into the carbonate radical ($CO_3^{\bullet-}$), nitrogen dioxide radical ($\bullet NO_2$), and hydroxyl radical ($\bullet OH$). The generation of free radicals initiates lipid peroxidation cascades, protein oxidation and nitration. Image modified from Hall, 2010. [54]

In vivo experimental evidence for hydroxyl radical ($\bullet\text{OH}$) formation following TBI was demonstrated in the focal TBI rat model wherein the salicylate trapping method implicated that within the first few minutes following TBI, $\bullet\text{OH}$ radicals significantly increased [55, 56] which was temporally concurrent with other neuronal injury models demonstrating lipid peroxidation, disruption of the blood-brain barrier [57] and glutamate release [58].

Equally useful experimental evidence of $\bullet\text{NO}_2$ radical formation has been generated through the indirect measurement of 3-nitrotyrosine (3-NT). 3-NT is the nitration of tyrosine residues on proteins which is primarily generated by the nitrogen dioxide radical ($\bullet\text{NO}_2$) [59, 60]. Accordingly, 3-NT is frequently used as a marker for $\bullet\text{NO}_2$ [61, 62]. 3-NT levels increased within the mouse brain simultaneously with lipid peroxidation within the first hour after injury in the weight drop model [63] and in the CCI model with an increase of oxidative damage and calpain-mediated cytoskeletal degradation [64]. Experiments using a lateral fluid percussion TBI model also demonstrated that after injury endothelial nitric oxide synthase (eNOS) is increased concurrent with blood-brain barrier disruption 24 hours after injury. eNOS generates $\bullet\text{NO}$ which as previously mentioned, reacts with superoxide radical to create peroxynitrite degradation products that form $\bullet\text{NO}_2$.

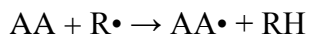
Additional *in vivo* support for the increase of deleterious nitrogen radicals was developed from rat TBI models utilizing nitric oxide scavenger tempol. Experimenters administered tempol to catalytically scavenge peroxynitrite derived radicals such as $\text{CO}_3^{\bullet-}$, $\bullet\text{OH}$, and $\bullet\text{NO}_2$ and demonstrated a dose dependent decrease in 3-NT following CCI in the mouse [65].

1.8 Lipid peroxidation

Free radicals e.g. $\bullet\text{OH}$, $\bullet\text{NO}_2$, and $\text{CO}_3^{\bullet-}$ induce the lipid peroxidation (LP) of polyunsaturated fatty acids (PUFA) including arachidonic, linoleic, docosahexaenoic and eicosapentaenoic acids within cell and organellar membranes. The LP begins with the abstraction of an electron from an allylic carbon by a free radical i.e. “initiation.” Subsequent reactions during “propagation” contribute to the overall demise of the fatty acid into a degraded aldehydic product such as 4-hydroxynonenal (4-HNE) or 2-propenal (acrolein; ACR). The following describes the reactions of this process in further detail with the fatty acid arachidonic acid (AA) as an example.

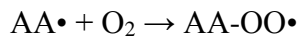
Initiation:

A highly electrophilic radical ($\bullet\text{OH}$, $\bullet\text{NO}_2$, or $\text{CO}_3^{\bullet-}$) steals an electron from hydrogen, bound to an allylic carbon (carbon surrounded by adjacent double bonds) of a PUFA e.g. AA. The carbon-bound hydrogen has an unequal distribution of electrons which facilitates relatively “easy” abstraction [66]. The attack of a free radical ($\text{R}\bullet$) converts the AA into a lipid or alkyl radical ($\text{AA}\bullet$). Subsequently the attacking radical is quenched by the electron-containing hydrogen.

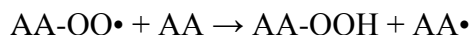


Propagation:

The alkyl radical (AA•) continues to react with a molecule of oxygen, which creates a lipid peroxy radical (AA-OO•).

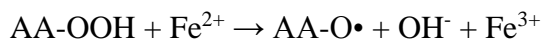


The peroxy radical (AA-OO•) continues to react within the membrane stealing an electron forming a lipid hydroperoxide (AA-OOH) and a second alkyl radical (AA•).

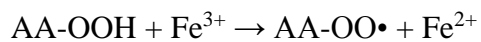


Iron-Catalyzed Propagation:

The lipid hydroperoxide AAOOH can be further decomposed by two forms of ionic iron. Ferrous (Fe²⁺) iron in the presence of hydroperoxide (AA-OOH) will react to form a lipid alkoxy radical (AA-O•).

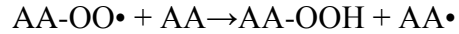
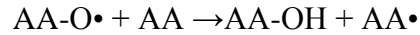


Or, in the presence of ferric (Fe³⁺) iron, the hydroperoxide (AA-OOH) is converted back into a lipid peroxy radical (AA-OO•).



Chain Branching Reactions:

Either alkoxy (AA-O•) or peroxy (AA-OO•) radicals arising from iron-catalyzed reactions will contribute to degradation of the nearby “chains.”



Scission and Fragmentation:

Among the products generated from the peroxidation of PUFAs are neurotoxic aldehydes such as 4-hydroxynonenal (4-HNE) and 2-propenal (acrolein; ACR) [67]. The following diagram demonstrates the creation of 4-HNE from AA.

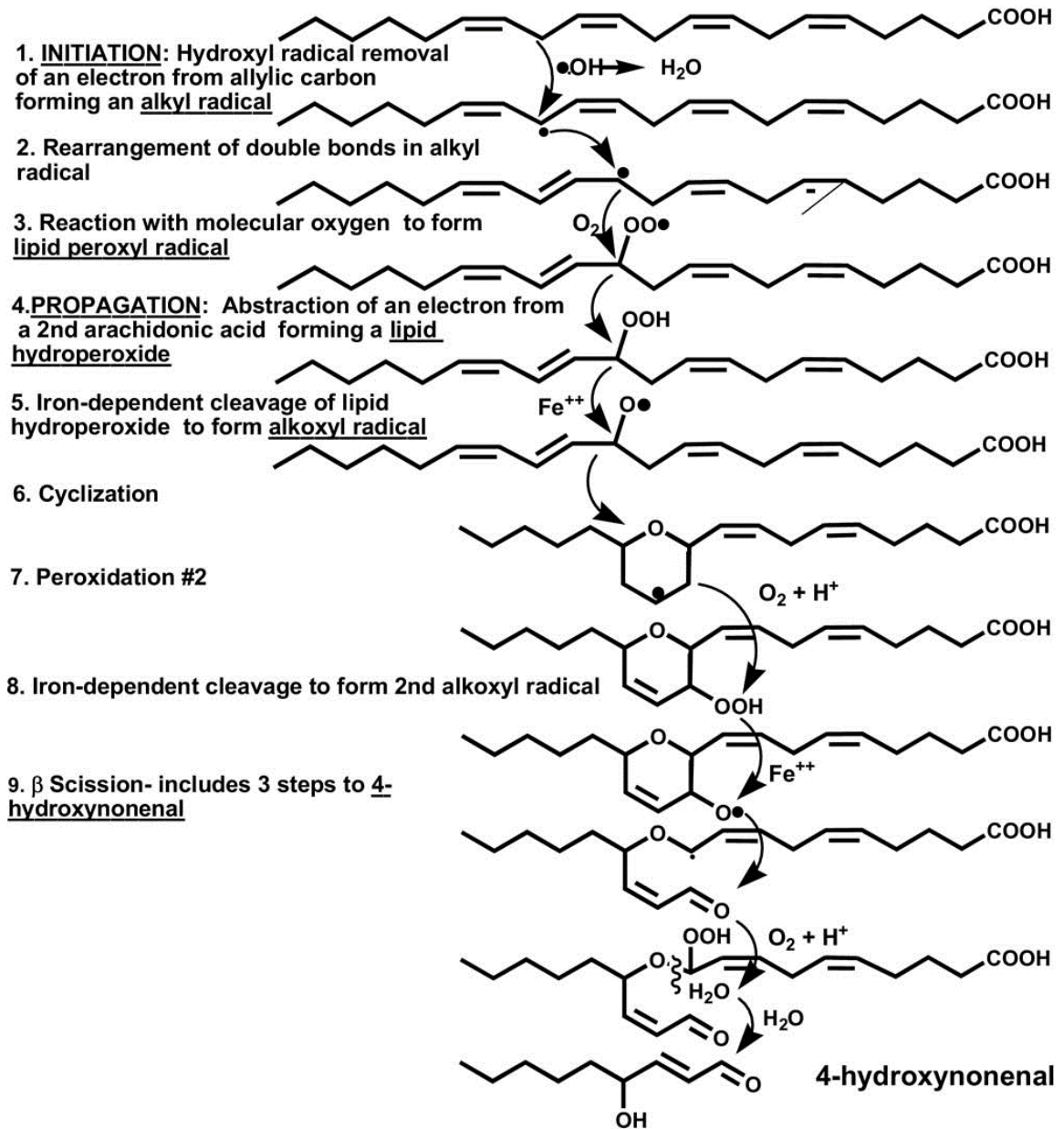


Figure 1.2 Chemical initiation, propagation, and termination of arachidonic acid to 4-hydroxynonenal (4-HNE). Adapted from Hall et al, 2010 [68].

Reactive aldehydes such as 4-HNE and ACR will be discussed in further detail in this chapter, however, these LP-derived breakdown products are highly toxic and bind to various amino acids or can create protein aggregates. Either consequence impedes or completely inhibits protein function thereby promiscuously disrupting normal cellular processes ranging from glutamate transport to mitochondrial function [69]. Other notable ramifications of LP are due to changes in membrane dynamics. Lipid peroxidized membranes exhibit decreased membrane fluidity, increased permeability to substrates and molecules that were otherwise impassable, and inactivation of membrane or lipid-bound enzymes [66]. *In vivo* experiments have determined that following hydroxyl radical formation within the first 5 minutes after CCI in the rat, LP progressively increases with the breakdown of the blood-brain barrier [57].

1.8.1 Treatment of Lipid Peroxidation

Multiple compounds have attempted to protect against LP and some have demonstrated neuroprotection (See Hall et al., 2010 for further review). However, one compound tirilazad mesylate (U74006F), uses a scavenging mechanism which parallels that of a compound of this current work, save that the target of the scavenger is different. Tirilazad scavenges the lipid peroxy radical (e.g. R-OO•) which limits LP by sequestering the ability of lipids to undergo chain branching. The mechanistic concept of tirilazad was verified in both mice [70] and rats [71] and demonstrated neuroprotective efficacy. Tirilazad underwent testing in phase II and phase III trials but due to complications in the randomization of patients the results were never released in North America. However,

European trials failed to demonstrate a beneficial improvement of Glasgow Coma Scale (GCS) score. Though post-hoc analysis revealed a significant reduction of mortality in patients suffering a severe TBI with subarachnoid hemorrhage (tSAH) [71], the compound lost sponsorship for further development and clinical testing.

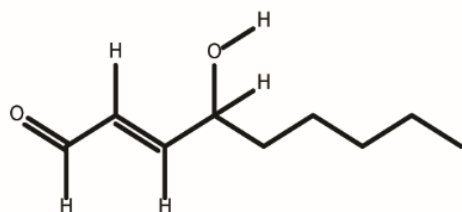
Pharmacological scavenging of lipid peroxy radicals has the potential, in theory and in practice, to be a feasible clinically relevant intervention for the treatment of TBI in humans. However, much criticism was received for tirilazad due to the limiting therapeutic window. Lipid peroxy radicals, much like many free radicals have relatively short-lived half-lives which requires early intervention if clinical efficacy is desired. As previously discussed in the section regarding Ca^{2+} regulation, it is our prerogative to investigate a scavenging compound. The work with tirilazad strongly supports the notion that scavenging is feasible as a neuroprotective mechanism especially if the scavenged substrates exhibit a longer half-life. Of the available scavenging targets, reactive aldehydes possess several characteristics that are ideal for scavenging and in the following sections the role of reactive aldehydes will be further discussed.

1.9 Reactive Aldehydes

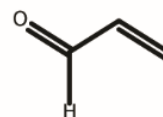
Lipid peroxidation compromises membrane integrity and interrupts phospholipid dependent proteins (e.g. ion channels and electrogenic ion pumps), however, the aldehydic breakdown products are additional, well-characterized toxic mediators of cellular damage as demonstrated in various experimental models of TBI [72-74].

Specifically, 4-HNE and ACR possess carbonyl functional groups (**Figure 1.3**) capable of covalently binding lysine, histidine, and cysteine amino acids of cellular and mitochondrial proteins via Schiff base and/or Michael adducts [75, 76]. (See **Figure 1.4**) These alterations induce conformational changes in protein structure compromising their function, which contributes to overall cellular demise. Both 4-HNE and ACR are highly electrophilic; the exception is the LP-derived 3 carbon containing molecule: malondialdehyde (MDA) [77]. MDA is a degradation product of LP and can be used in the assessment of LP, but it is non-toxic and often referred to as a “tombstone” marker. Free radical-induced LP is one of the most deleterious contributors of acute post-TBI pathophysiology [65, 78-82].

**Aldehydic Breakdown Products of Lipid Peroxidation
"Reactive Carbonyls"**



**4-Hydroxynonenal
4-HNE**



**2-Propenal
Acrolein, ACR**

Figure 1.3. Structure of 4-hydroxynonenal (4-HNE) and Acrolein (ACR), each possessing a nucleophilic aldehyde i.e. reactive carbonyl. 4-HNE and ACR are the aldehydic breakdown products of free radical-induced lipid peroxidation. Carbonyls refer to compounds that contain double bonded oxygen (CHO) functional group, to include reactive aldehydes: 4-HNE and ACR.

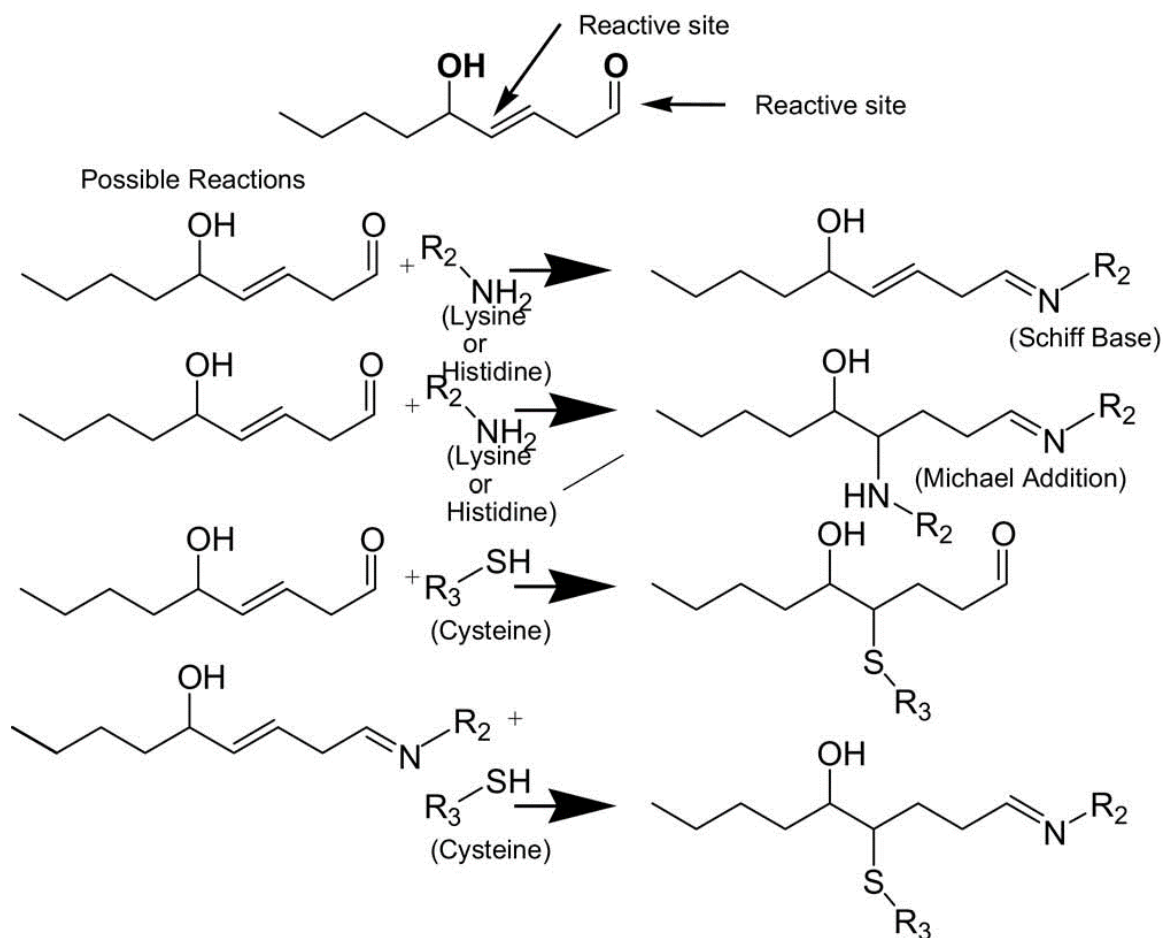


Figure 1.4: Example of 4-HNE and Schiff base and Michael additions to protein residues. Adapted from Hall et al, 2010 [68].

1.9.1 Reactive Aldehydes in Traumatic Brain Injury

In various articles the LP-derived breakdown products such as 4-HNE and acrolein have been referred to as reactive aldehydes, carbonyls, or lipid aldehydes. The term carbonyl simply refers to the COH bond in the parent compound. The aldehydic reference applies to the placement of the double bonded oxygen (O) in the compound; a terminal position indicates an aldehyde. For the remainder of this manuscript the terms reactive aldehydes and carbonyls will be used interchangeably in regards to specifically 4-HNE and ACR.

Reactive aldehydes or carbonyls, as previously mentioned, are capable of interrupting a wide variety of enzymatic processes [38]. And, carbonyls produced after traumatic brain injury are capable of disrupting vital cellular mechanisms such as those involved with signaling and mitochondrial function [83]. Not only are the processes interrupted but the structural integrity of the adducted protein is compromised [84]. Adduction is a term coined to identify proteins that have been modified by such carbonyls [85]. It is important to note that protein adduction is a stronger mediator of cytotoxicity than the depletion of cellular reducing agents such as glutathione [75], which implies the expressed concern relative to treatment in TBI.

Experimental models of mouse TBI *in vivo* have helped to appreciate the spatial and temporal magnitude of aldehydic production after injury. For instance, 4-HNE and 3-NT were found to increase in mouse cortical tissue as early as 30 minutes after injury as demonstrated by immunohistochemical (IHC) staining [64] and can last for at least a week

after injury [63]. (3-NT is considered a marker of oxidation as well, but does not possess the same species of reactivity as 4-HNE).

Although Scheff et al., published nearly identical experiments, results concerning the modification of proteins in the cortex versus the hippocampus were published in separate journals of the same year. Nevertheless, these experimental CCI-TBI rat models provided support for the acute increase and persistent modification of synaptic proteins by 4-HNE, acrolein, protein carbonyl, and 3-NT in the hippocampus [78] and cortex [86] concurrent with a depletion of antioxidant systems.

Lipid-derived breakdown products like 4-HNE and ACR are both neurotoxic and broadly disrupt cellular function in an acute and persistent fashion, but ACR reportedly demonstrates additional toxicity and reactivity. For instance, exogenously applied ACR was shown to exhibit a tenfold potency in the ability to reduce respiratory function compared to 4-HNE in naïve rat isolated mitochondria [50]. Acrolein has been shown to initiate membrane instability and initiate LP [87], but only recently was ACR reported to be involved in the destruction of myelin. In these experiments acrolein was reported to initiate and facilitate demyelination of neurons by interfering with glutamate uptake, which facilitates excitotoxicity. When ACR scavengers were applied to the system demyelination was prevented [88].

Reasons for the increased potency of ACR are primarily implicated by its reactivity. Acrolein, of all unsaturated aldehydes, is the most reactive and reacts 110-150 times faster with other biomolecules such as proteins compared to 4-HNE [87, 89-91]. Other aldehydes that contain electron-releasing substituents exhibit a reduced charge of the carbon cation

intermediary. Therefore, the lesser the partial positive charge of the 3-carbon the double bond will exhibit decreased electrophilicity and therefore reduced reactivity [89]. Experiments on ACR 1:1 adduct formation demonstrate that ACR possesses the highest second order reaction rate constant $121\text{M}^{-1}\text{s}^{-1}$ [89], meaning that the rate of the reaction is directly proportional to the square of ACR concentration. And, while the rate constant (k) is experimentally determined and does not change as a constant, the medium in which the reactants are permitted to interact can sterically interfere with the ability of the reagents to meet. Additional consideration should also be made for environmental conditions such as pH that can affect conformation of a targeted protein for which acrolein is attempting to adduct. In other words, in the case of TBI, wherein the cell exists in a state of distress, the rate of reactions is not solely determined by an experimentally determined rate constants. Rather, other influences such as pH, hydrophobicity, half-life, and proximity of reagents among other factors have appreciable weight in the reactivity of carbonyls to various targets.

1.10 Mitochondria

Mitochondrial are colloquially regarded as the “powerhouse of the cell”. The phrase is meant to convey the unequivocal contribution to cellular vitality. However, as Mr. Benjamin Parker eloquently regards: “With great power, comes great responsibility.” So, while empirically it is true that the mitochondria are responsible for the oxidative phosphorylation which provides far more energy than glycolysis, much care is provided by the cell to regulate its homeostasis. Else, dire ramifications usually yielding death are

likely should the cell be forced to reconcile insults for which it cannot compensate. These details and more will be elaborated, but before the pathology it is important to first introduce form and prototypical functionality.

The mitochondrion can be described according to its major constituents: the outer mitochondrial membrane (OMM), the inner mitochondrial membrane (IMM), the inner mitochondrial space (IMS) and the matrix. The OMM is a lipid bilayer that encompasses the other remaining elements. The IMM is also comprised of lipid bilayer. The tortuous shape creates folds called cristae that increases the surface area for which the electron transport system (ETS) can transduce energy [92]. The IMS exists between the OMM and the IMM and serves as the space for which protons collect, driven against their gradient by the ETS. The most internal aspect is the matrix. Wherein not complex computer programs exist, rather, enzymes necessary for the continued degradation of glucose in what is known as the tricarboxylic acid cycle (TCA), citric acid cycle, or Krebs's cycle.

1.10.1 Mitochondrial function

Adenosine triphosphate (ATP) is the molecule produced by mitochondria. ATP serves as a type of “energy currency” for the cell. And upon utilization, the chemical energy release from the removal of the phosphate groups can be used to drive other process or enzymes. This production of ATP involves several complex components, and will be briefly detailed as dictated by their relevancy and pertinence.

Glycolysis:

The generation of ATP begins outside the mitochondria in the cytosol during glycolysis. One molecule of glucose is broken down into two molecules of pyruvate which allows two “turns” of the TCA cycle described below. This process produces 4 molecules of ATP and 2 molecules of nicotinamide adenine dinucleotide (NADH), which is a conserved coenzyme required to drive complex I of the ETS. It should be noted that the net production of ATP is limited to 2 molecules, not 4, as the reaction necessitates the difference in ATP to complete.

Tricarboxylic Acid Cycle:

Pyruvate enters the mitochondria with NADH and is catabolized into acetyl coenzyme A (acetyl CoA). Acetyl CoA enters the TCA cycle wherein 8 specific reactions facilitate the reduction (gain of electrons) to specific electron carriers. For instance during this process a single acetyl CoA molecule is oxidized e.g. loses its electrons to other compounds and in doing so the acetyl CoA is converted into 2 molecules of carbon dioxide (CO₂). The other compounds that were reduced (received electrons from acetyl Co A) were created at various stages in the cycle and in different quantities. In this process the following molecules were reduced:

- 3 molecules of NAD⁺ were reduced to 3 molecules of NADH
- 1 molecule of FAD was reduced to FADH₂
- 1 molecule of GTP was created.

Flavin adenine dinucleotide (FAD) molecule mentioned above has similar functionality to NADH in that it has the capacity to oxidize and be reduced again. Guanosine triphosphate (GTP) is a purine nucleoside triphosphate and is regarded as a single ATP equivalent used frequently by G-protein based signal transduction.

Electron Transport System & Oxidative Phosphorylation:

The reduction of NAD^+ and FAD to create NADH and FADH_2 as described in the previous section are major components of the electron transport system (ETS). These molecules contribute their previously acquired electrons to various complexes associated with the IMM [93]. Complexes I-IV work in concert with other proteins to establish a proton gradient by oxidizing their respective substrates i.e. the complex receives high energy electrons from their substrates and the complex then contributes protons (H^+) across the IMM. The first two complexes describe below are both entry points for the ETS, and is the principle reason why data relative to mitochondrial respiration is expressed as Complex I and Complex II-driven respiration. (See **Figure 1.5**)

- Complex I: Known otherwise as “NADH: ubiquinone oxidoreductase” or NADH dehydrogenase (ubiquinone). Complex I accept electrons from reduced forms of NADH and contributes to 4 protons across the IMM.
- Complex II: Succinate dehydrogenase, receives electrons from FADH_2 , but does not contribute protons across the IMM.
- Ubiquinone: Known otherwise as “Coenzyme Q_{10} .” Although, not designated as a “complex,” ubiquinone receives the high energy electrons from either Complex I or II and “shuttles” electrons to Complex III.

- Complex III: Cytochrome bc_1 receives electrons from Ubiquinone and translocates 4 protons across the IMM through a series of complicated, nearly theatrical, reactions described by what is called the “Q cycle.” See Nicholls and Ferguson 2002, for further details.
- Cytochrome C: Another electron carrying molecule that transports electrons from Complex III to Complex IV.
- Complex IV: Cytochrome C oxidase is the last step in the ETS and catalyzes the transfer of 4 electrons ($4e^-$) from cytochrome C to O_2 the final electron acceptor. In addition to this reaction, Complex IV “pumps” 2 protons across the IMM.
- Complex V: ATP synthase spans the IMM. The proton gradient formed by the previous complexes is used by Complex V to transduce protons back into the matrix down the electrochemical gradient. In doing so, mechanical energy is created to join adenosine diphosphate (ADP) with inorganic phosphate to create ATP i.e. phosphorylate ADP.

The process of oxidizing substrates to generate a proton gradient is coupled to the phosphorylation of ADP to create ATP, hence the term oxidative phosphorylation.

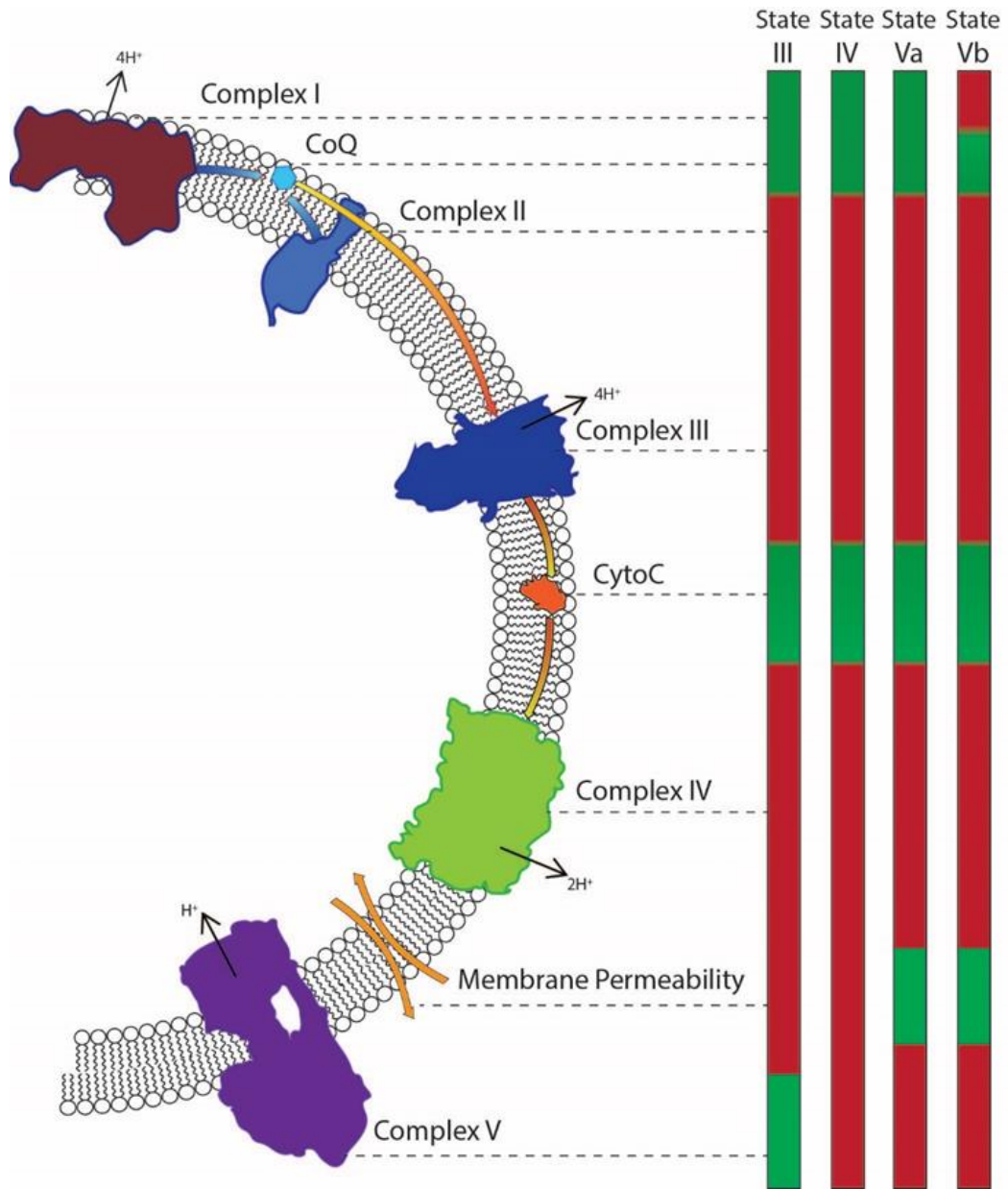


Figure 1.5 Illustration of the major components of mitochondrial electron transport system (ETS). Vertical bars represent four different states of mitochondrial respiration. Hashed lines can be followed from the protein complexes to the vertical bars; activated complexes are green bars while inactive complexes are red bars.

1.10.2 Mitochondrial States of Respiration

The rate of mitochondrial respiration can describe the speed at which oxidation and phosphorylation take place. However, this rate is a coupled mechanism involving multiple reactions that are tightly controlled and principally determined by the proton electrical potential (Δp) and the difference of redox potentials nearest to sites of proton translocation [93].

Experimental models that utilized the Oxytherm or Seahorse Bioscience to determine mitochondrial rates of respiration are capable of only measuring the amount of oxygen that mitochondria respire. This metric is representative of a single reaction (the rate at which O₂ becomes the final electron acceptor). In order to fully assess the components of respiration and better understand where and how dysfunction can be measured, various compounds can be introduced into the isolated mitochondrial solution. The addition of these compounds to experimentally investigate mitochondrial dysfunction is further described in the **Material and Methods** chapter.

Briefly, the addition of various substrates or inhibitors induces various “states of respiration” originally described by Chance and Williams [94] and later adapted by Nicholls and Ferguson [93]. The following introduces the states of respiration by the sequential addition of various compounds. (See **Figure 1.5**)

- **State I:** Mitochondria alone in the presence of inorganic phosphate (P_i)
- **State II:** Complex I substrates added e.g. pyruvate and malate.
- **State III:** Addition of Complex V substrate ADP.

- Describes the rate of coupled oxidative phosphorylation.
- **State IV:** Addition of Complex V inhibitor e.g. oligomycin.
 - Describes integrity of the IMM.
- **State V:**
 - **State Va:** Addition of protonophore e.g. FCCP
 - Describes maximal state of oxidative respiration for Complex I.
 - **State Vb:** Addition of Complex II substrates, and addition of Complex I inhibitor.
 - Describes maximal state of oxidative respiration for Complex II.

The respiratory control ratio (RCR) is a metric that can provide insight on the state of mitochondria, specifically it is an index of how “coupled” oxidative and phosphorylative mechanisms are. RCR is the ratio of State III respiration (in the presence of pyruvate, malate, and ADP) divided by State IV respiration (mitochondria in the presence of pyruvate, malate, ADP, oligomycin A-an inhibitor of ATP synthase).

1.10.3 Mitochondrial Superoxide Production

As promised, and likely to the reader's dismay, mitochondrial dysfunction especially in the context of TBI will be further discussed. The principle source of superoxide production occurs from "electron leak" during the ETS. During the transfer of electrons throughout the ETS, electrons can make a "quantum leap" from their intended destinations. And, while a benevolent Ziggy does not provide assistance in where the electrons are transferred, leaping electrons will preferentially partially reduce O₂. As a result superoxide is produced (O₂[•]). Recently reviewed, multiple sites within the ETS are capable of electron leak and subsequent superoxide formation [95]. Complex I and III are generally accepted as the principle producers of superoxide. Complex I produces superoxide at its flavin prosthetic group within the NADH sub-component and at the ubiquinone sub-component. Complex II at the flavin site and Complex III produces superoxide at the ubiquinone binding site [95]. However, other sources of superoxide formation exist in the ETS. For instance, in adjacent pathways to the ETS (not from pyruvate) rather the β-oxidation of fatty acids depend upon electron transferring proteins (ETF) [95]. Experiments in isolated mitochondria from naïve mice have contributed a wealth of knowledge regarding the idiosyncrasies of superoxide formation. In particular Complex I and III are frequently attributed as the primary sources; Complex I contributing far more than complex III. However, researchers have shown that the production of superoxide is complex (pun intended) and under conditions wherein Complex I is not able to function e.g. inhibited experimentally with rotenone, the enzymes within the matrix such as pyruvate dehydrogenase (PDH) and 2-oxoglutarate dehydrogenase (OGDH) produce more superoxide than Complex I in normal conditions [96]. This concept is important to

consider when trying to understand the wherein free radicals are produced following a TBI, especially considering that aldehydic breakdown products are capable of binding to a wide range of proteins to inhibit function.

1.10.4 Mitochondrial Peroxynitrite Formation

As previously mentioned, the product of $O_2^{\bullet-}$ and $\bullet NO$, forms a temporary peroxynitrite anion ($ONOO^-$) which degrades into further more toxic and reactive aldehydes. The production of $NO\bullet$ is produced by nitric oxide synthase and is important for cellular signaling. Of the three forms, endothelial NOS (eNOS), neuronal NOS (nNOS), and inducible NOS (iNOS), mitochondrial NOS is activated by the influx of Ca^{2+} . Given the relevancy of Ca^{2+} homeostasis by mitochondria, discussed in the next section, dysfunctional mitochondria can contribute further to formation of free radicals.

After injury in the experimental mouse CCI-TBI model protein nitration, an index of peroxynitrite formation, increased in the cortex and hippocampus significantly 24 hours after injury and peaked at 72 hours. The expression (mRNA) of eNOS did not increase, but protein levels of eNOS did significantly at 48 and 72 hours in the hippocampus and cortex. These experiments also demonstrated at least a partial temporal relationship between NOS protein and marker of oxidative damage 3-NT [97].

1.10.5 Role of Mitochondria in Calcium Homeostasis

Mitochondria play an important role in the regulation of Ca^{2+} , especially after CNS injury [98]. Should the neuron reach an intercellular concentration of approximately 500nM Ca^{2+}_i then mitochondria initiate means to accommodate the relatively high influx of Ca^{2+} [99]. Calcium regulation is driven by several Ca^{2+} channels. A Ca^{2+} uniporter exists to move Ca^{2+} into the matrix; this channel is compelled by the mitochondrial membrane potential ($\Delta\psi$). The efflux of Ca^{2+} on the other hand is driven by the $\text{Ca}^{2+}/n\text{Na}^+$ exchanger, whose functionality is partially dictated by the H^+/Na^+ exchanger [100]. The exact ratio of Ca^{2+} to Na^+ is presently undetermined [93]. To a certain point the influx of Ca^{2+} can be buffered in the matrix by the creation of a calcium-phosphate gel [93]. However, in the event of TBI mitochondria are often incapable of buffering the massive influx of Ca^{2+} .

1.10.6 Mitochondrial Dysfunction after TBI

In addition to the influx of Ca^{2+} from glutamate-mediated opening of NMDA channels, traumatic tearing, and failure of Na^+/K^+ ATPases in the cell membrane depolarize the cell. Two major ramifications are subsequent to the Na^+/K^+ failure: (1) the depolarization causes voltage-gated Ca^{2+} channels to open and aberrant Ca^{2+} influx [101]. (2) Loss of Na^+/K^+ ATPase functionality means the accumulation of intercellular Na^+ ; the accumulation instigates the reversal of membrane $\text{Ca}^{2+}/\text{Na}^+$ exchangers to pump Ca^{2+} into the cell.

Such a torrential influx of Ca^{2+} in the cell after TBI overwhelms the capacity of mitochondria to maintain homeostasis. The excessive Ca^{2+} loading or cycling [102] as well as oxidative stress [103] will induce mitochondrial permeability transition (mPT). The formation of the mPT allows the movement molecules up to ~150 kDa and the loss of the mitochondrial membrane potential ($\Delta\psi$), exacerbates ROS formation, increases lipid peroxidation, and initiates apoptotic cellular death pathways[104, 105]. In an attempt to preserve and institute the proton gradient Complex V (ATP synthase) reverses [106] and contributes overall depletion of energy.

Strong evidence for mitochondrial dysfunction as a result of mPT following experimental CCI-TBI was demonstrated in experiments that investigated the treatment of cyclosporin A (CsA) in isolated rat mitochondria and synaptosomes. In these experiments CsA treatment was able to reduce ROS formation and prevent mPT formation by excessive Ca^{2+} loading. CsA was postulated to mediate the observed effects by either (1) preventing mPT formation by interacting with cyclophilin D, (2) reducing glutamate-mediated cycling/uptake of Ca^{2+} , or (3) the CsA-cyclophilin complex could suppress calmodulin phosphatase which normally would activate NOS by phosphorylation [106]. CsA was later reported to spare 50% of otherwise lost cortical tissue following TBI in the same rat CCI-TBI model. [107].

As for the time course of mitochondria damage following TBI, experimental mouse CCI-TBI models were used to conclude that the onset of mitochondrial dysfunction is relatively early. Mitochondria isolated from the cortex of mouse brains following a CCI-TBI were reported to exhibit a significantly impaired ability to respire oxygen 30 minutes

after injury to the latest time point measured, which was less impaired but still significant at 72 hours following injury [73].

Despite the acute onset of mitochondrial dysfunction, the possible therapeutic range for pharmacological intervention was reported to exist within 5 minutes to 24 hours after CCI-TBI in isolated cortical mouse mitochondria [108]. The investigators concluded this by administration of carbonyl cyanide 4-trifluoromethoxy phenylhydrazone (FCCP). FCCP is protonophore which acts to “uncouple” oxidation of substrates from the phosphorylation of ADP. Though this treatment is considered an “insult” to the mitochondria, therapeutic worth is obtained in reducing Ca^{2+} influx, reportedly by reducing the membrane potential ($\Delta\Psi_m$) thereby reducing the chemiosmotic gradient and consequently reducing the influx of Ca^{2+} into the mitochondrial matrix. The importance and relevance of this experiment to the current work will become apparent in the Discussion; however, it is important to note now that therapeutic intervention can be applied within 24 hours (as shown with FCCP) because the mitochondria are able to be uncoupled. In other words, 24 hours post-injury mitochondria are still coupled regardless of how diminished.

Aside from Ca^{2+} dysregulation, mPT, and uncoupled state of mitochondria after injury, mitochondria are also seductive targets to potentiate another type, but related form of damage. Given the rich in environment of polyunsaturated fatty acids in the lipid bilayers and the intrinsic ability to generate reactive oxygen species in both normal and pathological conditions, mitochondria are targets for not only LP but subsequent aldehydic attacks.

Specifically, 4-HNE and ACR have been identified as reactive carbonyls capable of impairing mitochondrial respiration and contribute to the accumulation of oxidative damage markers [50, 73, 74, 109]. The impaired mitochondria become incapable of regulating ionic homeostasis, have severely reduced or completely inhibited ability to generate ATP through oxidative phosphorylation, and will initiate apoptotic cell death, thereby killing the neuron in which they reside [65, 73, 110-113]. It should be noted that while apoptotic cell death is the result of mitochondrial dysfunction, the death of ACR-treated neurons in culture is by necrosis which does not directly involve cytochrome c release [27, 114]

1.11 Carbonyl Scavenging

All of the previously described pathologic processes involve reactive aldehydes e.g. carbonyls. In each instance 4-HNE and acrolein are capable of either initiating, prolonging, or exacerbating all of the aforementioned processes involving, but not limited to free radical generation, lipid peroxidation, Ca²⁺ dysregulation, and mitochondrial function. Additionally, the pharmacological prevention or amelioration of each of these pathological processes independently has been met with some success, but currently no Food and Drug Administration (FDA)-approved pharmacological intervention for the treatment of human TBI exists.

Increasingly, researchers have begun to investigate carbonyl scavenging. Simply defined for the context of TBI: carbonyl scavenging is a means to prevent the binding of neurotoxic aldehydes to biological substrates, by offering an exogenous pharmacological

compound that will bind to the carbonyls instead. Carbonyl scavengers by definition exhibit a high reactivity to endogenous aldehydes [115], and the most effective scavengers contain a hydrazine pharmacophore [116]. The hydrazine moiety is a (-NH-HN₂) functional group capable of binding to reactive aldehydes. One of the more extensively studied hydrazine-containing compounds is the anti-hypertensive compound hydralazine (HZ).

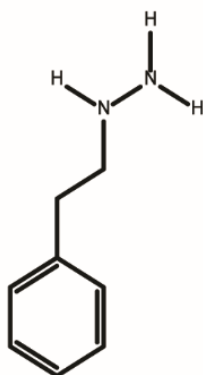
Hydralazine has shown potential for carbonyl scavenging in neurotrauma when first examined in spinal cord compression injuries. In these experiments spinal cords extracted from guinea pigs sustained an *ex vivo* compression injury followed by immersion in 500mM of hydralazine. Hydralazine-treated spinal cords exhibited significantly less membrane permeability, reduced superoxide production, and decreased acrolein accumulation by way of immunohistochemical staining (IHC) [117].

In other experiments also investigating the HZ compound, the utility of the hydrazine functional group was highlighted as an effective means to prevent adduct crosslinking [118]. Here, the authors were able to demonstrate that ACR rapidly causes cross-linking and oligomerization of acrolein adducted proteins and that HZ was able to prevent this even when added after the application of ACR. This experiment is pertinent and therefore important for two reasons: 1) ACR even after bound is still reactive and can cross-link other proteins. 2) Hydrazine-containing compounds are able to prevent this. The authors concluded that the majority of toxicity is attributed to this mechanism and that the neuroprotective effects are primarily due to preventing cross-linking by adduct trapping and not only scavenging free aldehydes [118, 119]. Given the efficacy in this and other model paradigms, hydralazine possess significant potential for TBI. However, HZ

possesses significant shortcomings. HZ is a potent vasodilator with a short half-life of approximately 30 minutes [120]. Early investigations with HZ advise that the therapeutic levels necessary for carbonyl scavenging are not tolerable *in vivo* considering the potency of the anti-hypertensive effects [120].

Another compound that retains the hydrazine moiety but does not possess hypotensive effects is the monoamine oxidase inhibitor (MAO-I) phenelzine (PZ). (**Figure 1.6**)

Carbonyl Scavenger



Phenelzine
PZ

Figure 1.6. Phenelzine (PZ) is an FDA-approved drug for the treatment of depression and anxiety. PZ is an inhibitor of monoamine oxidase A and B types which prevents the degradation of monoamines such as serotonin, norepinephrine, epinephrine and dopamine.

Phenelzine is an FDA-approved drug for the treatment of major depression by irreversibly inhibiting both A and B monoamine oxidase (MAO). MAO is contained within the presynaptic neuron and within in the outer mitochondrial membrane. The compound does contain a phenolic ring which is capable of acting as an anti-oxidant and a carbonyl scavenger, though predominantly by the latter means [116, 121]. Carbonyl scavenging (**Figure 1.7**).

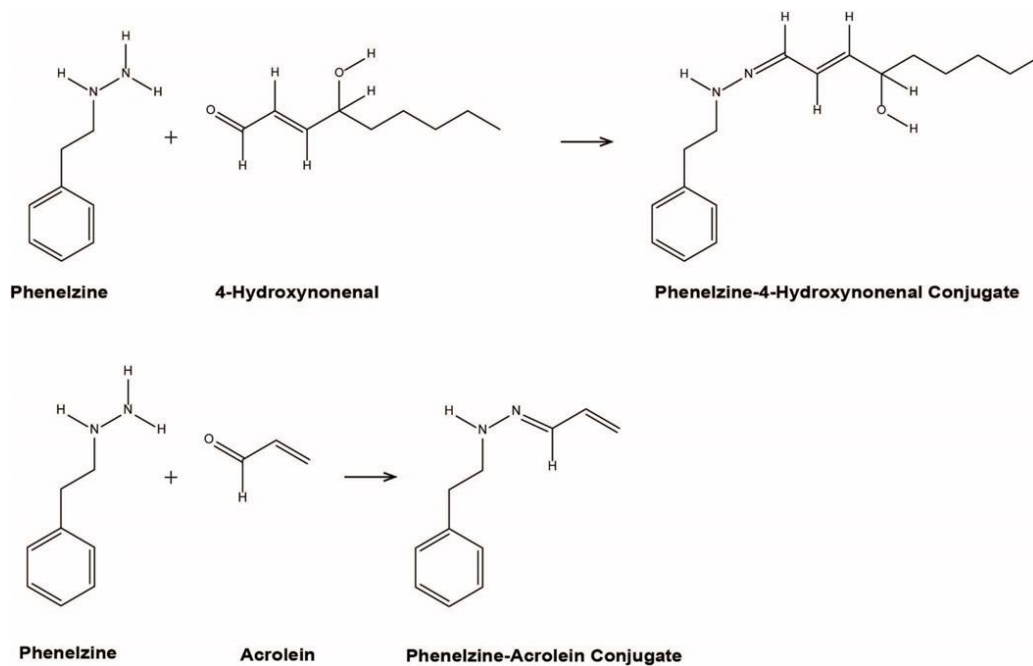


Figure 1.7 Chemical scavenging reactions of phenelzine with reactive carbonyls: 4-hydroxynonenal and acrolein.

When smooth muscle cells *in vitro* were exposed to various oxidized lipoproteins, PZ treated cells were capable of reducing cytochrome c release, reduce hydrogen peroxide and superoxide production, reduced mPT formation, and reduce the presence of cytotoxic carbonyls such as 4-HNE and other compounds reactive to thiobarbituric acid [116]. (Thiobarbituric acid reactive substances (TBARS) is an assay to detect malonodialdehyde which is not *exclusively* a by-product of lipid peroxidation.) The authors made special effort to indicate that MAO-I s in these assays did not contribute to the formation of superoxide radicals because the medium did not contain MAO substrates.

The investigation of PZ *in vivo* as a treatment for neurotrauma is presently underwhelming, but what currently exists is promising. *In vivo* experiments investigating the use of PZ in ischemia-reperfusion brain injury in the gerbil have demonstrated what the authors coined as “reduction of aldehyde load.” Though, this phrase will not be used in this manuscript the experiments were useful in that PZ was able to reduce neurotoxic aldehydes in this injury paradigm with up to a 3 hour delay of administration [122].

Recently our laboratory has begun to investigate the efficacy of PZ as a treatment for TBI. Initially the investigation of PZ took place in an *ex vivo* model, wherein cortical brain mitochondria were isolated from naïve mice and exposed to an exogenous application of 4-HNE. Our mitochondrial respirations studies demonstrated that a 5 minute pretreatment of PZ was able to significantly protect the ability of mitochondria to respire oxygen for both Complex I and Complex II-driven respiration. Similarly isolated, mitochondria exposed to a 5 minute pre-treatment of PZ significantly reduced 4-HNE, marker of oxidation via immunoblotting assay [50].

The investigation of PZ's ability to protect mitochondrial function was further studied *in vivo* using the rat CCI-TBI model. Rats were given a single 10 mg/kg subcutaneous injection of PZ 15 minutes after a severe CCI-TBI, and assessed 3 hours later for mitochondrial dysfunction. PZ treatment groups exhibited significant protection of mitochondrial respiration for Complex I and II-driven rates and overall RCR. Additional experiments investigated the ability of PZ to preserve cortical tissue in the rat two weeks after a severe TBI. PZ-treated rats using the same dosing paradigm as previously mentioned exhibited a significantly higher volume of spared tissue when compared to vehicle-treated (saline) animals [50].

1.12 Dissertation Hypothesis

Given the involvement of reactive aldehydes in a wide range of secondary injury mechanisms following TBI, and the potential of PZ to effectively scavenge those reactive carbonyls-- we seek to further investigate the potential of PZ as a treatment for TBI by addressing the following hypothesis.

The **Overall Hypothesis** of this dissertation is that carbonyl scavenging with phenelzine (PZ) will exert an antioxidant neuroprotective effect in the traumatically injured rat brain mechanistically related to PZ's hydrazine moiety reacting with the lipid peroxidation-derived reactive aldehydes 4-HNE and ACR.

Chapter 2

Materials and Methods

(Portions submitted for publication in Free Radical Biology and Medicine)

2.1 Animals

All experiments involving rats were performed with adult male Sprague-Dawley (SD) rats (Harlan, Indianapolis, IN) weighing 300-350g. Rats were exposed to food and water *ad libitum*. All protocols associated with this study are approved by the University of Kentucky Institutional Animal Care and Use Committee which abide by the National Institutes of Health Guidelines for the Care and Use of Animals.

2.2 Drug & Substrate Preparation

2.2.1 4-HNE and Acrolein

4-Hydroxynonenal (4-HNE) and 2-propenal (acrolein) were purchased from the manufacturer and prepared fresh before each experiment consistent with previously described methods and diluted in distilled water to the desired molarity [72]. Acrolein was purchased from Sigma-Aldrich (Supelco, Bellefonte, PA). 4-HNE was purchased from EMD Chemicals Inc. (Merck KGaA, Darmstadt, Germany). Stock solutions were stored according to the manufacture's suggestions at -20°C.

2.2.2 Pargyline

Pargyline hydrochloride (Eutonyl - P8013) was purchased from Sigma-Aldrich. Pargyline was titrated in 0.9% saline to working solution of 5 mg/ml. The final injected volume was calculated based on the weight of the rat to meet the desired dose concentration of 10 mg/kg. Maintenance doses, when used, were diluted to final concentration of 5 mg/kg.

2.2.3 Phenelzine

Phenelzine sulfate salt was purchased from MP Biochemicals (Solon, OH, USA) and titrated in 0.9% saline to working solution of 5 mg/ml. The final injected volume was calculated based on the weight of the rat to meet the desired dose concentration of 10 mg/kg. Maintenance doses, when used, were diluted to final concentration of 5 mg/kg.

2.2.4 Mitochondrial Substrates & Inhibitors

Preparation of mitochondrial substrates and inhibitors for use with Clark-type oxygen electrode were based upon previously published concentrations [72, 108, 123].

Table 2.1. Preparation of Mitochondrial Substrates and Inhibitors

Compound	Manufacturer	Stock	Preparation	
Pyruvate	Sigma P-2256	500 mM	550 mg	to 200 μ l of 1M HEPES in 10 ml diH ₂ O *
Malate	Sigma M-7397	250 mM	335 mg	to 200 μ l of 1M HEPES in 10 ml diH ₂ O *
ADP	Sigma A-5285	30 mM	128.2 mg	to 200 μ l of 1M HEPES in 10 ml diH ₂ O *
Oligomycin-A	Biomol CM-111	1 mg/ml	1 mg	to 1 ml of methanol
FCCP	Biomol CM-120	1 mM	2.542 mg	to 10 ml of 100% ethanol
Succinate	Sigma S-7501	1 M	2.36 g	to 400 μ l of 1M HEPES in 20 ml diH ₂ O *
Rotenone	Biomol CM-117	1 mM	3.94 g	to 10 ml of 100% ethanol*

* Adjust pH to 7.2 using KOH and HCl.

2.3 Controlled Cortical Impact Surgical Procedures

Young adult male Sprague-Dawley (SD) rats (Harlan Labs, Indianapolis, IN) weighing 300-350g were used in experiments wherein controlled cortical impact (CCI) procedures were used to induce a traumatic brain injury (TBI). Rats were anesthetized with 5% isoflurane (SurgiVet, 100 series) and oxygen (SurgiVet, O₂ flowmeter 0-4lpm). Heads were shaved and placed into a stereotaxic frame (Kopf Instruments, Tujunga, CA). Isoflurane was reduced to 2% for remainder of procedure.

Lubrication was applied to the eyes to prevent drying and a rectal probe was used to maintain body temperature at 37°C via electronic heat pad under the animal. A midline surgical incision was made to retract skin and expose the skull for a 6 mm unilateral craniotomy. The craniotomy was performed with a Michelle trephine (Miltex, Bethpage, NY) centered between bregma and lamda sutures, lateral to the sagittal suture. The cortex was exposed by removing the skull cap carefully without damaging the dura. The exposed brain was injured with an electronically controlled impact device (TBI 0310; Precision Systems & Instrumentation, Fairfax Station, VA, USA) in accordance with previously described methods [50, 73, 106, 107, 124]. The dura was injured by a 5 mm beveled tip that compressed the exposed cortex 2.2 mm at a velocity of 3.5 m/sec, and a dwell time of 500ms. A thin veil of Surgicel (Johnson & Johnson, Arlington, TX) was placed over the injury. A premade plastic cap with an 8 mm diameter was attached directly to the skull over the injury site with commercial cyanoacrylate. The cyanoacrylate was allowed to dry before the wound was closed with staples. Rats were removed from stereotaxis and placed into an incubation cage, which provided heat via conduction by an electronic water pump. Rats were monitored until the righting reflex was regained.

- *Sham* groups are defined as rats which were exposed to only craniotomy, but not CCI.
- *Vehicle* groups are defined as rats which are exposed to craniotomy, CCI, and received the vehicle solution (saline).
- *Treatment* groups are rats which received the craniotomy, CCI, and the drug solution in its respective vehicle. The drug administered in all *in vivo* experiments was phenelzine which required a saline vehicle. Rats were randomly assigned to designated groups.

2.4 Ficoll- Purified Mitochondrial Isolation and Protein Assay

Isolation of rat brain mitochondria was performed on ice and is consistent with previously published methods [50, 73, 125]. Rats were exposed to CO₂ for approximately 1 minute until flaccid. Brains were rapidly extracted after decapitated. Ipsilateral cortical tissue was dissected from the rest of the brain and a 8mm diameter circular punch was used to extract tissue corresponding to the site of impact including the penumbra. The cortical tissue was homogenized using Potter-Elvehjem manual homogenizer in 3mL of ice-chilled isolation buffer (215 mM mannitol, 75 mM sucrose, 0.1% bovine serum albumin, 20 mM HEPES, and 1 mM EGTA, pH adjusted to 7.2 with KOH). Differential centrifugation at 4°C was used to separate nuclei and cellular components from crude mitochondrial pellet. Tissue was exposed to two rounds of centrifugation (1300 x g for 3 min) at 4° C. After each centrifugation the supernatant was decanted and diluted in isolation buffer with EGTA. The supernatants were centrifuged at 13,000 x g for 10 minutes. The pellet was resuspended carefully in 400µL of isolation buffer with EGTA which was place inside a

nitrogen bomb (Parr Instrument Company, Moline, IL) at 1,200 psi for 10 minutes to disrupt synaptosomes. The samples were then added onto a discontinuous 7.5% and 10% Ficoll layered gradient. The samples layered on the Ficoll column were centrifuged at 100,000 x g for 30 minutes at 4° C within a Beckman SW 55ti rotor. The resultant pellet was resuspended in 25 to 50 µL isolation buffer without EGTA to yield a concentration of ~10 mg/mL. Final protein concentration was determined using BCA protein assay kit measuring absorbance at 562 nm with a BioTek Synergy HT plate reader (Winooski, VT). For each experiment, fresh mitochondria and buffer solutions were prepared.

2.5 Mitochondrial Bioenergetics Analysis

2.5.1 Clark-type Electrode for in Vivo Use

The Clark-type oxygen electrode (OXYT1/ED, Hansatech Instruments, Norfolk, UK) was used to assess the ability of mitochondria to respire oxygen i.e. a metric of mitochondrial function. Approximately 180µg to 200µg can be isolated from injured and uninjured cortical punches. However, 100 µg of isolated mitochondrial protein are used as previously described [126] to assess mitochondrial function. Mitochondria were suspended in respiration buffer (215 mM mannitol, 75 mM sucrose, 0.1% BSA, 20 mM HEPES, 2 mM MgCl, 2.5 mM KH₂PO₄, pH adjusted to 7.2) in a volume of 250µL which was continuously stirred in a sealed chamber at a constant 37° C.

In accordance with previously published manuscripts respiratory function was measured as the amount of oxygen consumed over time (nmoles/min) [73]. Substrates were added to chamber in the order presented in **Table 2.2**.

Table 2.2. Inducers of Various States of Respiration (at Final Concentrations)

State	Substrates	Amount	
I	no substrates	n/a	Equilibrate for one minute. Contains only mitochondria and Respiration buffer
II	Pyruvate + Malate	2.5 μ L of 5 mM Pyruvate+ 2.5 mM Malate	Complex I substrates allowed to mix with mitochondria and reach a steady rate
III	ADP	1.25 μ L of 150 μ M	Allowed to achieve maximal respiration with a second bolus of ADP
IV	Oligomycin	0.25 μ L of 1 μ M	Allowed to reach maximum effect in approximately 2 minutes
Va	FCCP	0.5 μ L of 1 μ M	Allowed to reach maximum effect in approximately 2 minutes
Vb	Rotenone	0.2 μ L of 1 mM	Allowed to inhibit Complex I respiration
	Succinate	5 μ L of 10 mM	Complex II substrates allowed to drive respiration.

2.5.2 Preparation of Seahorse Sensor Cartridge and Mitochondrial Substrates/ Inhibitors

The Seahorse Extracellular Flux Analyzer, XFe24 (Seahorse Biosciences) can be used to quantify cell culture or isolated mitochondrial bioenergetics.[127-131] In these experiments, XFe24 analyzer was used to quantify respiratory function and bioenergetics of mitochondria in intact and well-coupled (respiratory control ratio (RCR) >5). Mitochondria were isolated using Ficoll-gradient centrifugation as previously described [127]. The XFe24 analyzer offers a transient, 7 μ L chamber within 24-well microplates that enables the real-time determination of oxygen and proton concentrations.[107, 131] **Figure 2.1 A**, depicts a representative mitochondrial oxymetric trace. One day preceding experimentation 1.3mL of XF Calibrant solution (Seahorse Bioscience) was added to each well of the 24 well dual-analyte sensor cartridge (Seahorse Biosciences). The sensor cartridge was stacked on top of a Hydro Booster plate which was stacked on a Utility Plate (Seahorse Biosciences). The stacked plates were incubated overnight in a 37⁰ C incubator without CO₂. The sensor cartridge was removed from incubation and placed into the Seahorse XFe24 the day of experimentation, loaded with mitochondrial substrates and inhibitors at 10x concentrations. For the initiation of state III respiration e.g. activation of complex I and IV, Port A of the sensor cartridge received (50 mM) pyruvate / (25 mM) malate / (10 mM) ADP . Port B contained 10 μ M Oligomycin-A solution for the generation of state IV respiration. Port C contained 40 μ M solution of FCCP for uncoupled, ADP-driven [complex I] state IV respiration. Port D contained 100 nM solution of Rotenone (Company)/ 100 mM of Succinate (Company) for assessment of uncoupled, Succinate-driven [complex II] state IV respiration. During the automated sensor calibration, 7.5 μ g of isolated mitochondria were suspended in 50 μ L in mitochondrial

isolation buffer and added to each well of Cell Culture plate (Seahorse Biosciences) excluding background wells which contained respiration buffer alone. The plate was then centrifuged at 2000 rpm for 4 min at 4⁰C to attach mitochondria to the 24-well cell culture plate. After centrifugation 450 μ L of warmed (37⁰C) respiration buffer (215 mM Mannitol, 75 mM Sucrose, 0.1% BSA, 20 mM HEPES, 2 mM MgCl, 2.5 mM KH₂PO₄ adjusted to pH of 7.2 with KOH) was added gently to the corner of each well for a total volume of 500 μ L. **Figure 2.1 B** illustrates the electron transport system, substrates, and status of activity for respective complexes. Experiments investigating the treatments of phenelzine, pargyline, 4-HNE, or acrolein followed once the mitochondria were fixed to culture plate and are described below. The following **Table 2.3** list the protocol for Seahorse mitochondrial respiration assay.

Table 2.3. Standard Seahorse Mitochondrial Respiration Protocol

Standard Seahorse Mitochondrial Respiration Protocol	
1	Probe Calibration
2	Mix 1 minute
3	Time Delay: 1 minute and 30 seconds
4	Mix 25 seconds
5	Measure 2 minutes
6	Mix 1 minute
7	Injection Port A (pyruvate/ malate/ ADP)
8	Mix 25 seconds
9	Measure 2 minutes
10	Mix 1 minute
11	Inject Port B (oligomycin)
12	Mix 25 seconds
13	Measure 2 minutes
14	Mix 1 minute
15	Inject port C (FCCP)
16	Mix 25 seconds
17	Measure 2 minutes
18	Mix 1 minute
19	Inject port D (rotenone/ succinate)
20	Mix 25 seconds
21	Measure 2 minutes

4HNE and ACR Dose Response

Experiments were performed to determine the optimal concentration of 4-HNE and ACR to inhibit approximately 50% (suboptimal dose) of mitochondrial function. Isolated mitochondria affixed to culture plate (as described previously) were exposed to 4-HNE or ACR ranging from 10 μ M to 100 μ M and 1 μ M to 10 μ M, respectively. Following 4-HNE or ACR treatment mitochondria were assessed by the XFe24 for oxygen consumption rate (OCR) (pmoles O₂/min). OCR were generated by Seahorse algorithms designed to calculate area under the curve. Excel (Microsoft) software was used to isolate time specific points wherein the generated rate calculations reflected the OCR of Complex I and Complex II e.g. the specified time points following the auto-injection of pyruvate-malate and succinate, respectively. Because mitochondria possess the capability to eventually utilize all of the ADP substrates and there exists a delay before oligomycin can inhibit respiration, the highest time points for ADP rates and lowest time points for oligomycin rates are used in place of software generated averages. This is in accordance with previously published methods [127]. The current studies indicate optimal dose of 4-HNE and ACR was determined to be 30 μ M and 3 μ M, respectively.

PZ Dose Response to 4-HNE or ACR

Increasing concentrations of PZ (3 μ M, 10 μ M or, 30 μ M) were exposed to isolated mitochondria (7.5 μ g) in 24 well culture plates (Seahorse Biosciences) for 5 minutes. Immediately following PZ pretreatment mitochondria were exposed to reactive aldehydes such as 4-HNE and ACR (30 μ M and 3 μ M respectively) for 10 minutes. Culture plates containing PZ pretreated mitochondria with subsequent reactive aldehyde exposure were

assessed for their ability to respire oxygen with XFe24, via measurement of OCR (pmoles O₂/min).

PZ or PG Treatment against 4-HNE or ACR

Similar experiments were used to determine the efficacy of a PZ to prevent 4-HNE or ACR-induced respiratory inhibition. In these experiments, isolated mitochondrial were exposed to a 5 minute pretreatment of PZ 30 μM, followed by a 10 minute exposure to reactive aldehyde 4-HNE or ACR. Phenelzine pretreatment concentrations were chosen based on the PZ dose response to 4-HNE or ACR, and in accordance with previously published methods published in isolated cortical mouse brain mitochondria.[50, 72] Concentrations of pargyline (PG) were based on molar equivalency with the most effective dose of PZ.

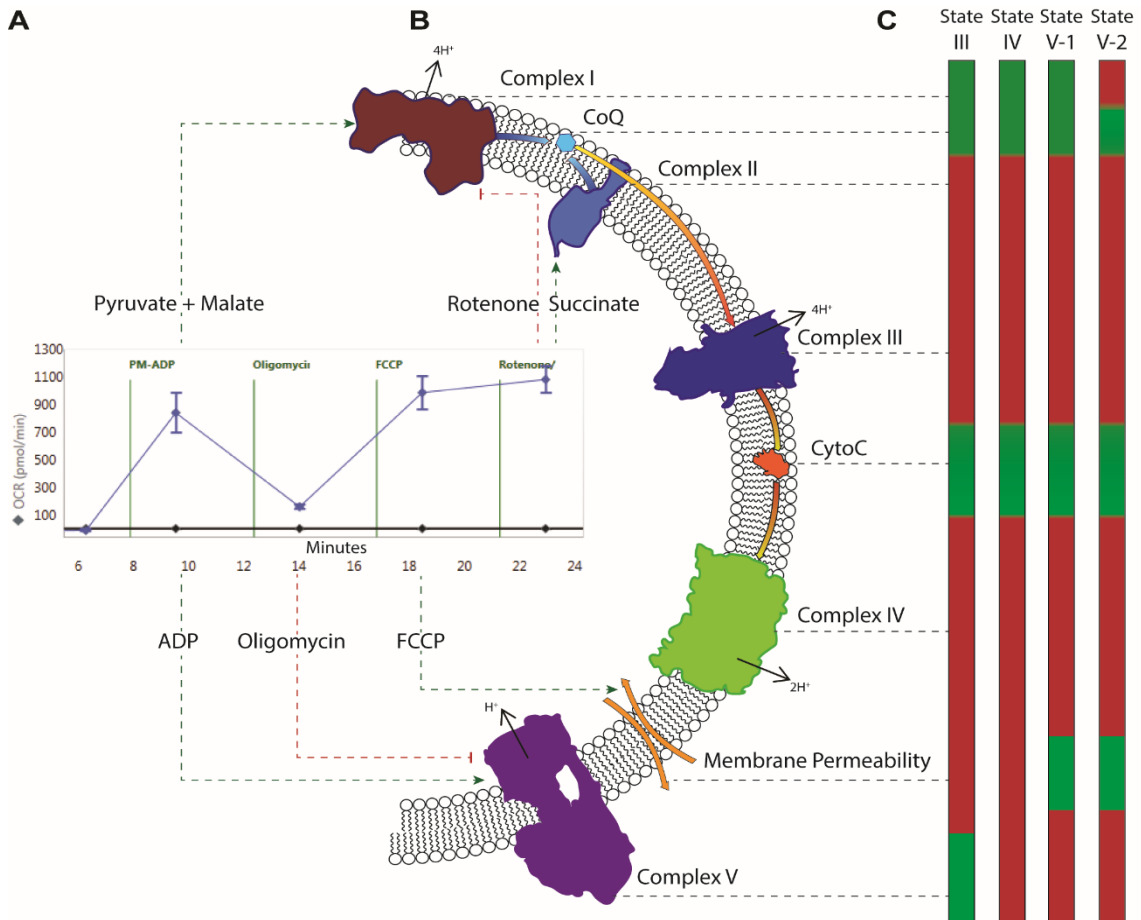


Figure 2.1. A) Typical oxymetric trace demonstrating mitochondrial bioenergetics as measured by oxygen consumption rate (y-axis). The addition of substrates to mitochondria is indicated along the x-axis. B) Illustration of the major components of mitochondrial electron transport chain (ETC). The addition and the effect of exogenous substrates on the ETC is indicated by green hashed arrows (activation) or blunt red arrows (inactivation). C) Vertical bars represent four different states of mitochondrial respiration. Hashed lines can be followed from the protein complexes to the vertical bars; activated complexes are green bars while inactive complexes are red bars. There are depicted two State V respiration states V-1 and V-2 which represent Complex I and Complex II-driven states, respectively. For example: at 14 minutes, oligomycin is added to the mitochondrial pool which inhibits (red blunt arrows) Complex V. Hashed lines emerging from Complex V depict that the complex is activated during State III respiration (green bars), but is deactivated in all other measured states (red bars).

2.6 Mitochondrial Calcium-Buffering

In order to determine the extent to which mitochondria can buffer calcium, mitochondria were isolated from injured rat brains as described above and in accordance with previously published methods [73, 124, 132, 133]. A spectrofluorometer (Shimadzu RF-5301) was used to measure extra mitochondrial Ca^{2+} . Mitochondria (100 μg) within the spectrofluorometer, were incubated in a cuvette at 37°C in a 2 mL solution containing respiration buffer (125 mmol/L KCl, 2 mmol/L MgCl_2 , 2.5 mmol/L KH_2PO_4 , 0.1% BSA, 20 mmol/L HEPES at pH 7.2) and 100nM Ca^{2+} -sensitive indicator Calcium Green 5 N (CaG5N) (Molecular Probes, Eugene, OR). CaG5N possesses an excitation wavelength at 506 nm and an emission wavelength at 532 nm, which is used to determine the point at which mitochondria can no longer sequester Ca^{2+} . The solution also contained 150 nM of tetramethyl rhodamine ethyl ester (TMRE) which is used to estimate the mitochondrial transmembrane potential ($\Delta\psi_m$).

Mitochondrial substrates were utilized to initiate respiration and were added in sequential order every minute starting with 5 mM pyruvate and 2.5 mM malate. At minute two 150 μM of ADP was added. At minute three 1 μM of oligomycin was added. At minute 5, a KD Scientific model 310 series infusion syringe pump (Holliston, MA) was used to infuse Ca^{2+} at a rate of 160nmol of Ca^{2+} per mg of mitochondrial protein per minute. Concentration of substrates and oligomycin inhibitor represent final concentrations.

Values reported in **Figure 5.9** were calculated based on the base-line CaG5N fluorescence readings before the infusion of calcium. Signal above 150% was considered the point at which mitochondria were unable to buffer calcium. This value was calculated by concentration of calcium infused (nmol/mg) prior to the point at which mitochondria

were 150 % above base-line. The value in the trace of **Figure 5.9** is the infusion rate of calcium per minute into the chamber divided by the amount of mitochondria in the chamber as measure previously by protein concentration assay: nmoles Ca^{2+} /mg protein/min [132].

2.7 Western Blot Analysis

2.7.1 Western Blot Analysis of Oxidative Damage Markers

In order to measure markers of oxidative damage (4-HNE and ACR) the following western blot analysis was used, which is in accordance with previously published methods [36, 134]. Mitochondrial samples assayed for 4-HNE adducts were separated on a precast gel (12% Bis-Tris w/v acrylamide; Criterion XT, Bio-Rad) with XT-MOPS buffer (Bio-Rad). Mitochondrial samples assayed for ACR adducts were separated on precast gel (4-12% gradient Tris-Acetate gels) using MOPS buffer (BioRad). Proteins separated on gel were transferred to nitrocellulose membranes with Semi-dry electrotransferring unit (BioRad) at 15 volts for 45 minutes at room temperature. Following transfer, membranes were blocked in 5.0% milk in TBS (Tris buffered solution; 20mM Tris HCl, 150 mM NaCl) for one hour at room temperature. Membranes were then incubated at 4⁰C overnight in primary 4-HNE or ACR antibody solution TBST (0.5mM Tween-20). 4-HNE rabbit polyclonal primary antibody (Alpha Diagnostics) was diluted 1:2,000. ACR mouse monoclonal antibody (Abcam, United States) was diluted at 1:1,000.

4-HNE and ACR primary antibodies were detected via 2 hour incubation at room temperature with goat rabbit immunoglobulin G (IgG) or anti-mouse IgG secondary antibody conjugated to infrared dye (1:5000, IRdye-800CW, Rockland) in TBST. Membranes were analyzed with LiCor Odyssey InfraRed Imaging System (Li-Cor

Biosciences, Lincoln, NE). 4-HNE and ACR protein smears were assessed from 150 kD to 50 kD and compared to single control group and expressed as percent of that group.

No primary controls for 4-HNE and acrolein have been provided in **Appendix B**.

2.7.2 Western Blot Analysis of Spectrin Degradation

The analysis of α -spectrin proteolysis by western blot analysis discussed below is in accordance with previously published manuscripts [36, 64, 65]. Cortical punch samples from rats as previously described were rapidly dissected on a glass stage chilled with ice and submerged in Triton lysis buffer (1% Triton, 20 mM Tris HCL, 150 mM NaCl, 5 mM EGTA, 10 mM EDTA, and 10% glycerol) which contained protease inhibitors (Complete Mini Protease Inhibitor Cocktail; Roche Diagnostics Corp., Indianapolis, IN). All samples were homogenized by sonication and centrifuged for 30 min (18,000 g at 4°C). The resulting supernatant was decanted and transferred to a new centrifuge tube; the pellet was discarded. Protein concentrations were determined using the BCA method described above. All samples were diluted to an optimal target concentration of 10 mg/mL. Samples were then separated on a 3-8% Tris-Acetate CriterionTM XT Precast gel (Bio-Rad, Hercules, CA). Proteins were then transferred from the gel to a nitrocellulose membrane with a semi-dry electro-transfer unit (Bio-Rad, Hercules, CA). Following transfer, membranes were blocked in 5.0% milk in TBS (Tris buffered solution; 20mM Tris HCl, 150 mM NaCl) for one hour at room temperature. Membranes were then incubated at 4°C overnight with primary mouse monoclonal anti-spectrin antibody (1:5000, Affiniti FG6090; Affiniti Biomol, Mamhead Castle, UK) in TBST (0.5mM Tween-20). The next

day, the membranes were washed in TBS-T solution three times for 10 minutes each. After wash, membranes were then probed for positive α -spectrin bands with a 1 hour incubation of secondary goat anti-mouse antibody (1:5000) conjugated to infrared dye (IRDye800CW, Rockland, Gilbertsville, PA). β -tubulin primary antibody (1:10,000) was incubated overnight, and probed with a goat anti-rabbit IgG secondary antibody conjugated to an infrared dye (1:10,000, A-21109, Alex Fluor; Invitrogen) after spectrin antibody probing. Membranes were quantified after scanning the membranes into the LI-COR Odyssey Infrared Imaging System (LI-COR Biosciences, Lincoln, NE). For every sample protein lane the 150 kDa and 145 kDa band was quantified by optical density in accordance with previously published methods [135], normalized β -tubulin, and expressed as percent of Untreated/ Sham control.

It is important to note that an alternative methodology of quantification and normalization of spectrin degradation does exist. This methodology quantifies by optical density, the proteolytic fragment bands of spectrin (145 kD or 150 kD) normalized to the intact actin band which is known as a poor calpain substrate. The pretense for this methodology is based, in part, as a means to overcome possibility of β -tubulin fragmentation which has been previously reported by calpain I and II [136]. As a result of possible proteolytic cleavage of β -tubulin, epitopes on β -tubulin could be altered in a means to change affinity or avidity of probing antibodies. Subsequent normalization of spectrin fragments with tubulin could potentially be skewed.

However, a limitation of the LI-COR Odyssey Infrared Imaging System (LI-COR Biosciences, Lincoln, NE) is in the quantification of drastically over exposed bands. If the

concentration of spectrin 280 kD band is beyond the detectable dynamic range of the imaging system, the band is inherently unquantifiable. Therefore, as a means to control for some spectrin 280kD samples representing overexposed banding, we have quantified based on β -tubulin normalization. β -tubulin normalization methodology is still consistent with recently published methodologies [64, 65, 135, 137]. Furthermore, for all western blots involving spectrin the optical density values of β -tubulin are exposed to the Grubbs' test for outliers (extreme studentized deviate); no β -tubulin values qualified as an outlier.

2.8 Mitochondrial Respiratory Control Ratio

For all mitochondrial respiration experiments untreated/ control animals were assessed for respiratory control ratio (RCR) and were determined to be above 5. The RCR can be used to determine how “coupled” mitochondria are e.g. coupled oxidative and phosphorylative mechanisms. General laboratory practices regard an RCR >5 to mean that mitochondrial membranes are “intact” after isolation procedures to still properly respire oxygen.

2.9 Tissue Processing and Histology

After 72 hours following TBI animals were anesthetized with an intraperitoneal overdose injection of pentobarbital (150 mg/kg) and transcardially perfused with 0.01 M phosphate buffer solution (PBS) followed by 4% paraformaldehyde (PFA) solution in 0.01 M PBS at pH 7.4. Brains were rapidly extracted and allowed to soak in 4% PFA. Brains

were removed after 24 hours and allowed to soak in 20% sucrose + PFA solution for an additional 24 hours. Tissue is rapidly frozen on the microtome platform at -20° for 10 minutes. A freezing microtome was used to cut coronal slices 40 μm thickness at a blade angle of 7.5° to the surface of the tissue. Sections were taken from the septal area (intra aural level 10.7) to the posterior hippocampus (intra aural level 0.3). Every tenth section was taken for mounting; a total of approximately 12 sections represented one brain.

Mounted sections were soaked in CHCl_3 (100mL) + EtOH (400mL of 95% EtOH) for 30 minutes. Then transferred to increasing concentrations of EtOH for dehydration (95%, 70%, 50%) for 3 minutes each then soaked in dH_2O for 3 minutes. Slides were then soaked in Nissl/ cresyl violet solution (5.64ml 1M acetic acid, 0.816g sodium acetate, 500ml dH_2O , and 0.2g cresyl violet powder [Sigma C1791]) for 5-10 minutes. Then slides were dipped 8 times in dH_2O , 50% EtOH, 70% EtOH, 95% EtOH + AcOH (500mL 95% EtOH + 12 drops of acetic acid), then 3 minutes in 95% EtOH, 5 minutes in 100% EtOH, 5 minutes in Citrisolv stock solution, then 5 minutes in a second batch of Citrisolv stock solution. Tissue on slides were lightly covered with permount and coverslipped.

Slides photographed under bright field microscope at $\times 1.25$. Tissue sparing across groups was processed utilizing ImageJ (NIH Bethesda, MD) software. Analysis of rat brains were blinded and employed the Cavalieri stereological protocol [138, 139]; the group for which each rat belonged (vehicle, PZ treatment type 1, or PZ treatment type 2) was unknown.

Each section was separated by a known distance (d), where d = mean section thickness multiplied by the number of sections between the sampled sections. The total

cortical area was measured by pixels and converted to mm². The total cortical area is defined as the dorsal aspect of lamina I to the dorsal aspect of the corpus callosum, and was measured for each hemisphere. Each area was multiplied by d to calculate a sub volume that when summed provided the respective total volume.

The volume of the ipsilateral hemisphere was compared to the contralateral hemisphere and expressed as percent of spared tissue (ipsilateral volume/ contralateral volume * 100) [50]. Ipsilateral to contralateral comparison provided effective means of measuring spared tissue without having to compensate for variability in tissue fixation or processing across different brains, and eliminated the need to euthanize 8 sham animals.

2.10 Statistical Analysis

2.10.1 Mitochondrial Respiration

In vitro results are calculated using Prism, GraphPad and expressed as means \pm SD. All experiments investigating mitochondrial respiration and oxidative damage *ex vivo* were analyzed by one-way analysis of variance (ANOVA), followed by Dunnet's post-hoc which allowed for multiple comparisons to a single control group. The exception was for experiments wherein multiple comparisons between groups were made, not to a single control group. Accordingly, it was necessary to analyze by one-way analysis of variance (ANOVA), followed by Student-Newman-Keuls multiple comparisons test (SNK). Additionally, SNK affords the advantage of testing multiple groups with more power

compared to Tukey's range test, where power is defined as the means to correctly reject the null hypothesis [140].

2.10.2 Calcium Buffering

Values of calcium buffering were computed as nmoles Ca^{2+} / mg mitochondrial protein / min for each measured sample. Groups were compared by one-way analysis of variance (ANOVA), followed by Student-Newman-Keuls multiple comparisons test (SNK). In all cases statistical significance was determined as $p < 0.05$.

2.10.3 Spectrin Degradation

As previously described every sample protein lane the 150 kDa and 145 kDa band was quantified by optical density in accordance with previously published methods [135], normalized β -tubulin, and expressed as percent control. Groups were compared by one-way analysis of variance (ANOVA), followed by Student-Newman-Keuls multiple comparisons test (SNK). In all cases statistical significance was determined as $p < 0.05$.

2.10.4 Histology

Total volume of spared tissue was measured blinded then calculated as percent volume spared as described above. Percentage of spared tissue for each rat within a single group was averaged and compared to other groups by one-way analysis of variance (ANOVA), followed by Student-Newman-Keuls multiple comparisons test (SNK). In all cases statistical significance was determined as $p < 0.05$.

Chapter 3

Dissertation Research Approach

3.1 Hypothesis

The hypothesis of this dissertation is that carbonyl scavenging with phenelzine (PZ) will exert an antioxidant neuroprotective effect in the traumatically injured rat brain mechanistically related to PZ's hydrazine moiety reacting with the lipid peroxidation (LP)-derived reactive aldehydes 4-hydroxynonenal (4-HNE) and acrolein (ACR).

3.2 Aim 1

Assess the ability of the carbonyl scavenger PZ to protect uninjured, isolated rat brain mitochondria from *ex vivo* exposure to the deleterious, LP-derived reactive aldehydes 4-HNE and ACR.

3.2.1 Aim 1 Rationale

Following traumatic brain injury (TBI) the generation of excessive free radicals initiates lipid peroxidation (LP) cascades. A result of LP is the creation and accumulation of LP breakdown products such as 4-HNE and ACR. 4-HNE and ACR are known neurotoxins capable of covalently binding to mitochondria and cellular protein targets via aldehydic, carbonyl functional groups.[75, 76] Given the nature of the rapidly reacting and

short-lived free radical, targeting and scavenging reactive aldehydes such as 4-HNE and ACR may be a more feasible approach for achieving pharmacological antioxidant neuroprotective intervention or provide a useful adjunct to traditional lipid peroxyl radical (LOO•) scavengers to provide a multi-mechanistic approach for stopping the posttraumatic lipid peroxidation process at multiple points.

As for the consideration of PZ, this compound possesses several advantages. Primarily, PZ possesses a hydrazine functional group (NH-NH₂). The hydrazine functional group (i.e. moiety), covalently binds carbonyl-containing compounds like 4-HNE and ACR.[116, 141, 142] Reports of *in vitro* cell cultures indicate that hydrazine-containing compounds are able to inhibit carbonyl cytotoxicity.[116, 118, 122, 143] Furthermore, PZ is reported to function as a neuroprotective agent by reducing aldehydic toxicity in focal and global ischemia-reperfusion stroke models.[122]

The investigation of mitochondrial respiratory functionality endpoint was chosen based on previously published reports that 4-HNE, and more potently, ACR inhibit mitochondrial functionality.[67]

In vivo experiments detailed in Aims 2 and 3 utilized isolated mitochondria which were from the same anatomical site of a controlled cortical impact (CCI)-induced TBI, but in uninjured “Sham” animals.

3.2.2 Experiment 1, Aim 1

4-HNE & ACR Dose Response

Our intent was to determine sub-optimal concentrations of 4-HNE or ACR to significantly, but not completely, inhibit mitochondrial function. Cerebral cortical mitochondria were isolated from uninjured, young adult rats and incubated for 10 minutes with increasing concentrations of 4-HNE or ACR in a dose-dependent manner. Mitochondrial function, and/or disruption thereof, was measured by the mitochondria's ability to respire oxygen using the Seahorse Biosciences XF24e Extracellular Flux Analyzer. Data were expressed in terms of Complex I and Complex II-driven respiration rates and compared to untreated mitochondria.

Table 3.1 Aim 1, Experiment 1; 4-HNE and ACR Dose Response

Aim 1 , Experiment 1			
4-HNE or ACR Dose-Response			
4-HNE		ACR	
Untreated	n = 4	Untreated	n = 4
10 μ M	n = 4	1 μ M	n = 4
30 μ M	n = 4	3 μ M	n = 4
100 μ M	n = 4	10 μ M	n = 4
Total	n=16	Total	n=16

Corresponds to **Figure 4.1**

Rationale

In order to determine the ability to PZ to protect mitochondria, it was necessary to first investigate which concentrations of 4-HNE or ACR are necessary to elicit *ex vivo* mitochondrial respiratory dysfunction. The tested concentrations of 4-HNE and ACR were broadly based on previously published concentrations of 4-HNE and ACR to significantly inhibit isolated mitochondria from rat brain and spinal cord[68] and the observation that ACR is ten times more potent than 4-HNE in regards to attenuation of isolated brain mitochondrial respiratory function.[72] It is important to note that no documented cases exist demonstrating PZ resurrecting dead mitochondria. Therefore, it was imperative to determine the “sub-optimal dose” of 4-HNE or ACR that significantly reduced mitochondrial function, but does not lead to their complete demise.

Unpublished pilot studies previously generated by our lab justified the 10 minute incubation wherein mitochondria were exposed to 4-HNE or ACR. This was used as the standard for all experiments wherein reactive carbonyls are exogenously exposed to mitochondria prior to oxymetric studies utilizing the Seahorse Bioscience XF24e Extracellular Flux Analyzer. Mitochondrial oxymetric studies performed by the Seahorse Analyzer and traditional Clarke electrode-based Oxytherm provide information that can be used to interpret multiple states of respiration.

3.2.3 Experiment 2, Aim 1

Phenelzine Dose Response.

Determine the most effective dose of PZ to prevent mitochondrial dysfunction by scavenging reactive aldehydes. Isolated mitochondria were exposed to a 5 minute dose-dependent pretreatment of PZ, followed by a 10 minute incubation with 4-HNE or ACR. Protective efficacy was determined by PZ's ability to prevent 4-HNE or ACR-induced mitochondrial respiratory dysfunction and PZ's ability to reduce markers of protein modification by the aldehydes as measured by western blot. Mitochondrial respiration was expressed in a similar manner as Experiment 1, but protection is compared to mitochondria treated by 4-HNE or ACR only. Phenelzine's ability to reduce markers of oxidative damage (4-HNE or ACR) is also compared to mitochondria treated with 4-HNE or ACR.

Table 3.2 Aim 1, Experiment 2; PZ Dose Response.

Aim 1 , Experiment 2			
PZ Dose Response			
4-HNE		ACR	
Untreated	n = 4	Untreated	n = 4
4-HNE 30 μ M	n = 4	ACR 3 μ M	n = 4
4-HNE 30 μ M + PZ 3 μ M	n = 4	ACR 3 μ M + PZ 3 μ M	n = 4
4-HNE 30 μ M + PZ 10 μ M	n = 4	ACR 3 μ M + PZ 10 μ M	n = 4
4-HNE 30 μ M + PZ 100 μ M	n = 4	ACR 3 μ M + PZ 100 μ M	n = 4
Total	20	Total	20

Corresponds to **Figure 4.2** (Respiration) and **Figure 4.4** (Oxidative Damage).

Rationale

The concentrations listed in the table at the time of experimentation were originally written as “sub-optimal concentration of 4-HNE or ACR,” which is data gleaned from Aim 1, Experiment 1. However, for the sake of continuity, the optimal dose of 4-HNE (30 μ M) and ACR (3 μ M) are listed in the table as discovered from experimentation.

The dose-response concentrations of PZ used to protect rat mitochondria from 4-HNE are broadly based on previously published experiments wherein equi-molar concentrations of PZ to 4-HNE were found to protect mice mitochondria *in vitro*. [144] PZ dose-response concentrations to protect mitochondrial from ACR insult were the same concentrations used as 4-HNE. However, ACR is approximately ten times more potent and the concentration was adjusted as in the previous experiment.

The rationalization of pre-incubation of PZ to mitochondria before exposure to ACR or phenelzine is entirely a proof of principle concept. The intent of the experiment is to determine if PZ can scavenge reactive carbonyls at a known concentration. Other experiments test this idea, under the complex pathophysiology of TBI.

The endpoints of mitochondrial respiration and markers of oxidative damage are used as an index of both mitochondrial function and an indication of the physical presence of deleterious 4-HNE- or ACR-protein adducts.

3.2.4 Experiment 3, Aim 1

Phenelzine (PZ) versus Pargyline (PG)

Investigate the mechanism by which PZ may be able to protect mitochondrial dysfunction and prevent oxidative damage. Isolated mitochondria were exposed to a 5 minute pretreatment with the hydrazine-containing MAO inhibitor PZ or the structurally similar MAO inhibitor PG which lacks the hydrazine moiety, followed by a 10 minute incubation of 4-HNE or ACR. Sub-optimal doses for 4-HNE and ACR defined in Experiment 1 were used. Isolated mitochondria from a single rat brain represents n=1. Each pool consisted of enough mitochondria to be divided into two groups. The first group was tested with 4-HNE and the second group was tested with ACR. Optimal dose of PZ defined in Experiment 2 was used for PZ and PG. Protective efficacy was determined by PZ's or PG ability to prevent 4-HNE or ACR-induced mitochondrial respiratory dysfunction. The ability to reduce oxidative damage was also determined for both compounds and assessed by western blot.

Table 3.3 Aim 1, Experiment 3; PZ vs PG.

Aim 1 , Experiment 3			
PZ v PG			
4-HNE		ACR	
Untreated	n = 6	Untreated	n = 6
4-HNE 30 μ M	n = 6	ACR 3 μ M	n = 6
PZ 30 μ M + 4-HNE 30 μ M	n = 6	PZ 30 μ M + ACR 3 μ M	n = 6
PG 30 μ M + 4-HNE 30 μ M	n = 6	PG 30 μ M + ACR 3 μ M	n = 6
Total	24	Total	24

Corresponds to **Figure 4.3** (Respiration) and **Figure 4.5** (Oxidative Damage).

Rationale

Phenelzine is an MAO inhibitor that possesses a hydrazine pharmacophore which is capable of covalently binding to carbonyl functional groups [116]. It is through this means we believe that PZ is able to scavenge deleterious carbonyls. However, PZ could provide mitochondrial protection by simply providing steric hindrance between reactive carbonyls and mitochondrial proteins. Therefore, it is advantageous to determine if another structurally similar compound PG, which does not contain the hydrazine moiety, can provide mitochondrial protection against 4-HNE or ACR.

Pargyline and PZ are structurally similar, have similar molecular weights, and both are MAO-I (**See Figure 3.1**). Therefore, the optimal concentration of PZ determined by experimentation was the same molar concentration used to test PG.

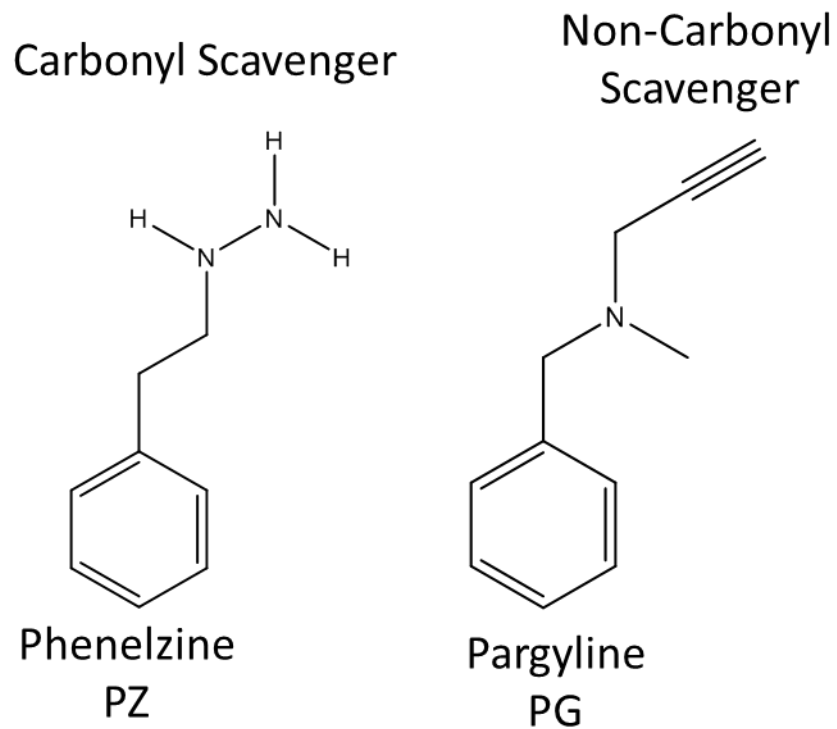


Figure 3.1. Structural differences between phenelzine (PZ) and pargyline (PG). Both compounds are monoamine oxidase inhibitors. PZ possesses a hydrazine moiety (HN-NH₂) functional group whereas PG possesses a propyne (H₃C≡CH) functional group.

3.3. Aim 2

Determine the ability of the carbonyl scavenger PZ to protect mitochondria after a controlled cortical impact induced traumatic brain injury in young, adult rats.

3.3.1 Aim 2 Rationale

Exogenous application of TBI-derived deleterious compounds to isolated mitochondria is a proof of principle *ex vivo* assay. In order to determine if PZ possess the ability to protect mitochondria in the wake of the complex pathophysiology of TBI, PZ was evaluated in this environment.

This Aim seeks to determine if PZ is capable of protecting mitochondrial respiratory function, reducing the endogenous accumulation of 4-HNE and ACR and maintaining mitochondrial Ca⁺⁺ buffering capacity after TBI *in vivo*.

3.3.2 Experiment 1, Aim 2

In Vivo PZ Protection of Mitochondrial Respiration.

Determine the ability of PZ to protect mitochondrial respiratory function 72 hours after a CCI-TBI. Rats will receive a severe TBI followed by a 15 minute post-injury dose of PZ 10 mg/kg SubQ, followed by subsequent doses of PZ at 5 mg/kg every 12 hours up to 72 hours. Extent of protection is determined by the PZ ability to protect mitochondrial respiration. Mitochondria were isolated from the cortical injury site 72 hours after injury.

Data is expressed in terms of State III / State IV respiration i.e. the respiratory control ratio (RCR).

Table 3.4 Aim 2, Experiment 1 *In vivo* Mitochondrial Respiration

Aim 2, Experiment 1	
<i>In vivo</i> mitochondrial respiration	
Sham	n = 5-6
Sham + PZ (10 mg/kg)	n = 5-6
TBI + Vehicle	n = 8-9
TBI + PZ (10 mg/kg)	n = 8-9
Total	26-30

Rationale

In this experiment the dosing of PZ is modified to include “maintenance dosing.” Previous publications by our lab used a single 10 mg/kg subcutaneous dose 15 minutes after injury[144]. This is a slight reduction of the dosing paradigm which has been previously reported for neuroprotection studies performed in gerbils [122]. However, this was intentionally reduced to minimize the monoamine oxidase inhibitory (MAOI) effects of phenelzine in rats [145]. The inclusion of the repeated maintenance dosing paradigm of intended to overlap the time course peak accumulation carbonyls which peak at 72 hours post-TBI [72]. The administration of PZ every 12 hours is intended to match the 11.6 hour blood serum half-life of PZ in rats, published by the original manufacture Pfizer under the drug name Nardil © [146]. Additional support for the 12 hour repeated dosing paradigm is derived from a study in which a single dose of PZ (15 mg/kg, subcutaneously) was able to increase brain ornithine levels after prior monoamine oxidase inhibition but PZ’s effects were only effective for approximately 12 hours after administration [147].

Previous work indicates that after spinal cord injury the accumulation of 4-HNE and ACR peaks at 48-72 hours[45]. Therefore, in order to provide the maximum opportunity for PZ to scavenge 4-HNE and ACR, we administer PZ 15 minutes post-TBI and every 12 hours until 72 hours to maintain theoretical concentration at 10 mg/kg.

The choice of *ex vivo* oxymetric analysis is the Oxytherm, a traditional Clarke-type electrode system chosen primarily for consistency with our other recently published *in vivo* experiments published in our lab [144].

3.3.4 *Experiment 2, Aim 2*

In vivo PZ Protection of Mitochondrial Oxidative Damage.

Determine the ability of PZ to protect mitochondria by decreasing 4-HNE or ACR markers of oxidative damage 72 hours after injury. Rats exposed to a severe CCI-TBI will receive the same PZ 10 mg/kg dosing paradigm from Experiment 2. Western blot quantification will be used to analyze the accumulation of lipid peroxidative markers 4-HNE or ACR, in mitochondrial proteins isolated from the injury.

Table 3.5 Aim 2, Experiment 2

Aim 2, Experiment 2	
<i>In vivo</i> mitochondrial oxidative damage	
Sham	n = 5-6
Sham + PZ (10 mg/kg)	n = 5-6
TBI + Vehicle	n = 8-9
TBI + PZ (10 mg/kg)	n = 8-9
Total	32

In vivo Mitochondrial Oxidative Damage

Rationale

This experiment is designed to determine if PZ possesses the same capabilities of scavenging carbonyls and protecting mitochondria from the accumulation of oxidative damage markers *in vivo* as demonstrated *ex vivo*.

3.3.5 Experiment 3, Aim 2

In Vivo PZ Protection of Mitochondrial Ca²⁺ Buffering

Assess the ability of PZ to protect mitochondria against TBI-induced Ca²⁺ buffering dysfunction. Rats exposed to a severe CCI-TBI will receive PZ 10 mg/kg 15 minutes after injury, and 5 mg/kg every 12 hours, up to 24 hours. At 24 hours, rats will be euthanized, mitochondria isolated, and assessed for the ability to buffer calcium.

Table 3.6 Aim 2, Experiment 3; Mitochondrial Calcium Buffering

Aim 2, Experiment 3	
<i>Mitochondrial Calcium Buffering</i>	
Sham	n = 8-9
Vehicle	n = 8-9
TBI + PZ (10 mg/kg)	n = 8-9
Total:	24

Rationale

Mitochondria attempt to compensate for the large influx of Ca^{2+} after TBI by taking up (i.e. buffering) the excess cytoplasmic Ca^{2+} . However, excessive cycling and loading of Ca^{2+} can induce mitochondrial permeability transition (mPT) [102]. The formation of the mPT facilitates the loss of the mitochondrial membrane potential ($\Delta\psi$) which exacerbates ROS formation, increases lipid peroxidation, release of the Ca^{2+} and initiates apoptotic cellular death pathways [104, 105].

This experiment is designed to assess the ability of mitochondrial to buffer calcium after TBI. Dysfunctional mitochondria have a reduced ability to buffer this calcium influx [108, 110]. Previous reports demonstrate that mitochondria exhibit significantly diminished Ca^{2+} buffering capacity at 3 and 12 hours following CCI-TBI in the mouse. Additionally, subsequent to the loss of Ca^{2+} homeostasis, calcium sensitive cysteine proteases begin to degrade spectrin as early as 15 min after injury[148] and have been reported to remain active for at least 24 hours[149]. Therefore, in the present experiment we chose to examine whether PZ can protect the ability of mitochondria to buffer Ca^{2+} 24 hours after CCI-TBI in the rat. The 24 hour window is consistent with previously published reports indicating that time point is within an optimal window of therapeutic treatment [108].

3.4.1 Aim 3

Determine the extent to which PZ is able to provide neuroprotection in rats following a CCI TBI.

3.4.2 Aim 3 Rationale

PZ has previously demonstrated the ability to spare cortical tissue in rats. These experiments utilized a single SubQ injection of PZ 10 mg/kg 15 minutes after a severe TBI and were assessed for cortical sparing two weeks after injury. PZ treated rats demonstrated a significant increase in cortical tissue compared to vehicle (saline)-treated animals [144].

This aim is to determine if the ability of PZ in the current dosing paradigm (which has an added maintenance dosing aspect: single bolus 10 mg/kg dose followed by a maintenance dose of 5mg/kg every 12 hours) is capable of sparing cortical tissue as the previously published single dose study. Additionally, this aim seeks to determine if the PZ has a clinically relevant therapeutic window.

3.4.4 Experiment 1, Aim 3

In Vivo Therapeutic Window

Determine the maximum therapeutic window of PZ to function as a neuroprotective agent. Neuroprotection will be determined by PZ_m's ability to prevent cortical cytoskeletal

degradation by immunoblotting of spectrin degradation products after a CCI-TBI in young, adult rats. Rats will be given the PZ_m dosing paradigm (which contains maintenance dosing for 72 hours).

Rats will be given a single subcutaneous dose of PZ (10 mg/kg) at *X* time after injury followed by an additional dose of 5 mg/kg every 12 hours for 72 hours. At 72 hours rats will be euthanized and cortical tissue will be harvested, processed, and analyzed for cytoskeletal degradation e.g. spectrin breakdown products (SBDP). Where, *X* = the length of time PZ_m treatment will be delayed: 15 minutes, 3 hours, 6 hour, 12 hours, or 18 hours. All delayed time points will utilized the same PZ_m dosing paradigm as histological sparing with the same number of doses. This dosing paradigm is consistent with the dosing paradigm intended to theoretically maximize the ability of PZ to scavenge reactive carbonyls.

Table 3.8 Aim 3, Experiment 1; *In Vivo* neuroprotection; therapeutic window

Aim 3, Experiment 1					
<i>In vivo</i> Therapeutic Window					
<i>Treatment</i>	<i>15 min</i>	<i>3 hrs</i>	<i>6 hrs*</i>	<i>12 hrs*</i>	<i>18 hrs*</i>
Sham	n = 8	n = 8	n = 8	n = 8	n = 8
Vehicle	n = 8	n = 8	n = 8	n = 8	n = 8
PZ (10 mg/kg)	n = 8	n = 8	n = 8	n = 8	n = 8
Total:	24	24	24	24	24

**Time points: 6hrs, 12hrs, and 18hrs were discontinued.*

Rationale

This experiment was intended to address to the maximum delay of treatment that the PZ_m treatment can be delayed after injury and still have a clinically relevant therapeutic window. The assessment of spectrin degradation was chosen as it is reliable marker of TBI damage and reported to have a rapid onset after TBI [150].

As described in **Chapter 1**, the connection between mitochondrial dysfunction and calpain activation leads to the proteolytic cleavage of spectrin. And, given the rapid onset of degradation, ability of PZ to increase calcium buffering, and increase histological sparing, the spectrin degradation is theoretically a viable assay to determine therapeutic value.

Should it become evident that PZ_m is no longer able to reduce spectrin degradation, the last time point to significantly reduce spectrin degradation will designate maximum post-TBI time point that initiation of PZ treatment could be delayed (i.e therapeutic window).

3.4.3 Experiment 2, Aim 3

Histological Neuroprotection

Investigate the ability of PZ to spare cortical tissue following a CCI-TBI in young adult rats. Rats will receive a unilateral severe CCI-TBI, followed by either a single 10mg/kg PZ treatment 15 minutes after injury (PZ_s) or multiple doses of PZ (PZ_m). Extent

of histological neuroprotection will be determined at 72 hours post-injury, by the ability of PZ_s or PZ_m to increase spared cortical tissue, compared to vehicle-only treated rats.

Table 3.7 Aim 3, Experiment 2; *In Vivo* neuroprotection, Tissue Sparing

Aim 3, Experiment 2	
<i>In vivo</i> neuroprotection; tissue sparing	
Vehicle	n = 8
PZ _m	n = 8
PZ _s	n = 8
Total:	24

- **PZ_m** =10 mg/kg, 15 minutes after injury, then 5 mg/kg every 12 hours.
- **PZ_s** = 10 mg/kg, 15 minutes after injury, not maintenance dosing.

Rationale

This experiment will serve as a means to investigate the ability of PZ to spare cortical brain tissue. The PZ_m dosing paradigm is intended to maximize the scavenging of carbonyls which peak at 72 hours. This effort requires an additional “maintenance” aspect of the original dosing paradigm PZ_s which was published with a limited sample size ($n = 4$) [144]. Therefore, this experiment will serve two purposes: 1) expand sample size (n) of the previously published and 2) differentiate the ability of the two dosing paradigms to protect cortical brain tissue. The 72 hour time point was chosen to determine the effects of a completed PZ_m dosing regimen versus a single PZ_s treatment regimen. Furthermore, this time point would help to understand how much cortical tissue is preserved at an earlier time point.

Chapter 4

Phenelzine protects brain mitochondrial respiratory function from oxidative damage by scavenging the lipid peroxidation-derived reactive carbonyls 4-hydroxynonenal and acrolein

(Portions submitted for publication)

4.1 Specific Aim

Assess the ability of the carbonyl scavenger PZ to protect uninjured, isolated rat brain mitochondria from *ex vivo* exposure to the deleterious, LP-derived reactive aldehydes 4-HNE and ACR.

4.2 Introduction

A crucial component to keeping the neuron alive after traumatic brain injury is to stabilize mitochondrial function. And, the most definitive way to protect mitochondrial dysfunction is to prevent either free radical production or the subsequent LP cascade. For many years, researchers have explored the possibility of pharmacological compounds to scavenge free radicals or interrupt LP cascades. In particular, tirilazad during a phase III clinical trial was capable of scavenging lipid peroxyl radicals (LOO•) during the “propagation” phase of the cascade [68]. However, a timely pharmacological intervention by a LOO• scavengers is limited by the narrow therapeutic window intrinsic to rapidly reacting lipid peroxyl radicals. Additionally, LOO• scavengers only interrupt LP cascades;

they are not capable of reversing it. Fortunately, an alternative means exist to prevent free radical-induced LP by targeting the latest stage of the cascade: the generation of the aldehydic breakdown-products. Scavengers that target the deleterious breakdown products i.e. reactive carbonyls (4-HNE and ACR) are adeptly known as “carbonyl scavengers.” The use of carbonyl scavengers may have the potential to expand the clinical therapeutic window and possibly to reverse LP-mediated damage.

But, not all scavengers are equal. The most effective carbonyl scavengers are capable of covalently binding carbonyls via a hydrazine functional group (-NH-NH₂) [116, 141, 151]. The most ideal scavengers would be those already possessing FDA-approval for clinical use. Two such available compounds are hydralazine (HZ) and phenelzine (PZ). HZ is used generally to treat hypertension as a potent arterial vasodilator while PZ has been used in a variety of conditions, primarily as a monoamine oxidase inhibitor (MAO-I) for the treatment of depression. Regardless, both compounds possess a hydrazine moiety and have demonstrated the ability to inhibit carbonyl toxicity within cell culture models [116, 118, 122, 143]. Additionally, HZ and PZ have both been shown to exhibit neuroprotective effects in multiple models of neurotrauma. HZ was demonstrated to function as neuroprotectant in the context of spinal cord injury (SCI) while simultaneously reducing acrolein accumulation[117].

On the other hand, PZ has was reported as a neuroprotectant in focal and global ischemia-reperfusion models of stroke, and similarly reduced a deleterious “aldehyde load” [122]. While both HZ and PZ seem as equally promising candidates for carbonyl scavenging in the treatment of TBI, HZ is contra-indicated as its ability to induce hypotension which may already exist in patients who have sustained a TBI.

Therefore, the intent of this study is to demonstrate that the most clinically relevant drug, PZ is able to protect mitochondrial dysfunction as measured by oxythermic respiration and oxidative damage markers. Additionally, we investigate the importance of the hydrazine functional group by which PZ is believed to be capable of scavenging reactive carbonyls. While our lab has previously demonstrated the ability of 4-HNE to inhibit mitochondrial respiration and subsequently PZ's ability to prevent oxidative damage [50], the current studies have never been conducted in the high-throughput assay utilizing the Seahorse XFe24 analyzer. In the present study, we conducted experiments to determine the dose-response relationship for antagonism of 4-HNE and ACR by comparing the mitochondrial protective effects of PZ, which contains the hydrazine group, against the structurally similar compound PG, which lacks the hydrazine group. Moreover, since both compounds are MAO inhibitors, the comparison of the two allows for a determination of whether MAO inhibition might contribute to the protective effects of PZ.

4.3 Results

4.3.1 4-HNE and Acrolein Inhibit Brain Mitochondrial Respiration

Ficoll-isolated cortical mitochondrial bioenergetics were assessed using Seahorse XFe24 analyzer 10 minutes post-exposure to 4-HNE and ACR. As depicted in **Figure 4.1**, *ex-vivo* isolated mitochondria exposed to a 5 minute PZ pretreatment followed by 10 minute exposure to increasing concentrations of **(A-B)** 4-HNE 10 μ M, 30 μ M, 100 μ M or **(C-D)** ACR 1 μ M, 3 μ M, 10 μ M inhibited mitochondrial respiration in a significant, dose-dependent manner for complex I and complex II-driven OCR. For mitochondria exposed

to 4-HNE, only 30 μM and 100 μM concentrations significantly inhibited complex I and II-driven OCR ($p < 0.05$). 4-HNE at 30 μM was deemed a sub-optimal concentration to reduce, but not completely inhibit of mitochondrial respiration for both complex I & II. However, ACR was able to significantly reduce complex I and II respiration at all tested concentrations compared to controls: 1 μM , 3 μM , 10 μM ($p < 0.05$). ACR at 3 μM was deemed sub-optimal. Suboptimal concentrations of ACR (3 μM) were found to be approximately ten fold more potent than 4-HNE (30 μM) to inhibit mitochondrial complex I and complex II OCRs.

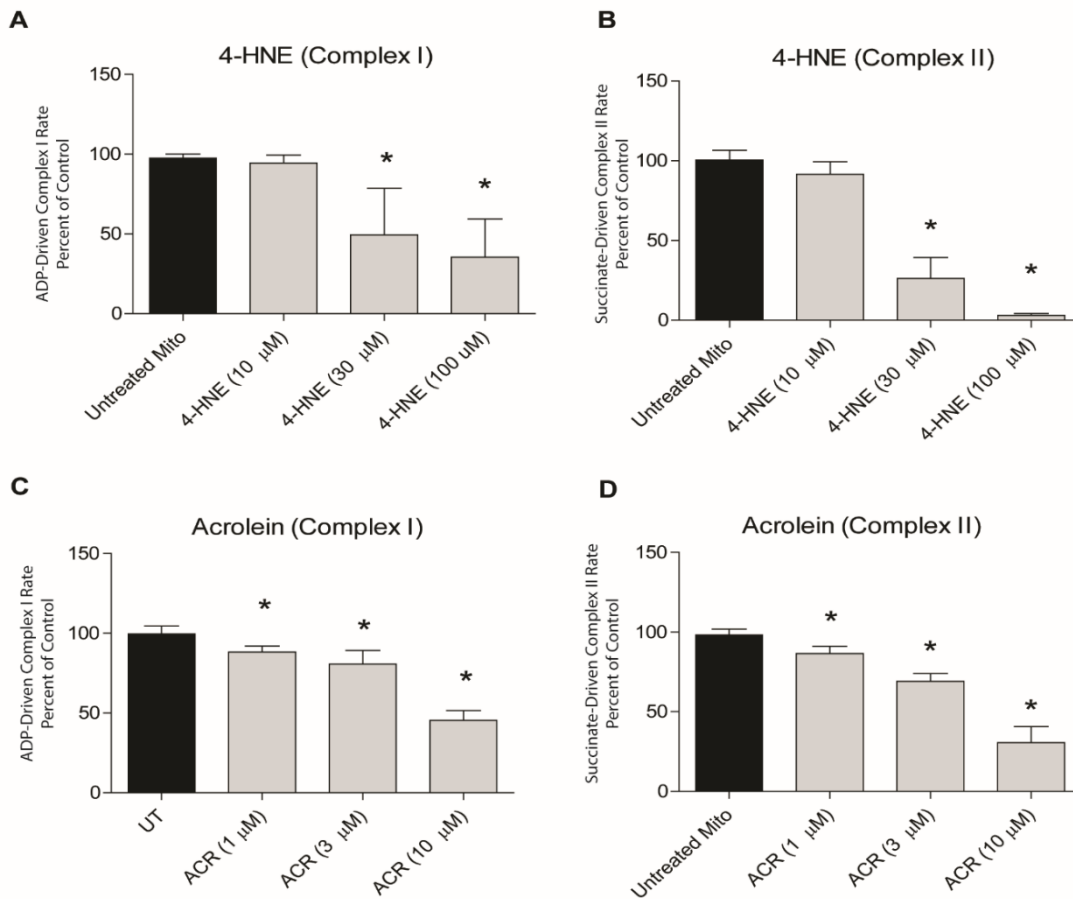


Figure 4.1 4-hydroxynonanal (4-HNE) and Acrolein (ACR) reduce Complex I and Complex II driven respiration in a dose dependent fashion in cortical mitochondria isolated from young adult, uninjured SD rats. Isolated mitochondria were exposed to increasing concentrations of 4-HNE for 10 minutes at room temperature and immediately assessed for oxygen consumption rates. 4-HNE at 30 μ M and 100 μ M significantly inhibited both Complex I and Complex II driven respiration. ACR at all tested concentrations 1, 3, and 10 μ M was able to significantly inhibit mitochondrial respiration. One-way ANOVA followed by Dunnett's Multiple Comparison post-hoc test. * = $p < 0.05$. Error bars represent +/- SD. N = 4 rats per group.

4.3.2 Phenelzine Protects Against 4-HNE or ACR-Induced Mitochondrial dysfunction in a Concentration -Dependent Fashion

The Seahorse XFe24 analyzer was used to determine the ability of PZ to protect cortical, isolated mitochondrial OCR exposed for 10 minutes to 4-HNE [30 μ M] or ACR [3 μ M] (**Figure 4.2**). Concentrations of 4-HNE and ACR were chosen based on previous experiments (**Figure 4.1**). Mitochondria were incubated with a 5 minute pretreatment of increasing concentrations of PZ (3 μ M, 10 μ M, 30 μ M) then incubated with a 10 minute treatment of 4-HNE or ACR. Mitochondrial OCR rates are reported for complex I and complex II. For mitochondria exposed to 4-HNE, significant protection was observed in complex I-driven OCR with 10 μ M and 30 μ M concentrations of PZ ($p < 0.05$) (**Figure 4.2a**). As for 4-HNE insulted mitochondria, complex II-driven OCR was only significantly protected by the maximum tested PZ concentration: 30 μ M ($p < 0.05$) (**Figure 4.2b**). In similar experiments, PZ, only at the maximum dose tested (30 μ M) was able to significantly protect ACR-insulted mitochondria for both complex I and II driven OCRs ($p < 0.05$). (**Figure 4.2 c, b**).

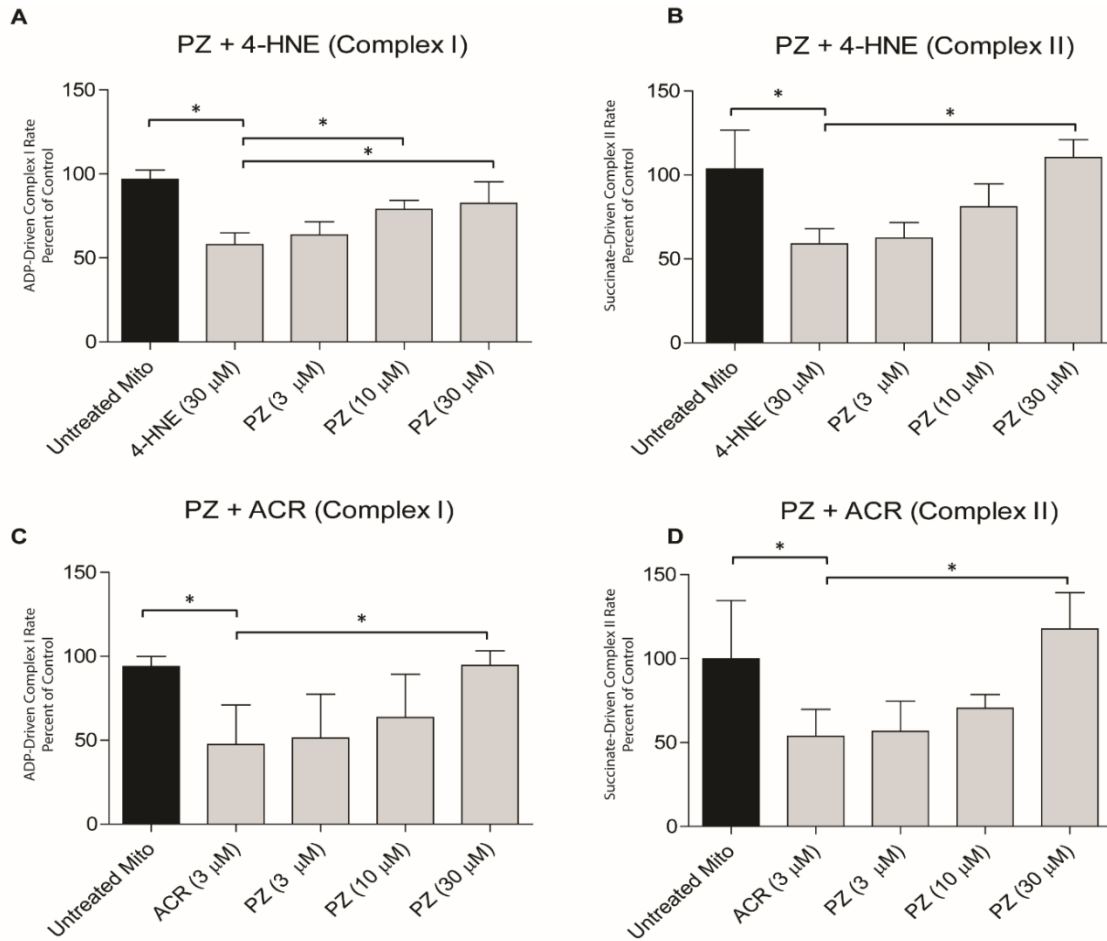


Figure 4.2. Isolated mitochondria were exposed to a 5 min phenelzine (PZ) pretreatment, followed by a 10 min incubation of 4-hydroxynonenal (4-HNE) and Acrolein (ACR) and immediately assayed for oxygen consumption rates. PZ pretreatment was able to protect mitochondrial respiration in a dose dependent manner. **A)** PZ at 10 μM and 30 μM was able to significantly protect mitochondrial function against an insult of 4-HNE at 30 μM for Complex I driven respiration. **B)** PZ was also able to significantly protect Complex II-driven respiration from a 30 μM insult of 4-HNE. **C & D)** PZ at 30 μM was able to significantly protect Complex I and Complex II-driven respiration from 3 μM ACR. One-way ANOVA followed by Dunnett's Multiple Comparison post-hoc test. * = $p < 0.05$. Error bars represent \pm SD. N = 4 rats per group.

4.3.3 Phenelzine, but not Pargyline, Protects Against 4-HNE and ACR-Induced Mitochondrial Dysfunction

The comparative abilities of PZ or PG to prevent mitochondrial dysfunction was assessed with Seahorse XFe24 analyzer (**Figure 4.3**). Concentrations of 4-HNE [30 μ M] or ACR [3 μ M] were chosen based on their demonstrated efficacy to significantly inhibit mitochondrial OCR (**Figure 4.1**). Similarly, the concentration of PZ [30 μ M] was chosen based previous experiments demonstrating significant prevention of mitochondrial dysfunction (**Figure 4.2**). With these conditions established, isolated cortical mitochondria were treated with either a PZ or PG pretreatment for 5 minutes, followed by ACR or 4-HNE exposure for 10 minutes. Mitochondrial OCR was expressed as percent control for ADP or succinate-driven respiration rates e.g. complex I and complex II, respectively. Mitochondria exposed to 4-HNE [30 μ M] or ACR [3 μ M] significantly ($p < 0.05$) inhibited complex I (ADP) and complex II (succinate) driven OCR compared to untreated controls (**Figure 4.3**). However, mitochondria exposed to PZ [30 μ M] pretreatment significantly prevented 4-HNE or ACR-induced mitochondrial OCR for both tested complexes ($p < 0.05$). No significant difference was found between PZ-protected mitochondria and untreated controls. In the same experiment, mitochondria were instead pretreated with an analogue compound pargyline [30 μ M] followed by 4-HNE or ACR insult. Pargyline possesses a similar structure to PZ and also serves as a MAO inhibitor, but lacks a hydrazine moiety functional group. Consistent with the hypothesized importance of the hydrazine functional group in carbonyl scavenging, PG treated mitochondria demonstrated no significant protection and no difference between 4-HNE or ACR only insulted mitochondria.

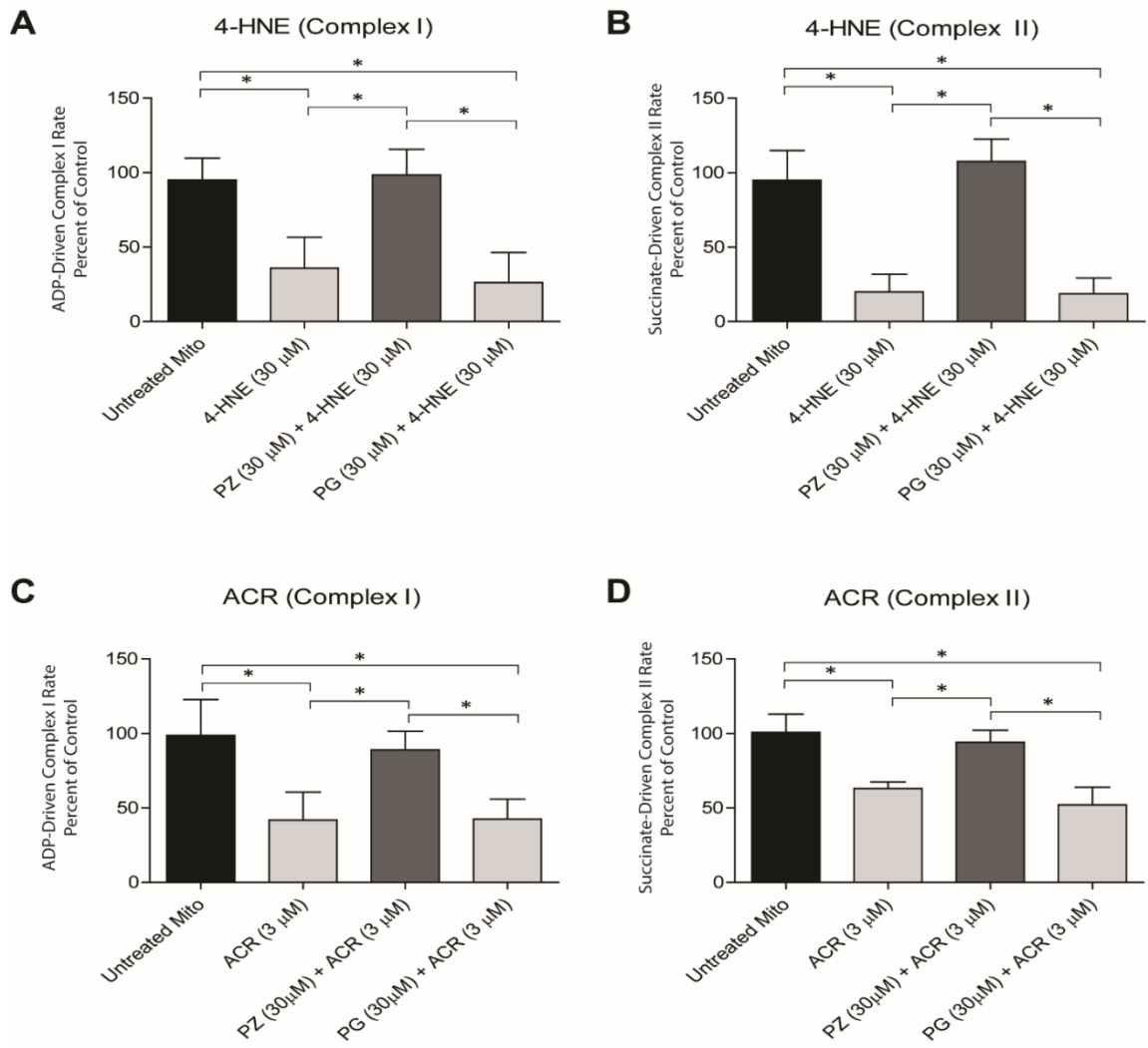


Figure 4.3. Phenzazine (PZ) protects mitochondrial respiration from 4-hydroxynonenal (4-HNE) and Acrolein (ACR) insult, but pargyline (PG) does not. Isolated mitochondria incubated with 4-HNE (30 μ M) or ACR (3 μ M) exhibited significantly impaired mitochondrial function for both Complex I and Complex II-driven respiration. However, a 5 min pretreatment of PZ (30 μ M) significantly protected mitochondrial respiration for both Complex I and Complex II-driven respiration. Pargyline, which is also a MAO inhibitor, but lacks a hydrazine moiety was not able to effectively protect mitochondrial respiration from 4-HNE or ACR insult. One-way ANOVA followed by Student Newman-Keuls post-hoc test. * = $p < 0.05$. Error bars represent \pm SD. $n = 6$ rats per group.

4.3.4 Phenelzine Prevents Mitochondrial Oxidative Damage Ex Vivo in a Dose-Dependent Fashion

Western Blot analyses were used to determine if increasing concentrations of PZ could reduce oxidative damage to mitochondrial proteins. 50 µg of isolated cortical mitochondria were utilized in the same manner as described earlier in this manuscript. A 5 minute PZ exposure to isolated mitochondria demonstrated dose-dependent protection against exogenously applied 4-HNE [30 µM] or ACR [3 µM] (**Figure 4.4**). Phenelzine at either 10 µM or 30 µM concentrations significantly reduced 4-HNE adducts (i.e. oxidative damage markers) when compared to 4-HNE only treated mitochondria ($p < 0.05$). Similarly, PZ at 10 µM and 30 µM significantly reduced ACR adducts ($p < 0.05$).

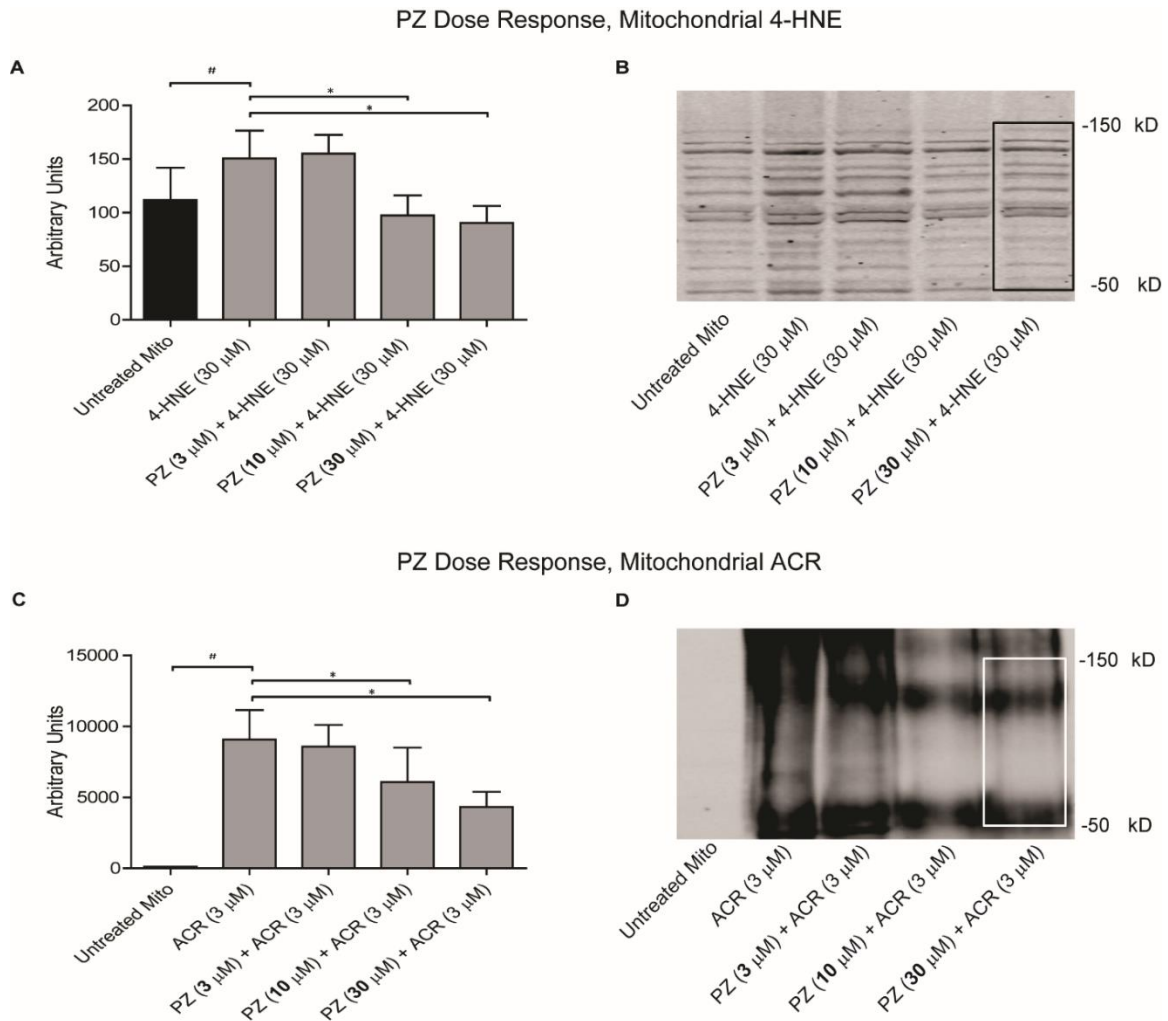


Figure 4.4. Phenzelzine reduces 4-hydroxynonenal (4-HNE) and Acrolein (ACR) in a dose-dependent manner. Mitochondria were isolated from the cortex of uninjured SD rats and exposed to increasing concentrations of PZ pretreatment 3, 10, and 30 μM for 5 min, followed by 4-HNE or ACR for 10 minutes. Mitochondria were then assessed for oxidative damage markers 4-HNE or ACR by Western Blot analysis between 150 kD and 50 kD. 4-HNE (30 μM) or ACR (3 μM) significantly increased oxidative damage. Phenzelzine at 10 and 30 μM was able to significantly ameliorate 4-HNE or ACR in mitochondria. One-way ANOVA followed by Dunnett's Multiple Comparison post-hoc test. Student t-test compared untreated to 4-HNE or ACR. #, * = $p < 0.05$. Error bars represent \pm SD. N = 6 rats per group.

4.3.5 Phenelzine, but not Pargyline, Protects against Mitochondrial Oxidative Damage Markers 4-HNE and ACR

Isolated cortical mitochondria exposed to 5 minute pretreatments of PZ (30 μ M), but not PG, were able to significantly prevent accumulation of oxidative damage markers of 4-HNE or ACR by western blot analysis ($p < 0.05$) (**Figure 4.5**). Mitochondria exposed to 4-HNE (30 μ M) or ACR (3 μ M) revealed a significant increase of banding intensity compared to untreated controls. PG + ACR or PG + 4-HNE treatments were not significantly different from 4-HNE or ACR treated mitochondria, respectively. Additionally, PZ-only or PG-only treated mitochondrial (controls) were not significantly different than untreated mitochondria.

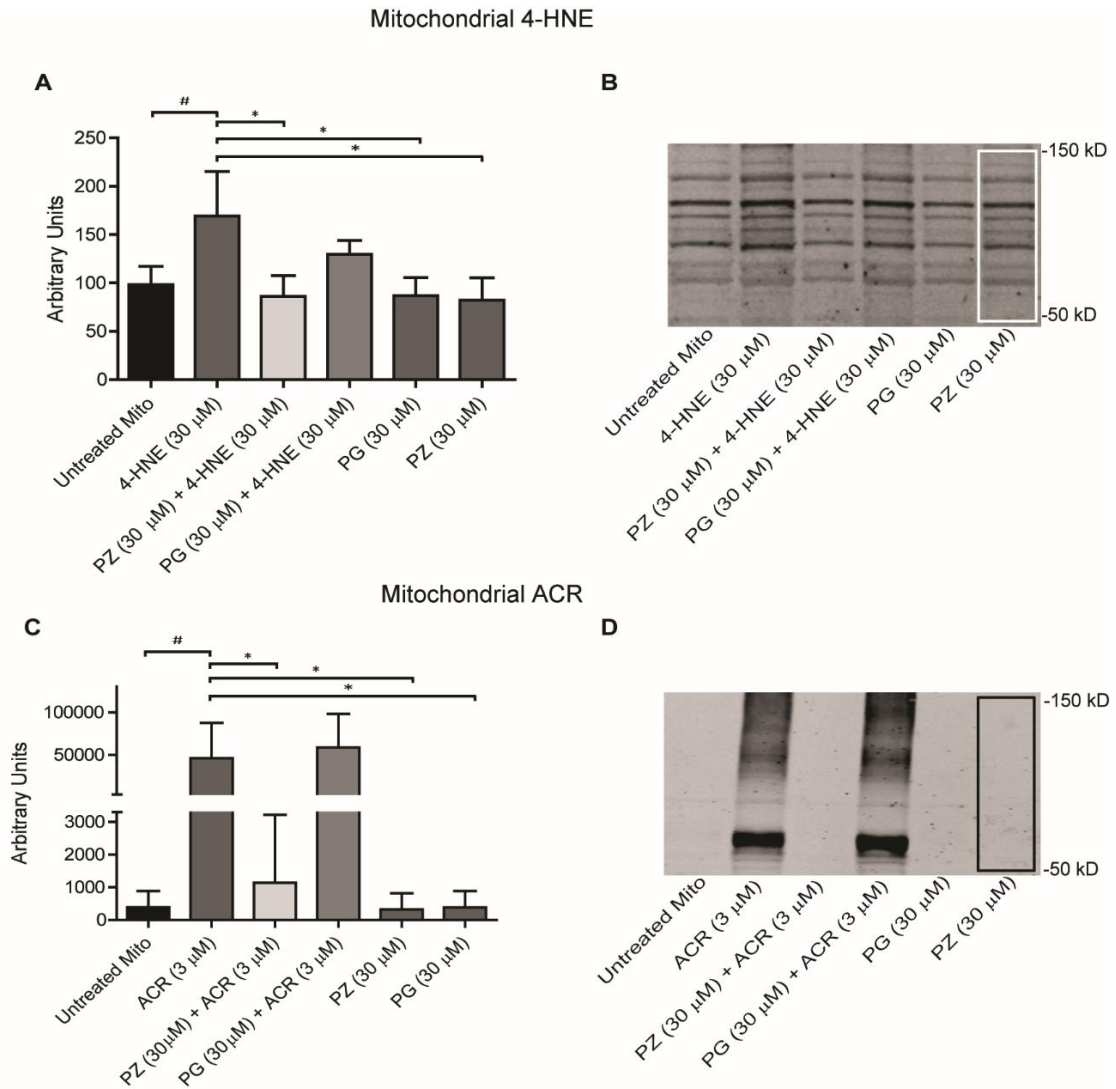


Figure 4.5 Phenzelzine (PZ) reduces 4-hydroxynonenal (4-HNE) and Acrolein (ACR), but pargyline (PG) does not. Uninjured rat mitochondria were isolated from cortex and were incubated with a 5 min PZ or PG pretreatment followed by a 10 min incubation of 4-HNE (30 μ M) or ACR (3 μ M). Samples were then assessed by Western Blot analysis for measures of oxidative damage. 4-HNE (30 μ M) or ACR (3 μ M) treated mitochondria exhibited statistically significant elevations of 4-HNE or ACR compared to untreated groups. However, PZ at 30 μ M was able to significantly ameliorate 4-HNE or ACR accumulation. One-way ANOVA followed by Dunnett's Multiple Comparison post-hoc test. Student t-test compared untreated to 4-HNE or ACR. #, * = $p < 0.05$. Error bars represent \pm SD. N = 6 rats per group.

4.4 Discussion

Free radical induction of LP is one of the most validated secondary injury mechanisms in TBI. Numerous studies have demonstrated that compounds (antioxidants) possessing the ability to interrupt the LP cascade are protective in TBI models. [68] Most notably, tirilazad mesylate (U74006F) was able to inhibit the propagation phase of LP and improved post-TBI survival in patients with traumatic subarachnoid hemorrhage in phase III clinical trials.[152] Unfortunately, these compounds have an inherently limited therapeutic window as their targets rapidly evolve during the course of the LP cascade. It should be noted, however, that much of the damage caused from LP is attributed to the deleterious aldehydic breakdown products.[153] Two notorious reactive aldehydes, 4-HNE and ACR, are broadly characterized by their electrophilic functional groups and relatively long half-lives. Such characteristics allow 4-HNE and ACR to become ideal targets for pharmacologic scavenging.

Scavenging reactive aldehydes or “carbonyl scavenging” is a treatment approach that essentially serves to provide sacrificial targets for 4-HNE and ACR. Both 4-HNE and ACR can be scavenged in this way.[85] However, one compound in particular, PZ, provides the following distinct advantages as a carbonyl scavenger for the treatment of TBI. Primarily, PZ is an FDA-approved and is readily available in a clinical setting. Because PZ is not a hypotension-inducing compound, unlike HZ, it would not be contraindicated for the acute treatment of TBI in which hypotension is not uncommonly seen as an injury-induced complication. Finally, PZ possesses the ability to function as an antioxidant against superoxide radical, [116] scavenge unbound carbonyls, and scavenge reactive aldehydes already bound to proteins. Interestingly, 4-HNE and ACR bound to

proteins via Michael addition will retain an exposed carbonyl capable of contributing further damage, however, PZ in a process dubbed “adduct-trapping” is able to covalently bind, sequester the carbonyl, and prevent subsequent damage. [118]

While the therapeutic advantages of PZ are apparent, studies only recently have begun to elucidate the true implications PZ treatment in neurodegeneration. Additionally, the collapse of mitochondrial functional integrity is tightly associated with neuronal cell death.[154] Therefore, the purpose of the current study was to investigate the ability of PZ to function as a carbonyl scavenger and protect mitochondria in an *ex vivo* model of TBI.

In order to test PZ’s ability to scavenge reactive aldehydes it was necessary to first establish that inhibition of mitochondrial respiration by 4-HNE or ACR could be measured in the Seahorse Flux Analyzer and was consistent with previous studies that were (oxythermic i.e. Clark Type electrode-based). [50, 72] Accordingly, we were able to demonstrate a concentration-dependent relationship for 4-HNE and ACR to inhibit respiration. When mitochondria were exposed to PZ followed by sub-optimal doses of 4-HNE or ACR mitochondria respiration dysfunction could be prevented. Additionally, PZ pre-treatments were able to attenuate the accumulation of mitochondrial protein oxidative damage markers measured via western blot.

The basis of PZ neuroprotection can exist in several modalities. For instance the PZ ring structure can function as an antioxidant for superoxide radical. Or, due to the fact that PZ inhibits MAO activity, it may provide mitochondrial and therefore neuronal protection by the reduction of hydrogen peroxide and other aldehydes [155]. However, in the present manuscript we were able to show that PZ was able to protect mitochondrial

respiratory function to 4-HNE or ACR insult, whereas the non-hydrazine MAO inhibitor PG was not. Given that these compounds are structurally and functionally related but only PZ prevents mitochondrial dysfunction and accumulation of oxidative damage markers in mitochondria, two reasonable conclusions can be made: 1) PZ scavenges carbonyls through its hydrazine moiety which is consistent with previous predictions [122, 151], and 2) A mere mechanical separation of protein target and reactive aldehyde is not sufficient to prevent oxidative dysfunction, otherwise PG + ACR or 4-HNE treatment groups would have reduced mitochondrial dysfunction and decreased oxidative damage markers. Additionally, PG + ACR or 4-HNE groups were not statistically different than 4-HNE or ACR alone.

It should be noted that while there was a 10 -fold concentration difference between 4-HNE and ACR use to decrease mitochondrial respiration and increase oxidative damage, this is consistent with our previous studies.[50, 72] ACR is more potent than 4-HNE, however, PZ was able to still prevent mitochondrial dysfunction for both complex I & II – driven respiration. Although, the reported data appears that complex II is insulted more heavily by 4-HNE and ACR, and therefore PZ treatment has a greater protection for complex II these protein complexes are not operating under the same respiration states. Complex I-driven respiration is measured during state III respiration wherein oxidation and phosphorylation are coupled. Complex II-driven respiration is reported from state V uncoupled respiration. When inhibition and protection are compared for complex I and complex II respiration, in similar uncoupled states, complex one appears to be primarily insulted (Data not shown).

Furthermore, it appears that Complex II is more susceptible to the same dose of insult that is used to inhibit Complex I as seen **Figure 4.1**. However, the nature of the preparation and assessment of mitochondrial complexes is performed in a linear manner and the assessment of Complex II has several minutes of increased exposure time during the measurement of respiration. In other words, 4-HNE and ACR have significantly longer time to induce or exacerbate damage as the Seahorse device measures Complex I before Complex II.

In conclusion we are the first to demonstrate in an *ex vivo* TBI model that PZ can function as a carbonyl scavenger to prevent 4-HNE or ACR- induced brain mitochondrial respiratory failure and oxidative damage in a dose-dependent manner. Other experiments will investigate the ability of PZ to produce neuroprotective effects *in vivo* using the rat controlled cortical impact, brain injury model.

Chapter 5

Phenelzine protects mitochondrial respiratory and calcium buffering functions together with a reduction in mitochondrial oxidative damage after traumatic brain injury

5.1 Specific Aim

Determine the ability of the carbonyl scavenger PZ to protect mitochondria after a controlled cortical impact induced traumatic brain injury (TBI) in young, adult rats.

5.2 Introduction

The link between mitochondrial dysfunction and TBI is well established and discussed in detail in **Chapter 1**. Experimental injury models have consistently demonstrated that mitochondria sustain acute and prolonged dysfunction [51, 156, 157]. Injured mitochondria exhibit decreased ability to respire oxygen, impairment of the electron transport system (ETS), and a decreased ability to maintain calcium (Ca^{2+}) homeostasis.

A major source of free radical production following TBI is due to mitochondrial reactive oxygen species (ROS) leakage. Increased ROS production after experimental brain and spinal cord injury increases lipid peroxidation (LP) [79, 111, 158-160]. Increases in LP results in the accumulation of LP degradation products such as 4-HNE and acrolein (ACR) in injured central nervous system tissue proteins [45].

Dysfunctional mitochondria are less capable of buffering the influx cytosolic Ca^{2+} after neuronal injury [107, 161]. Ionic calcium (Ca^{2+}) is electrochemically attracted to the negative matrix environment surrounded by the inner mitochondrial membrane. However, following TBI excessive glutamate stimulation of *N*-methyl-D-aspartate (NMDA) receptors increases cytosolic Ca^{2+} and overwhelm the mitochondria [162]. Excessive Ca^{2+} increases ROS production, release of cytochrome C, and induces the formation of the mitochondrial permeability transition pore (mPT) [110, 163]. Loss of mitochondrial membrane potential is a mediator of these pathological mechanisms and is largely in response to the influx of Ca^{2+} into the mitochondrial matrix. Membrane potential ($\Delta\Psi_m$) is a key component of the chemiosmotic theory of how the electron transport system (ETS) functions to create ATP, without $\Delta\Psi_m$ mitochondria exhibit reduced mitochondrial function [73].

Previously, our laboratory elaborated the acute time course of mitochondrial dysfunction which is significantly elevated 30 minutes after a severe TBI followed by a subsequent recovery and then a progressive decline beginning at 24 hours which is at its worst 72 hours after injury [73]. Additionally, we have demonstrated in **Chapter 4** that the exogenous application of LP-derived damage markers such as 4-HNE and even more so ACR inhibit mitochondrial respiration *ex vivo* [72, 124, 144]

Experimental evidence supports that, following TBI, elevated Ca^{2+} can induce mitochondrial dysfunction [106, 111, 164, 165]. The ability of mitochondria to buffer Ca^{2+} is compromised significantly at 3 and 12 hours post-injury [73]. Mitochondrial Ca^{2+} dysregulation leads to increases of cytosolic Ca^{2+} which activates calpains whose proteolytic activity is elevated acutely as early as 3-4 hours after injury, peaks at 24-72

hours and although slowly declining thereafter remains elevated for up to 7 days [33, 166]. Oxidative damage markers such as the reactive aldehydes 4-HNE and ACR also have been documented beginning within minutes post-injury, and reaching peak levels 48-72 hours after injury [64].

Our *ex vivo* work detailed in **Chapter 4** indicates that PZ is capable of scavenging reactive aldehydes, preventing oxidative damage and improving mitochondrial respiration in isolated mitochondria exposed to 4-HNE or ACR. The primary objective of this chapter is to determine if the carbonyl scavenger PZ (10 mg/kg s.c. at 15 minutes after TBI followed by maintenance doses of 5 mg/kg s.c every 12 hours for 72 hours) is able to protect mitochondria *in vivo* after a severe controlled cortical impact (CCI)-TBI in young adult rats. Given the relevance described above, the metrics of mitochondrial function assessed in this chapter were assessed 1) the ability of mitochondria to respire oxygen, 2) accumulation of oxidative damage markers, and 3) the ability of mitochondria to buffer Ca^{2+} .

5.3 Results

5.3.1 Mitochondrial Respiration

Following CCI-TBI young adult rats received a subcutaneous injection of either normal saline vehicle or PZ (10 mg/kg) 15 min after injury and maintenance doses of 5 mg/kg every 12 hrs for 72 hrs. Rat were euthanized at 72 hours and did not receive the 72 hour time point injection. Cortical brain tissue was dissected via cortical punch and mitochondria were isolated via ficoll gradient centrifugation (See **Chapter 2: Materials**

and Methods). Immediately following mitochondrial isolation, mitochondria were assessed for their ability to respire oxygen using a Clark-type electrode which is consistent with methods our lab has previously published for *in vitro* [144] and *in vivo* experiments[73, 124]

The ability of PZ to protect TBI-induced mitochondrial dysfunction is expressed in two forms. **Figure 5.1**, depicts mitochondrial function as respiratory control ratio (RCR). RCR is a ratio of states III and IV, a purported sensitive metric of mitochondrial function [108]. Additionally, PZ's ability to protect mitochondria is expressed as rate of oxygen consumed for each state of respiration as moles of oxygen used per mg of mitochondrial protein per minute, **Figure 5.2-5.6**.

5.3.2 Respiratory Control Ratio

Mitochondria isolated from PZ treated rats exhibited a significant ($p < 0.05$) increase of RCR after injury compared to vehicle only treated rats and were not significantly different than sham only controls. (**Figure 5.1**) Vehicle treated rats' mitochondria exhibited a significant reduction of RCR after injury when compared to sham controls ($p < 0.05$) and sham + PZ controls ($p < 0.05$). Additionally sham + PZ controls compared to sham only controls was not significantly different. Sham and Sham + PZ groups were significantly different compared to Vehicle groups. RCR of PZ treatment was significantly increased compared to vehicle and not significantly different from either sham control variant (Sham or Sham + PZ). One-way ANOVA followed by Student Newman-

Keuls post-hoc test. * = $p < 0.05$. Error bars represent +/- SD; n = 8-9 rats per group except sham where n = 5 rats per group.

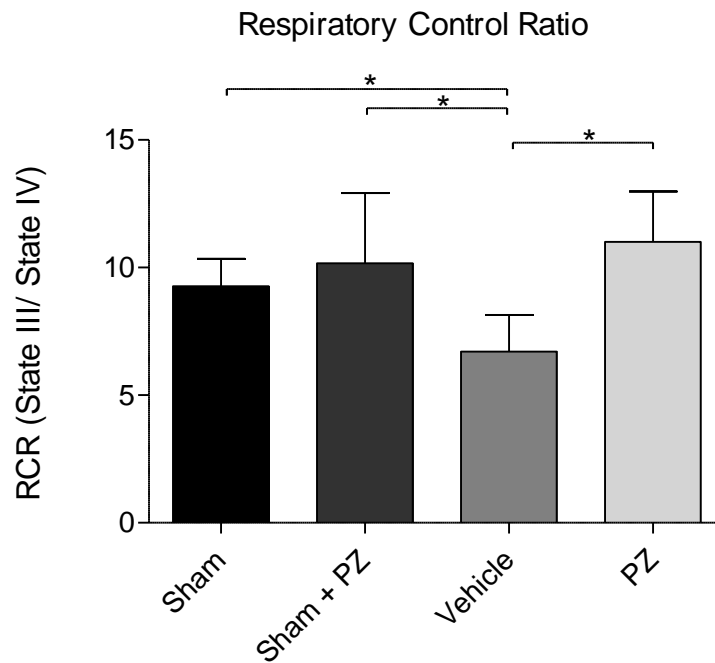


Figure 5.1 Effects of phenelzine (PZ) on cortical mitochondrial bioenergetics 72 hours after injury following severe controlled cortical impact. Mitochondrial respiration was measured with Clark-type electrode expressed as respiratory control ratio (RCR). The RCR is rate of oxygen consumption during State III divided by State IV respiration. Substrates during State III and IV are define within the text. Animals received PZ (10 mg/kg s.c.) 15 minutes after injury followed by maintenance dosing (5 mg/kg s.c.) every 12 hours; rats were euthanized at 72 hours. Sham and Sham + PZ groups were significantly different compared to Vehicle groups. RCR of PZ treatment was significantly increased compared to vehicle and not significantly different from either sham control variant (Sham or Sham + PZ). One-way ANOVA followed by Student Newman-Keuls post-hoc test. * = $p < 0.05$. Error bars represent +/- SD; n = 8-9 rats per group except sham where n = 5 rats per group.

5.3.3 States of Respiration

The following details and results represent data obtained from the same experiment that generated the RCR values; however, data is expressed as individual mitochondrial states of respiration. Defined states of respiration are slightly modified from their original concept [94] to that of more conveniently accepted protocol [93, 167] as indicated in **Methods**.

State II

As a brief reminder, these assayed mitochondria are the same as those used to determine RCR values in section **5.3.1**. Mitochondria in this state are incubated with pyruvate and malate but not ADP. There were no significant difference between controls: Sham *versus* Sham + PZ. However, there was a significant rate reduction detected between PZ group *verses* that of Sham + PZ ($p < 0.05$), but not between PZ *versus* Sham only. Additionally, PZ treated rats' mitochondria demonstrated significantly decreased dysfunction compared to vehicle ($p < 0.05$). There was not a significant reduction of respiration detected in vehicle compared to either sham groups (Sham or Sham + PZ).

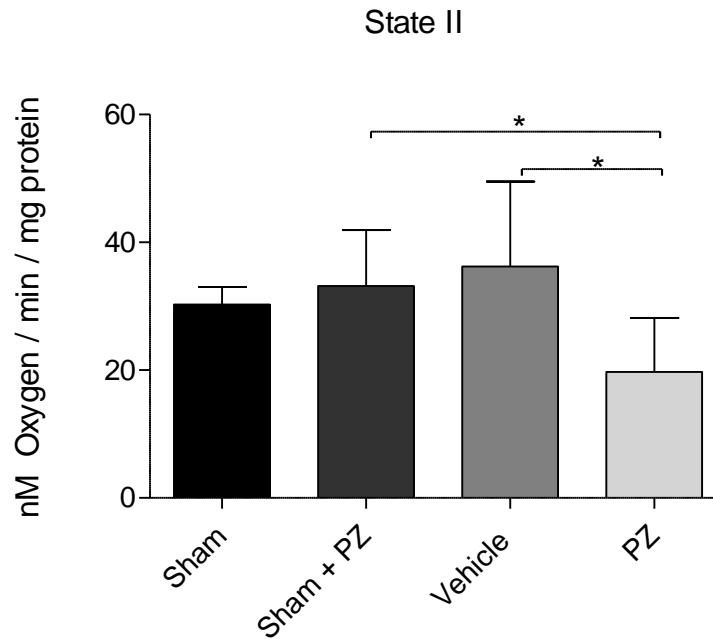


Figure 5.2 Rate of oxygen consumption calculated as nM of oxygen consumed per minute per mg of mitochondrial protein during State II respiration in the presence of pyruvate and malate but no ADP. State II is the theoretical functional equivalent to State IV respiration and is reported here as an internal control for consistency. Animals received PZ (10 mg/kg) 15 minutes after injury followed by maintenance dosing (5 mg/kg) every 12 hours; rats were euthanized at 72 hours. PZ treatment exhibited significantly decreased respiration compared to vehicle and Sham + PZ, respectively. One-way ANOVA followed by Student Newman-Keuls post-hoc test. * = $p < 0.05$. Error bars represent +/- SD; n = 8-9 rats per group except sham where n = 6 rats per group.

State III

State III is the state of respiration wherein Complex I substrates pyruvate and malate are present in addition to ADP for activation of Complex V (ATP synthase). Together Complex I and ATP synthase drive State III oxidative phosphorylation. PZ exposed mitochondria after TBI exhibited significantly decreased State III respiration rates compared to Sham ($p < 0.05$) and Sham + PZ ($p < 0.05$), respectively. In fact, PZ treatment was not statistically different than vehicle (TBI + saline). The injury effect was present, that is, the vehicle treated group was significantly reduced from both sham variants (Sham and Sham + PZ) ($p < 0.05$).

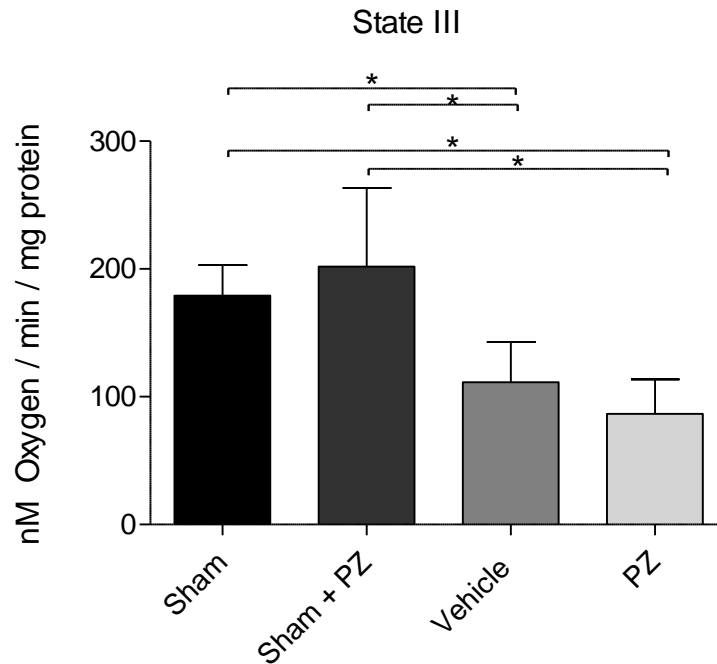


Figure 5.3 Rate of oxygen consumption calculated as nM of oxygen consumed per minute per mg of mitochondrial protein during State III respiration in the presence of pyruvate and malate and ADP. Animals received PZ (10 mg/kg) 15 minutes after injury followed by maintenance dosing (5 mg/kg) every 12 hours; rats were euthanized at 72 hours. Injury effect was present: Vehicle group significantly decreased from Sham and Sham + PZ). PZ treatment exhibited significantly decreased respiration compared to Sham and Sham + PZ, respectively. One-way ANOVA followed by Student Newman-Keuls post-hoc test. * = $p < 0.05$. Error bars represent +/- SD; n = 8-9 rats per group except sham where n = 6 rats per group.

State IV

During this state of respiration, the previously added ADP has been converted to ATP by Complex V driven by the proton gradient supplied by Complex I oxidation of substrates (pyruvate + malate). This is a State IV ADP-limited resting state. However, in State IV the addition of oligomycin to mitochondrial pools completely inhibits Complex V activity. In naïve isolated mitochondria, this state would exhibit diminished respiration as the ability to respire oxygen is theoretically still coupled to the ability to generate ATP. If respiration continues then we can deduce that oxidation and phosphorylation is uncoupled. In other words, State IV can be used to evaluate mitochondrial leak/ uncoupled respiration.

PZ exposed mitochondria following TBI, again, exhibited significantly decreased rate of oxygen consumption compared to both sham ($p < 0.05$) and sham + PZ ($p < 0.05$) and vehicle treated TBI groups ($p < 0.05$) **Figure 5.4**. Interestingly, saline following TBI (vehicle group) did not exhibit an injury effect as expected; vehicle group was not statistically different than either control variant (Sham or Sham + PZ). Controls were not significantly different from each other.

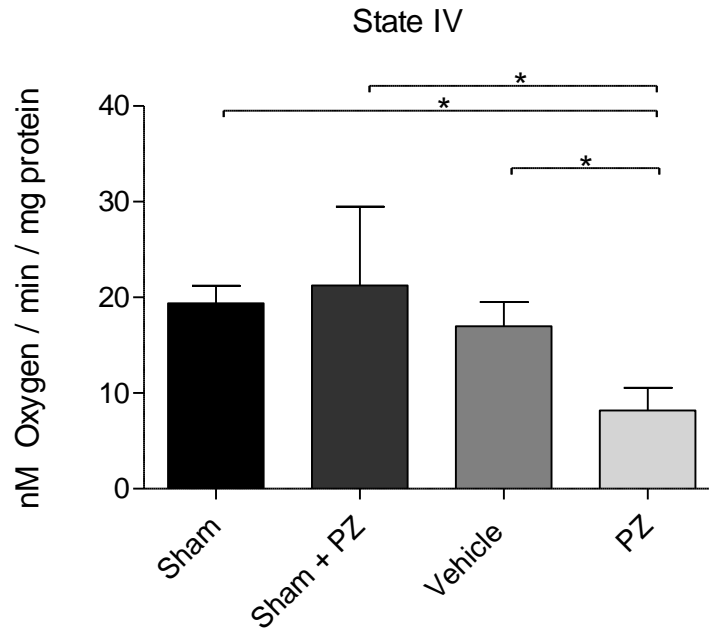


Figure 5.4 Rate of oxygen consumption calculated as nM of oxygen consumed per minute per mg of mitochondrial protein during State IV respiration in the presence of pyruvate, malate, ADP, and oligomycin. Animals received PZ (10 mg/kg) 15 minutes after injury followed by maintenance dosing (5 mg/kg) every 12 hours; rats were euthanized at 72 hours. PZ treatment was significantly decreased compared to Sham, Sham + PZ, and Vehicle groups, respectively. One-way ANOVA followed by Student Newman-Keuls post-hoc test. * = $p < 0.05$. Error bars represent +/- SD; n = 8-9 rats per group except sham where n = 6 rats per group.

State Va

State V respiration is expressed as State Va and State Vb. Va indicates State V, Complex I-driven respiration after the addition of FCCP, a protonophore. The protonophore allows the mitochondrial membrane to be synthetically uncoupled. Respirations reported for this state communicate the maximum respiration rate for which Complex I is capable, in the provided conditions without the limiting “tether” of Complex V. In other words, State Va is the maximum respiratory capacity of Complex I in an uncoupled state.

Mitochondria from PZ treated rats exhibited a significant respiratory impairment compared to sham ($p < 0.05$) and sham + PZ ($p < 0.05$) groups. See **Figure 5.5** However, unlike State IV respiration, the injury effect was apparent in State Va respiration: vehicle groups exhibited significantly reduced rates of respiration compared to both sham ($p < 0.05$) and sham + PZ ($p < 0.05$) groups. Controls (Sham and Sham + PZ) were not different from each other.

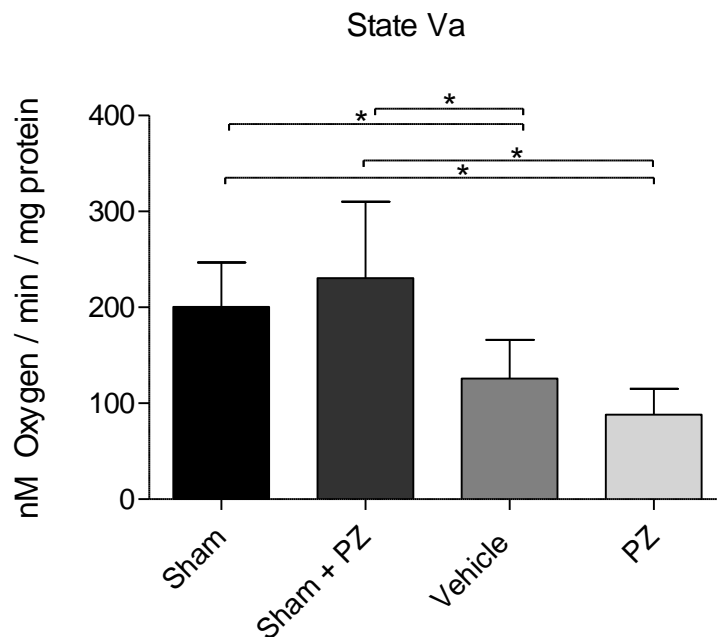


Figure 5.5 Rate of oxygen consumption calculated as nM of oxygen consumed per minute per mg of mitochondrial protein during State Va respiration after the addition of pyruvate, malate, ADP, oligomycin, and FCCP—an uncoupling protonophore. Animals received PZ (10 mg/kg) 15 minutes after injury followed by maintenance dosing (5 mg/kg) every 12 hours; rats were euthanized at 72 hours. PZ treatment was significantly decreased compared to both Sham groups, respectively. Vehicle group was significantly reduced compared to both Sham groups, respectively. One-way ANOVA followed by Student Newman-Keuls post-hoc test. * = $p < 0.05$. Error bars represent +/- SD; n = 8-9 rats per group except sham where n = 6 rats per group.

State Vb

The state of respiration described here is maximal respiratory capacity of Complex II (as opposed to State Va which is maximal respiration for Complex I). For this state of respiration rotenone was added to inhibit Complex I activity. Succinate was added to elicit activation of Complex II. And, since FCCP was previously added, Complex II now possesses the conditions to maximally respire oxygen when uncoupled.

Consistent again with previous states reporting diminished ability of PZ treated groups to facilitate Complex I-driven respiration, PZ + TBI group also exhibits a significantly diminished ability to respire oxygen compared to Sham ($p < 0.05$) and Sham + PZ ($p < 0.05$) and vehicle ($p < 0.05$) groups. Controls were not significantly different from each other. An injury effect was not apparent, i.e. the Vehicle-treated group did not exhibit significantly reduced respiration rates when compared to Sham or Sham + PZ groups.

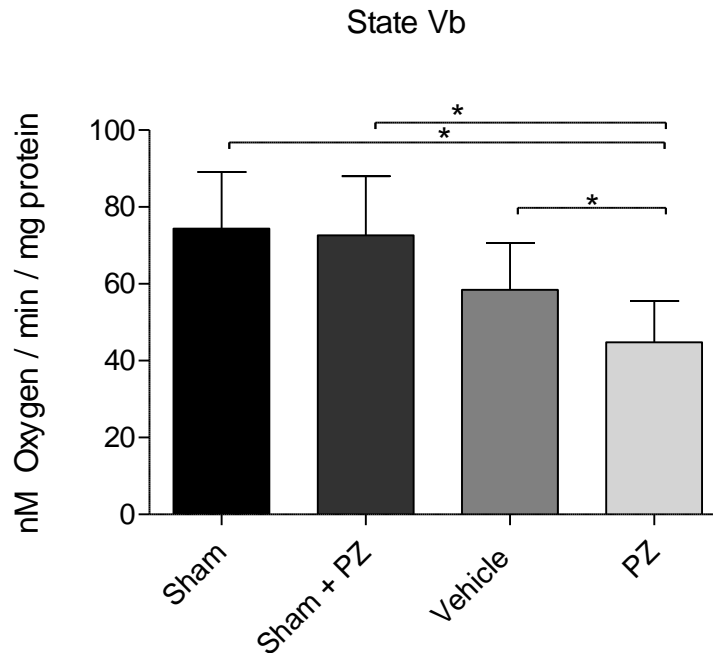


Figure 5.6 Rate of oxygen consumption calculated as nM of oxygen consumed per minute per mg of mitochondrial protein during State Va respiration after the addition of pyruvate, malate, ADP, oligomycin, FCCP, rotenone and succinate. Animals received PZ (10 mg/kg) 15 minutes after injury followed by maintenance dosing (5 mg/kg) every 12 hours; rats were euthanized at 72 hours. PZ treatment was significantly decreased compared to both Sham groups and Vehicle group, respectively. One-way ANOVA followed by Student Newman-Keuls post-hoc test. * = $p < 0.05$. Error bars represent +/- SD; n = 8-9 rats per group except sham where n = 6 rats per group.

5.3.4 Mitochondrial Oxidative Damage

In a similar but separate experiment with an additional cohort of rats, the ability of PZ to reduce markers of oxidative damage was assessed by western blot analysis. As described in **Methods**, isolated mitochondria were prepared from Sham, Sham + PZ, TBI + Vehicle, and TBI + PZ treatment groups. Neither variant of sham controls (Sham or Sham +PZ) received injury. PZ-treated rats followed the same dosing paradigm in **5.3.1**, that is, PZ 15 minutes following injury 10 mg/kg was injected subcutaneously, followed by 5 mg/kg maintenance injections every 12 hours for 72 hours. Mitochondria after isolation, were frozen at -80°C until assessed for protein concentration immediately prior to immunoblotting procedure.

Western blots of isolated mitochondria revealed that PZ treatment after injury was able to significantly ($p < 0.05$) reduce the 4-HNE marker of oxidative damage although not to the level of Sham only group **Figure 5.7**. 4-HNE accumulation was significantly ($p < 0.05$) elevated compared to both Sham and Sham + PZ control groups. Control groups (sham and sham + PZ) were not significantly different from each other.

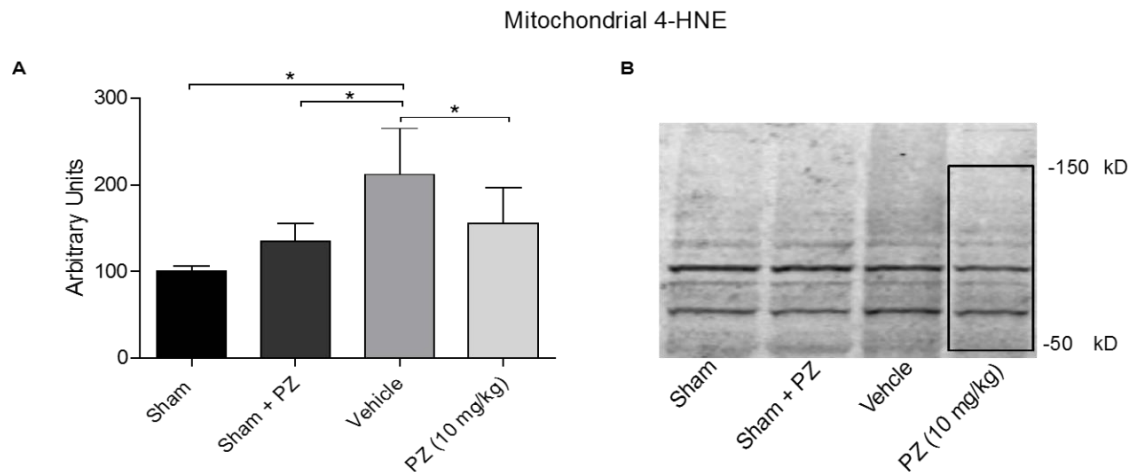


Figure 5.7 Phenzelzine reduces 4-hydroxynonenal (4-HNE) accumulation in mitochondria after severe CCI-TBI when treated 15 minutes after injury at 10 mg/kg, followed by 5 mg/kg every 12 hours. Rats were euthanized at 72 hours. **A)** Quantification of markers of oxidative damage in cortical mitochondria. **B)** Mitochondria were assessed for markers of oxidative damage by western blot analysis between 150 kd and 50 kd. 4-HNE was significantly elevated in Vehicle group compared to both Sham groups, respectively. PZ treatment group exhibited significantly reduced oxidative damage compared to Vehicle group, but did not return to Sham levels. ANOVA followed by Student Newman-Keuls post-hoc test. * = $p < 0.05$. Error bars represent \pm SD; n = 8-9 rats per group except sham where n = 5 rats per group.

5.3.5 Mitochondrial Calcium Buffering

Following severe TBI, subcutaneous injections of either vehicle (saline) or PZ treatment were administered 15 min after injury (See **Materials and Methods**). Phenelzine treatment again consisted of 10 mg/kg every 15 minutes after injury and subsequent 5 mg/kg dose at 12 hours. (See **Rationale** for dosing at 24 hours). Cortical mitochondria were dissected via punch, isolated from the excised cortical tissue via ficoll gradient and assayed for the ability to buffer Ca^{2+} . A typical trace is depicted in **Figure 5.9**. A spectrofluorometer was used to assess extra-mitochondrial Ca^{2+} levels by measuring the intensity of a fluorescent Ca^{2+} -sensitive indicator CaG5N. Mitochondria were incubated in sequential additions of pyruvate and malate at minute 1, ADP at minute 2, oligomycin at minute 3, and at minute 5 the Ca^{2+} infusion began.

One-way analysis of variance (ANOVA) followed by Student Newman-Keuls post-hoc analysis revealed multiple findings (See **Figure 5.8**). Firstly, mitochondria from vehicle treated rats had significantly reduced ability to buffer Ca^{2+} when compared to sham control groups ($p < 0.05$); this is consistent with previously published reports that TBI reduces mitochondrial buffering capacity [73, 124]. Additionally, rats treated after injury with a 24 hours PZ treatment paradigm exhibited a significantly ($p < 0.05$) increased ability to buffer Ca^{2+} when compared to vehicle treated rats. However, while PZ-treated rats' mitochondria were better able to buffer Ca^{2+} , the TBI + PZ treatment group's ability to buffer Ca^{2+} was not statistically different that Sham values.

Mitochondrial Calcium Buffering Capacity

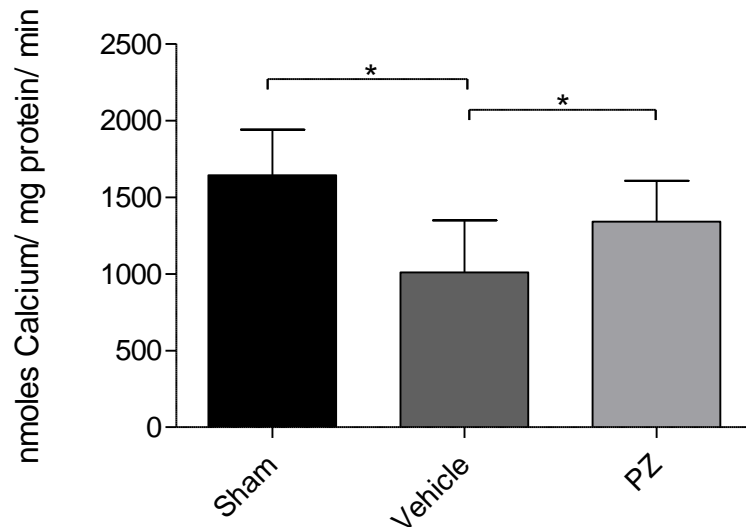


Figure 5.8 Quantification of cortical mitochondrial calcium buffering capacity 24 hours after severe CCI-TBI in the rat. Phenelzine (PZ) treatment consisted of single 10 mg/kg injection 15 minutes after injury followed by maintenance dosing every 12 hours at 5 mg/kg. Rats were euthanized at 24 hours. Mitochondria from vehicle treated rats demonstrated a significantly decreased ability to buffer increasing concentrations of Ca^{2+} (Ca^{2+}) compared to Sham. PZ treatment significantly improved Ca^{2+} buffering when compared to Vehicle. PZ treatment after TBI was not statistically different than Sham group. ANOVA followed by Student Newman-Keuls post-hoc test. * = $p < 0.05$. Error bars represent +/- SD; n = 8-9 rats per group.

Mitochondrial Calcium Buffering Traces

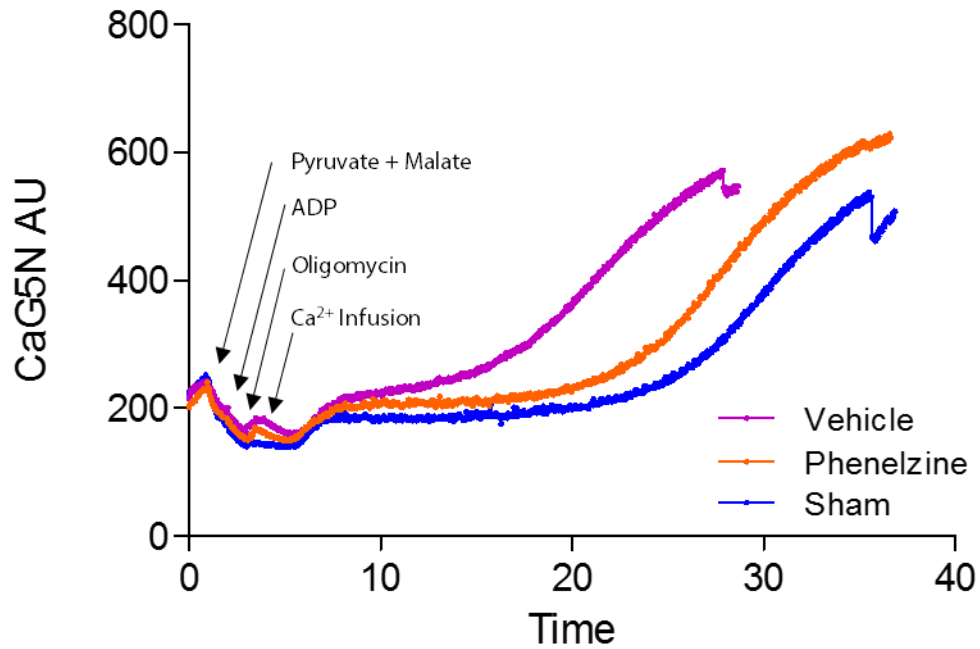


Figure 5.9 Typical mitochondrial Ca²⁺ buffering trace. A spectrofluorometer was used to assess extra-mitochondrial Ca²⁺ levels by measuring the intensity of a fluorescent Ca²⁺-sensitive indicator CaG5N. Mitochondria were incubated in sequential additions of pyruvate and malate at minute 1, ADP at minute 2, oligomycin at minute 3, and at minute 5 the Ca²⁺ infusion began.

5.4 Discussion

Face value interpretation of these experiments demonstrate that a 15 minute post-injury administration of PZ_m is able to protect against TBI-induced deficits in mitochondrial respiratory function when expressed in terms of RCR, mitochondrial Ca²⁺ buffering, and reduce mitochondrial markers of oxidative damage. (*PZ_m designates a single s.c. injection of 10 mg/kg 15 minutes after TBI and 5 mg/kg every 12 hours thereafter for 72 hours; the exception being Ca²⁺ buffering experiments wherein cortical mitochondria were isolated at 24 hours.*) While this is certainly true, further consideration of RCR (**Figure 5.1**) data compared to independent states of respiration (**Figures 5.2-5.6**) are seemingly contradictory.

In fact, PZ demonstrated significantly ($p < 0.05$) reduced respiration for every state of respiration measured (State II, III, IV, Va and Vb). How can PZ seem to improve mitochondrial respiration (RCR), reduce markers of oxidative damage, increase Ca²⁺ buffering but, simultaneously decrease individual states of respiration? Does the reckoning of this undermine or support PZ's presumed ability to protect mitochondria as demonstrated *in vitro* as detailed in **Chapter 4**? The following sections entertain 3 possibilities.

5.4.1 Hypothesis 1: Phenelzine-induced Monoamine Oxidase Inhibition Could Have a Greater Proportional Effect on Overall Mitochondrial Oxygen Consumption in Injured Mitochondria

The first consideration regards artifactual bias. Inherently, one must always consider their own ability to perform experiments, but this is not the artifact for which this author is considering. Rather, the isolated mitochondrial preparation itself has inherent limitations. As mentioned in **Chapter 1**, the mitochondrial respiration assays that we employed are only able to detect one component of respiratory function: oxygen consumption. However, the measurement of increased or decreased oxygen consumption following the addition of multiple substrates or inhibitors is helpful in dissecting the status of the individual states of respiration [93].

In the case of the injured mitochondria exposed *in vivo* to PZ treatment, when individual states of respiration are assessed, every *individual* state is significantly reduced compared to the Sham only cohort. However, when PZ treatment is compared to Sham and expressed as RCR, PZ provides protection. Under closer inspection of the individual states of PZ-treated groups, there is a reduction of State IV rate, more so than the decrease in State III. The quotient of these two numbers generates an RCR. Because RCR is a ratio, a relative increase in State III or a relative decrease in State IV will increase the overall RCR. The PZ-treated group as reported by RCR (**Figure 5.1**) consists of a State III (**Figure 5.3**) divided by disproportionately *decreased* State IV (**Figure 5.4**). One possibility that might account for the systematic reduction of the individual respiration states in injured, but not in non-injured mitochondria, could be due to the effect of PZ-induced monoamine oxidase (MAO) inhibition as source of reduced oxygen consumption.

Phenelzine is an irreversible, non-specific inhibitor of MAO [151]. The majority of monoamine oxidases exist in the outer mitochondrial membrane (OMM) [168]. Therefore, it is possible that PZ is preventing the degradation of monoamines by MAO, which consume oxygen as a part of the normal processes to breakdown monoamines. Because our assay only can detect total amount of oxygen consumed, we attribute decreased oxygen utilization with decreased respiratory function. However, decreased oxygen utilization could be attributed to the inhibition of normal basal catabolic reactions of monoamine degradation that normally consume oxygen.

In other words, in PZ-treated injured mitochondria, the relative contribution of background MAO activity-induced oxygen consumption, compared to the oxygen consumption by the injury-compromised electron transport chain, might be greater than that occurring in normal mitochondria. Where the ratio of oxygen utilization by MAO activity is minor compared to the amount of oxygen consumed by oxidative phosphorylation. This could explain why PZ appears to be exacerbating the TBI-induced respiratory dysfunction in the injured, but not in the Sham (non-injured mitochondria). Additionally, the reduction of respiration specifically during state IV, would lessen the extent of uncoupled respiration and lead to an overall beneficial increase of RCR. Mitochondria could be uncoupled but PZ is reducing the effect by decreasing the respiration disproportionately in State IV.

Admittedly, this possibility is undermined by the fact that the concentration of monoamines in the mitochondrial preparation, and thus the actual oxygen utilization attributable to MAO oxidation of those monoamines, is not presently known.

5.4.2 Hypothesis 2: Phenelzine-induced MAO Inhibition Leads to Increased levels of Monoamine Neurotransmitters Leading to Autoxidation-induced Free Radical Production

The second hypothesis, also related to PZ inhibition of MAO, as to how PZ could exhibit negative effects of mitochondrial respiratory states is through a potential increase in dopamine neurotoxicity. Immediately following post-injury administration of PZ, excitotoxic levels of monoamines (e.g. dopamine) could increase *in vivo* due to inhibition of their principal degrading enzyme (MAO). As already pointed out, PZ is a MAO inhibitor [151] and prevents the degradation of dopamine which elicits neurotoxicity when dopamine autoxidizes in the synaptic cleft [169]. Dopamine autoxidation leads to formation of amiochrome-protein adducts and free radicals [170] that inhibit normal cellular processes and facilitates lipid peroxidation (LP), respectably. These effects could reasonably happen during the 72 hour treatment time *in vivo* and serve to “pre-injure” or even exacerbate mitochondrial dysfunction before mitochondria are isolated for assessment of respiratory function. This would explain why reduction of respiration is only seen in animals with PZ treatment after injury (and not in Sham + PZ animals). In other words, PZ might be exacerbating only the injury effect on the mitochondrial respiratory state through dopamine neurotoxicity while mitochondria are still in the rat brain, which would account for not seeing this effect *in vitro*.

Yet, dopamine neurotoxicity does not account for our laboratory’s previously published results showing that a single injection of PZ given 15 minutes after TBI can improve mitochondrial RCR when assessed 3 hours after injury [144]. If inhibition of MAO increases dopamine levels (sufficient to induce neurotoxicity) which would decrease mitochondrial function, our previous experiment would not demonstrate that PZ treatment

increases mitochondrial respiration. On the other hand, the fact that mitochondria are protected by PZ when assessed at 3 hours post-injury does not preclude the possibility that dopamine accumulation and possible dopamine autoxidation might develop more slowly and become apparent, particularly in injured mitochondria, by 72 hours. However, this would require increased lipid peroxidation which we do not see there.

Other researchers have published evidence that undermine this dopamine neurotoxicity hypothesis. In fact, MAO inhibitors (both A and B types) have been shown to reduce mitochondrial dysfunction by preventing the degradation of dopamine [168] which increase respiration by reducing the degradation products of monoamine catabolism such as H₂O₂ and superoxide radical O⁻ that would otherwise hinder oxidative phosphorylation [171]. Additionally, the better preserved RCR in 72 hour post-TBI mitochondria and a decrease in oxidative damage (i.e. 4-HNE accumulation) at the same time point runs counter to the notion that PZ-induced MAO inhibition is increasing monoamine oxidation to the point of causing additional oxidative damage.

5.4.3 Hypothesis 3: Possible Negative Effects of Phenelzine-induced GABA Transaminase Inhibition Exacerbating Post-TBI GABA Excitotoxicity

GABA is generally regarded as an *inhibitory* transmitter which hyperpolarizes mature neurons by the influx of chloride ions (Cl⁻), the result is less electrical signaling and reduced Ca²⁺ influx [172]. However in early development and following neuronal injury [173], GABA receptors respond to GABA in an *excitatory* manner to *increase* Ca²⁺ influx

[174-176] as a means to modulate growth cones, enhance neuritic outgrowth and mature synapses [177-180].

Chen and colleagues carefully investigated the GABA *excitatory* actions and demonstrated that endogenous levels of GABA in the synaptic cleft after injury is able to depolarize Cl^- reversal potential that facilitate the efflux of Cl^- leading to neuronal depolarization instead of the normal Cl^- influx that underlies GABA-mediated repolarization [181]. Furthermore, application of GABA to traumatized cultured neurons has been shown to cause depolarization mediated via increased Ca^{2+} influx through normally Cl^- permeable channels[173]. Consequently, voltage-activated Ca^{2+} channels (L and N type) open and Ca^{2+} floods the cell with concentrations reaching over 600nM [173]. GABA excitotoxicity has been documented in multiple neuronal injury models and reports confer that the reversed role of GABA (e.g. excitatory effects of GABA) occur within a window starting approximately 3 hours after injury/insult, exhibit maximum response at 48 hours, then diminish gradually for the next 2 weeks [173]. *Maximum response is defined by manuscript's authors as 63% of the neurons in explanted hippocampal or cortical tissue responding to GABA with a Ca^{2+} influx.*

GABA excitotoxicity can be exacerbated by PZ which can increase GABA levels due to an inhibition of GABA metabolism. Interestingly, PZ is not only an inhibitor of MAO but a substrate for it. Phenelzine oxidation by MAO yields phenylethylidenehydrazine (PEH) [147]. PEH is a potent inhibitor of GABA-transaminase (GABA-T) and GABA-T is the primary means of synaptic GABA clearance [182]. Phenelzine has been reported to decrease MAO activity and simultaneously elevate GABA

levels. A single dose of PZ (15 mg/kg) in the rat inhibits 100% of GABA-T activity for 8 hours, which tapers off to 24 % inhibition 24 hours after injection[183].

Given that injured neurons are known to exhibit a reversed, excitatory role for GABA and that PZ increases GABA levels, PZ could be exacerbating GABA excitotoxicity. Too much GABA stimulation following trauma would exhibit the same drastic Ca^{++} influx that is associated with glutamate excitotoxicity.

Our data indicate that PZ is capable of scavenging neurotoxic carbonyls which can have beneficial effects like improving mitochondrial respiration (at least in regards to RCR) and reducing lipid peroxidative damage (i.e. 4-HNE) to mitochondrial proteins. However, PZ multiple dosing over a 72 hour period may aggravate GABA-mediated excitotoxic consequences. The PZ dosing paradigm utilized a single 10 mg/kg s.c. dose 15 minutes after injury and 5 mg/kg s.c. every 12 hours. This dosing paradigm was intentionally extended to allow maximum exposure of PZ to scavenge reactive aldehydes, but this dose may also elevate GABA levels during the period when injured neurons are most susceptible to GABA excitotoxicity (e.g. 48 hours).

Our previously published mitochondrial work indicated that a single dose (10mg/kg) of PZ was capable of increasing RCR, 3 hours after injury [144]. The increase in respiration suggests that a single dose of PZ may not contribute as drastically to GABA excitotoxicity as would multiple doses every 12 hours for 3 days. Additionally, neurons exhibit a limited excitatory response to GABA 3 hours after injury [173] which suggest early administration of PZ could also mitigate the GABA excitotoxic response. Which begs the question: *Would you rather get hit in the face once, or every 12 hours for 3 days?*

GABA Excitotoxicity on Calcium Buffering

Our Ca^{2+} buffering experiments in **Figure 5.8** demonstrate that PZ also protects the ability of mitochondria removed from the injured brain to buffer Ca^{2+} . According to the presented GABA excitotoxicity hypothesis, preservation of Ca^{2+} buffering may be a double-edge sword. On one hand mitochondria are able to better buffer increases of cytosolic Ca^{2+} that would otherwise activate Ca^{2+} -mediated proteases which could destroy the cell. On the other hand, increased Ca^{2+} within the mitochondrial matrix could disrupt the redox potentials which facilitate proton translocation and electron transfer e.g. PZ would decrease mitochondrial respiration. The notion that increased Ca^{2+} buffering decreases mitochondrial respiration is indirectly supported by other labs, which concluded that reducing Ca^{2+} in the mitochondria by pharmacologic uncoupling increases mitochondrial respiration and tissue sparing [108]. The uncoupling agents were concluded to reduce mitochondrial Ca^{2+} buffering which lead to restored mitochondrial respiration after moderate TBI in the rat.

In all, PZ is protecting mitochondria dysfunction after TBI *in vivo* by scavenging carbonyls and improving the ability of mitochondria to buffer Ca^{2+} . Diminished mitochondrial respiration in PZ-treated rats suggests that PZ may be exerting a self-limiting effect due to GABA-mediated Ca^{2+} elevations in the mitochondrial matrix which reduce the ability of mitochondria to oxidize substrates, translocate protons, and transfer electrons.

In summary, the neuroprotective properties of PZ appear to be complicated. We have demonstrated that the hydrazine moiety of PZ is able to scavenge deleterious carbonyls in normal mitochondria exposed to either 4-HNE or ACR *in vitro* together with

a decrease in aldehydic modification of mitochondrial proteins (**Chapter 4**), and that these effects are also seen in mitochondria assayed from rats subjected to CCI TBI and assessed at 72 hours after injury. Additionally, we have demonstrated that PZ is capable of improving mitochondrial Ca^{2+} buffering capacity after TBI. However, PZ is a GABA-T inhibitor and reduction in functionality of this enzyme could conceivably increase GABA levels. Normally a GABA increase might serve to decrease excitotoxicity, but after neuronal injury a GABA agonist will exacerbate the injury by facilitating a cytotoxic influx of Ca^{2+} . Even though, PZ treated mitochondria possess higher buffering capacities for this increased Ca^{2+} , this can translate physiologically to a reduction of mitochondrial respiration. Thus, it appears that PZ treatment may contribute to healthier brain mitochondria that exhibit less oxidative damage after TBI and increased ability to buffer Ca^{2+} , but they are limited in their maximal respiratory response.

Given the strong influence of PZ metabolites to modulate intracellular Ca^{2+} , the next chapter will investigate PZ's role in terms of spectrin degradation and histological sparing.

Chapter 6

Role of phenelzine in histological sparing of cortical tissue and spectrin degradation

6.1 Specific Aim 3

Determine the extent to which phenelzine (PZ) is able to provide neuroprotection in rats following a controlled cortical impact brain injury.

6.2 Introduction

In the previous chapter, the importance of calcium (Ca^{2+}) homeostasis was described as a function of mitochondrial condition. Specifically, the preservation of mitochondrial Ca^{2+} buffering could prevent cytosolic elevations of Ca^{2+} which would preempt the activation of degrading enzymes such as calpains. Additionally, proper Ca^{2+} homeostasis maintains the chemiosmotic gradient which is vital for the production of adenosine triphosphate (ATP)[93]. This chapter primarily focuses on the investigation PZ's therapeutic window and assessment of neuroprotection by characterization of spectrin degradation and histological tissue sparing.

Experimental models of TBI have long established the perturbation of Ca^{2+} homeostasis after injury [184]. One of the most well-established means by which Ca^{2+} homeostasis is lost after TBI is induced via glutamate excitotoxicity. Wherein, the primary insult to the brain serves as a mechanical depolarization stimulus that 1) activates the opening of voltage-dependent ion channels (Na^+ , K^+ , and Ca^{2+}) and 2) initiates the release

of excitatory neurotransmitters such as glutamate which stimulate N-methyl-D-aspartate (NMDA) and AMPA receptors on postsynaptic targets. Over-excitation of these receptors elicits the influx of Na^+ and Ca^{2+} ions into the neuron [21, 185, 186].

Rapid accumulation of Ca^{2+} can compromise cytoskeletal integrity by activation of calcium-sensitive proteases. Especially important, the rise of cytosolic Ca^{2+} activates cysteine proteases such as calpains.[187] Calpains target membrane-associated proteins and cytoskeletal components that upon cleavage have been reported to increase the incidence of cell death.[188] One specific target of Ca^{2+} -activated proteases is α II-spectrin [150], which has become a widely used and reliable means to assess the cytoskeletal integrity as a metric of neuroprotection [33, 34, 36, 149, 189] since its original characterization [33].

α II-spectrin is enzymatically degraded into what are referred to as spectrin breakdown products (SBDP). The particular SBDP exhibit a specificity to the proteolytic enzymes which degraded full length spectrin (280 kDa). For instance, cleavage by calpain results in fragments 150 kDa and 145 kDa whereas degradation of spectrin by caspase-3 results in formation of fragments 150 kDa and 120 kDa all of which can be detected by western blot analysis.[190] The ability to differentiate which proteolytic enzymes provide considerable insight into the type of neuroprotection a drug can offer. For instance, if calpain enzymatic activity is increased but not caspase, then with reasonable confidence one can argue that mitochondria have not undergone mPT and are relatively stable. Otherwise, these mitochondria would have induced pore formation and released cytochrome c, the activator of caspase-9. Caspase-9 is the activator of caspase-3 [191].

Caspase-3 cleavage of spectrin is detectable in spectrin degradation immunoblot analysis [190].

Spectrin degradation analysis not only an attempt to qualify neuroprotective properties of phenelzine (PZ), but it is also a means to measure therapeutic window. Therapeutic window in the context of the following experiments, is described as the maximum amount of time that PZ treatment can be delayed and still provide neuronal protection. Spectrin degradation in the rat controlled cortical impact (CCI) brain injury model is detectable as early as 15 min after injury[148]. Therefore, this endpoint has been used to determine the neuroprotective therapeutic window by evaluating the ability to attenuate spectrin degradation after CCI-TBI with treatment initiation delay times ranging to 15 min. to as long as 12 hours [192, 193]. Increasing the delay of PZ treatment would help determine the therapeutic window.

In addition to the assessment of spectrin degradation, the following experiments attempt to measure the extent to which PZ can spare tissue after CCI-TBI. Histological stains have previously been reported to correlate strongly in both location and timing of calpain-mediated spectrin degradation [33, 148, 194].

Thus far, PZ has been described as a monoamine oxidase inhibitor (MAO-I) and a carbonyl scavenger capable of binding lipid peroxidation-derived reactive aldehydes such as 4-hydroxynonenal (4-HNE) and acrolein (ACR). To date, PZ does not possess the ability to directly bind cytosolic Ca^{2+} . However, it is plausible that PZ could indirectly modulate cytosolic Ca^{2+} and provide neuroprotection by preserving mitochondrial function. We have documented in the previous **Chapter 5** that PZ is able to protect the

ability of mitochondria to buffer Ca^{2+} . It is well established that cytosolic Ca^{2+} concentration is a key regulator in the activation of proteolytic enzymes responsible for cytoskeletal degradation. Therefore, PZ may provide neuronal protection by allowing mitochondria to buffer Ca^{2+} which would reduce the cytosolic Ca^{2+} and subsequently preempt activation of Ca^{2+} sensitive proteolytic enzymes such as calpains and caspases [108, 184, 190].

On the other hand, PZ may exacerbate γ -aminobutyric acid (GABA) excitotoxicity. GABA typically binds to GABA receptors to suppress action potentials and decrease neuronal activity by facilitating the influx of chloride ions (Cl^-) which contributes to the hyperpolarization of the cell. Two exceptions to this “suppressant” role of GABA are thought to exist to modulate neurite outgrowth during embryonic development and after injury [176, 177]. In this role, GABA is an excitatory transmitter that causes a polarization reversal to efflux Cl^- (rather than the typical influx). Subsequently, the Cl^- influx causes voltage-gated Ca^{2+} channels to activate and facilitate the influx of Ca^{2+} ions. The excitatory role of GABA after neuronal injury is reported in cortical and hippocampal explants to elicit Ca^{2+} influx in approximately 38% of total neurons 3 hours after injury, maximum response of approximately 68% of neurons at 24 hours after injury, and only 9% of neurons two weeks after injury [173]. Thus, while PZ can protect mitochondrial Ca^{2+} buffering, it could simultaneously be exacerbating Ca^{2+} overload through PZ-metabolite GABA transaminase (GABA-T) inhibitory action which would act to increase GABA which in the post-injury state is largely excitatory and able to cause an increased Ca^{2+} influx [147]. Nevertheless, given the role of PZ to improve mitochondrial Ca^{2+} buffering, reduce oxidative damage and possibly influence critical components of Ca^{2+} homeostatic

regulation, we aimed to demonstrate the ability of PZ to influence spectrin degradation and to preserve cortical tissue sparing. Should PZ be able to decrease spectrin degradation, we intended to develop a therapeutic window to describe the maximum amount of time that the initiation of posttraumatic PZ treatment could be withheld after CCI-TBI in the rat and still provide neuroprotection. Additionally, two dosing paradigms were used to investigate tissue sparing. Increasing PZ dosing could theoretically result in an increase of neurological protection due to increased carbonyl scavenging, or it could result in a possible decrease in tissue sparing likely due to GABA excitotoxicity.

6.3 Results

6.3.1 Spectrin Degradation

Phenelzine treatment was delayed 15 minutes and 3 hours after a severe CCI-TBI in the rat. PZ dosing consisted of a single 10 mg/kg s.c. injection followed by repeated 5 mg/kg s.c. injections every 12 hours. Male rats were euthanized at 72 hours. Tissue dissected from rat brains by cortical hole punch and was assayed by immunoblotting technique for 150 and 145kD spectrin degradation products. Data were expressed as optical density as percent of sham for either 150 or 145 kD bands, normalized to β -tubulin.

15 minute Delay

Phenelzine or vehicle (0.9% Saline) treatments were delayed 15 minutes after CCI-TBI. Vehicle (saline) treated animals exhibited significantly higher ($p < 0.05$) banding intensities for 150 and 145 kD bands compared to sham. The PZ and Vehicle treatment

groups exhibited significantly increased banding intensities ($p < 0.05$) compared to the Sham group. However, PZ treatment group was not significantly different than vehicle treated group. See **Figure 6.1**.

Spectrin Degradation; PZ_m treatment delayed 15 minutes

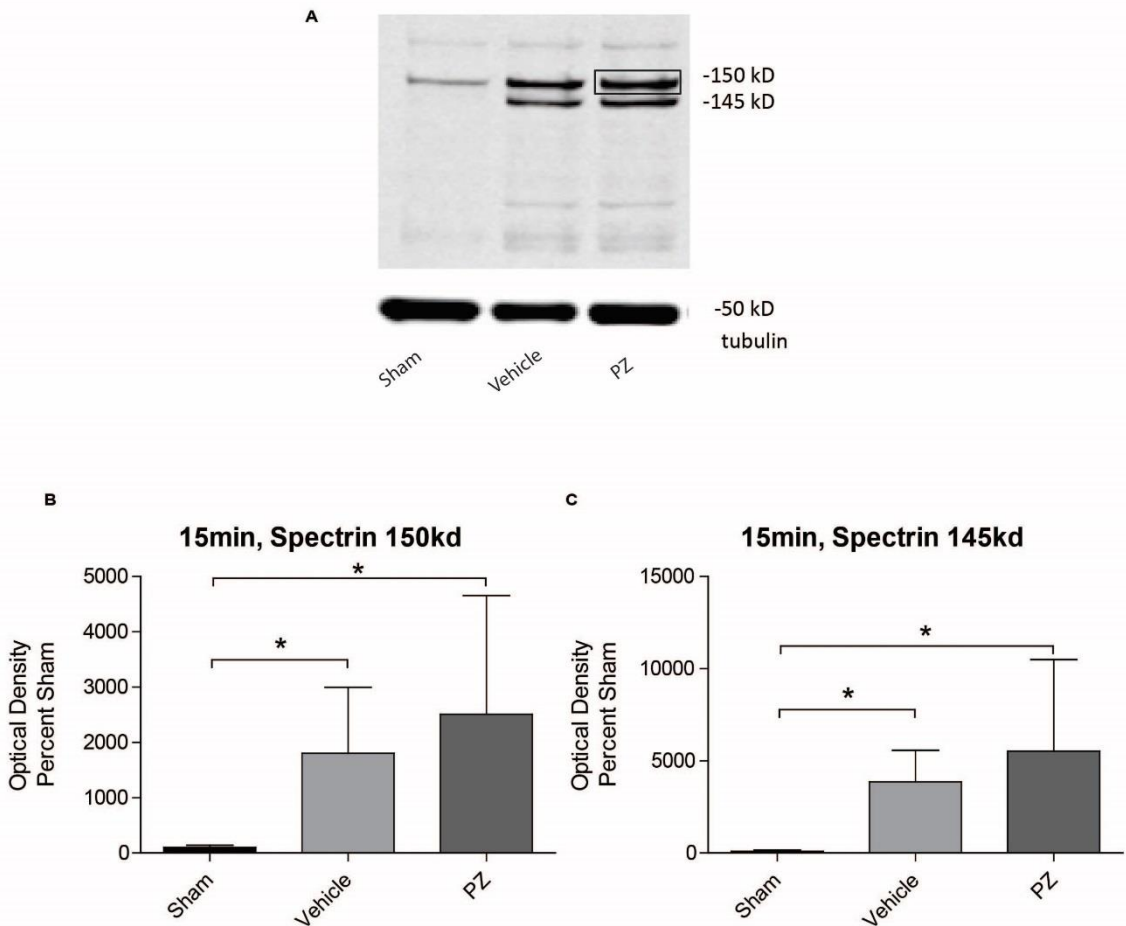


Figure 6.1 **A)** Western blot of spectrin degradation products. Phelzine (PZ) treatments were delayed 15 minutes after severe CCI-TBI. PZ was injected at 10 mg/kg 15 minutes after injury and 5 mg/kg every 12 hours thereafter. Rats were euthanized at 72 hours. **B-C)** Spectrin breakdown products (SBDP) are quantified by optical density, normalized to β -tubulin and expressed as percent control. **B)** 150 kD band for vehicle and PZ treatment groups were significantly elevated compared to sham, respectively. PZ was not significantly different from Vehicle group. **C)** 145 kD band for Vehicle and PZ treatment groups were significantly elevated compared to sham, respectively. However, PZ was not significantly different from sham control. One-way ANOVA followed by Student Newman-Keuls post-hoc test. * = $p < 0.05$. Error bars represent \pm SD; n = 8 rats per group.

3 hour Delay

In a second round of experiments, PZ or Vehicle treatments were delayed 3 hours after CCI-TBI. Similar to the 15 minute delay, Vehicle

treated animals exhibited significantly higher ($p < 0.05$) banding intensities for 150 and 145 kD bands compared to Sham. PZ treatment group also exhibited significantly increased banding intensities ($p < 0.05$) compared to Sham group. However, PZ treatment group was not significantly different than the vehicle treated group. See **Figure 6.2**.

Spectrin Degradation; PZ_m treatment delayed 3 hours

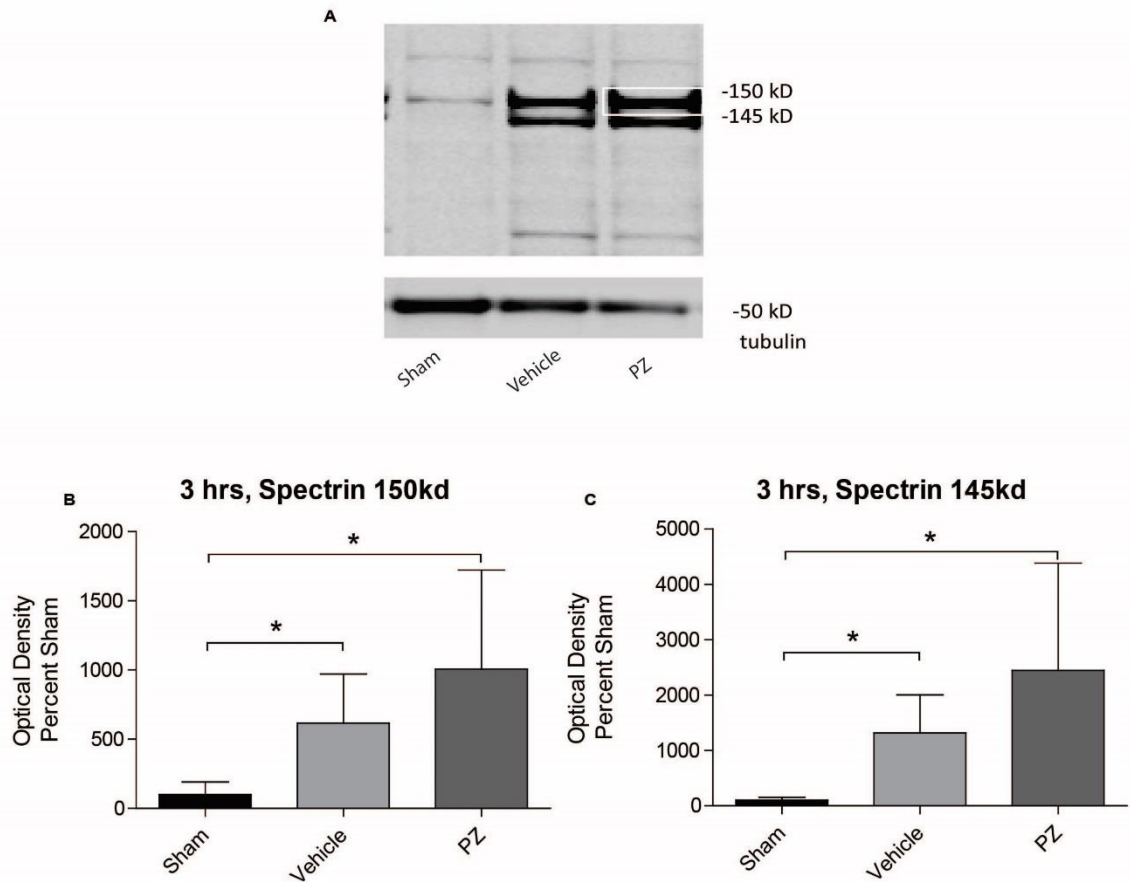


Figure 6.2 **A**) Western blot of spectrin degradation products after 3 hour delayed phenelzine (PZ) treatment. Phenelzine (PZ) treatments were delayed 3 hours CCI-TBI. PZ was injected at 10 mg/kg 3 hours after injury and 5 mg/kg every 12 hours after first injection. Rats were euthanized at 72 hours. **B-C**) Spectrin breakdown products (SBDP) are quantified by optical density, normalized to β -tubulin and expressed as percent control. **B**) 150 kD band for vehicle and PZ treatment groups were significantly elevated compared to sham, respectively. PZ was not significantly different from Vehicle group. **C**) 145 kD band for Vehicle and PZ treatment groups were significantly elevated compared to sham, respectively. However, PZ was not significantly different from sham control. One-way ANOVA followed by Student Newman-Keuls post-hoc test. * = $p < 0.05$. Error bars represent +/- SD; n = 8 rats per group.

6.3.2 Cortical Tissue Sparing

Two dosing paradigms were tested PZ_s and PZ_m .

- PZ_s is a single dose of PZ 10 (mg/kg) injected s.c. 15 minutes after a severe TBI. This single dose had previously been shown by our laboratory to increase tissue sparing in the rat when assessed at 14 days post-injury [144].
- PZ_m is a single dose of PZ (10 mg/kg) also injected s.c. 15 minutes after severe TBI in the rat followed by an additional maintenance 5 mg/kg dose given s.c. every 12 hours.

In both dosing paradigms, rats were euthanized at 72 hours after the first injection. Twelve brain sections were assessed for area of intact cortical tissue and then used to determine the volume of cortical sparing as described in **Chapter 2: Materials and Methods**. Data are expressed as percent of tissue spared compared to contralateral (non-injured) hemisphere.

Although perhaps showing an increase in tissue sparing compared to the Vehicle group, the PZ_s group was not statistically different than Vehicle treated group. However, PZ_m exhibited statistically significant ($p < 0.05$) increase of tissue sparing compared to the Vehicle group.

Phenelzine Cortical Tissue Sparing

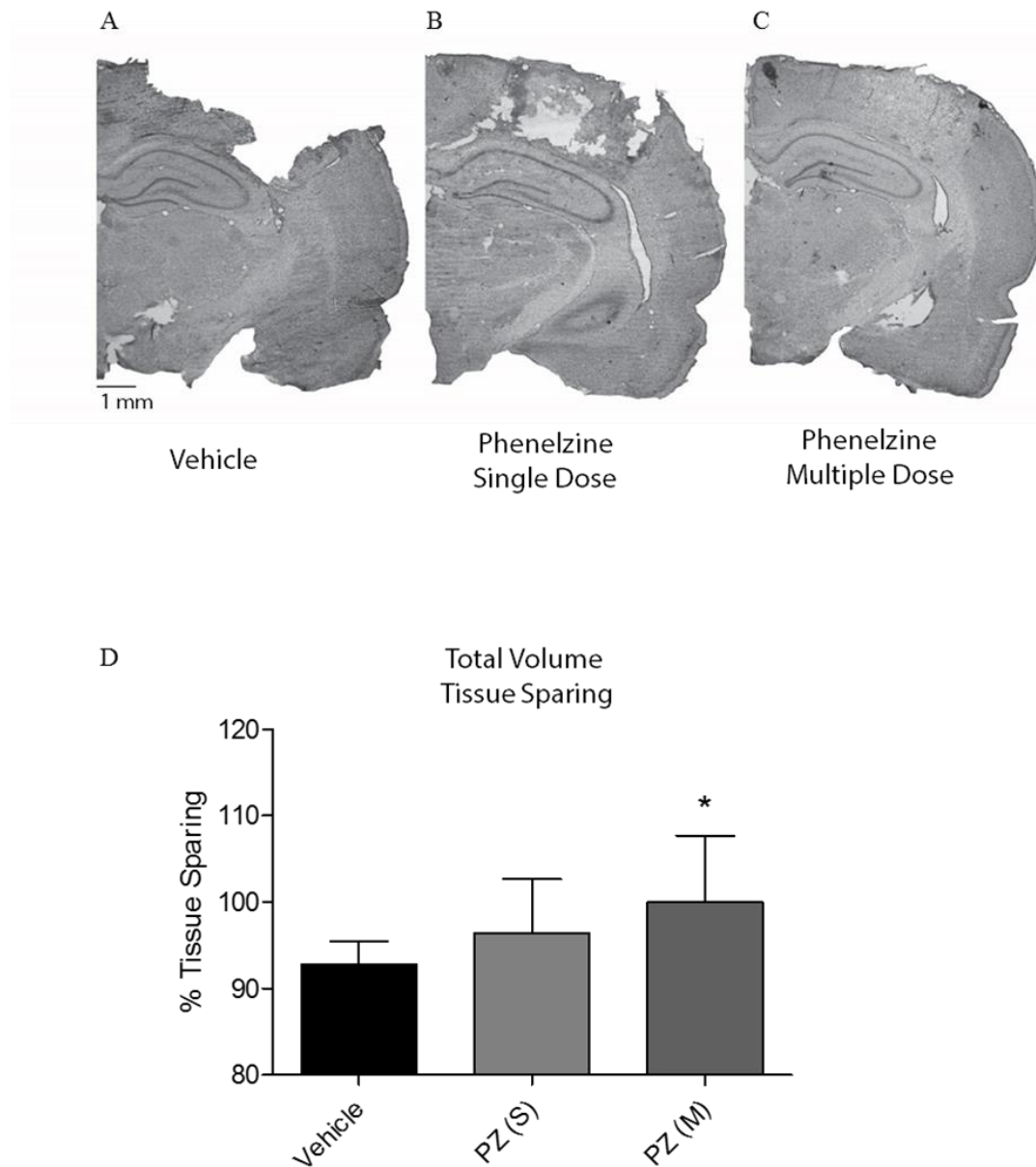


Figure 6.3 Coronal sections of ipsilateral rat brains rat taken at 1.2x magnification. **A)** Vehicle (0.9% saline) treated rat brain injected 15 minutes after TBI. **B)** Phenelzine (PZ_s) single dose treated animal, injected with a *single* dose of PZ, 15 minutes after injury at 10 mg/kg. **C)** Rat brain of PZ treated with a multiple dosing paradigm (PZ_m): single subcutaneous injection of PZ 15 minutes after injury, followed by maintenance dosing of 5 mg/kg every 12 hours thereafter. All groups (Vehicle, PZ_s, PZ_m) were

euthanized 72 hours after first injection. Black bar represents 1mm. **D)** Percent of tissue sparing followed by either Vehicle (saline), PZ_s, or PZ_m treatment. Rats were euthanized in all treatment paradigms at 72 hours after first injection. PZ_s did not exhibit a statistically significant amount of cortical tissue sparing when compared to Vehicle. However, PZ_m significantly increased the total volume of spared cortical tissue. One-way ANOVA followed by Dunnett's post-hoc test. * = $p < 0.05$. Error bars represent +/- SD; n = 8 rats per group.

6.4 Discussion

6.4.1 Multiple Phenelzine Dosing Protects Cortical Tissue but Does Not Decrease Spectrin Degradation Compared to Sham

The neuroprotective therapeutic window for PZ in terms of a possible reduction in posttraumatic calpain-mediated spectrin degradation was assessed by increasing the delay of PZ administration after injury. The multiple dose PZ paradigm was injected in rats after injury with either a 15 minute delay after TBI or, in another cohort, a 3 hours delay. All animals were euthanized and assessed for spectrin degradation 72 hours after the first injection. In both PZ-treated groups (15 minutes and 3 hours delay), neither group exhibited a reduction of spectrin degradation when compared to Vehicle-treated injured animals.

However, the same multiple dosing paradigm that did not demonstrate spectrin protection was able to spare cortical tissue, whereas the *single* dose of PZ did not. It is conceivable that the multiple dosing with PZ over 72 hours would provide more scavenging molecules that protect cortical tissue from deleterious carbonyls which would result in the observed protection of cortical tissue. However, this does not account for why spectrin degradation was not reduced. Theoretically, little prevention of spectrin degradation would imply that cortical tissue will *not* be spared due to the presumed “degraded” states of cytoskeletal components e.g. spectrin. The following section provides some ideas as to this dichotomy between PZ’s ability to increase histologically measured tissue sparing while not reducing spectrin degradation.

6.4.2 *Phenelzine Could Actually Exacerbate Spectrin Degradation*

As previously described in **Chapter 5**, the PZ metabolite PEH can inhibit γ -aminobutyric acid transaminase (GABA-T) leading to immediate increases in the “inhibitory” neurotransmitter GABA [195]. However, beginning immediately after injury neurons will utilize GABA as an *excitatory* neurotransmitter that reverses movement of chloride ions (Cl^-) to now exit the cell causing subsequent activation of voltage gated calcium channels and the influx of Ca^{2+} [173]. In consideration of this, PZ possesses the ability to increase GABA levels and therefore to exacerbate neuronal Ca^{2+} influx [196]. This idea suggest that PZ could worsen neuronal cytoplasmic Ca^{2+} overload, calpain activation and spectrin degradation. However, both PZ treatment delay groups (15 minutes and 3 hours) only showed a trend to exacerbate spectrin degradation; neither group was significantly worse than Vehicle. How can PZ have the propensity to exacerbate spectrin degradation, but not demonstrate this?

6.4.3 *Phenelzine Could Increase Total Intact Spectrin*

It is possible that PZ is worsening spectrin degradation, but it is also possible that PZ is simultaneously increasing the expression of spectrin. The result of which, would be a null effect as observed in our spectrin degradation assays. It is theoretically possible that increasing more intact spectrin could yield the potential of even more SBDP. However, as calpain is an enzyme it is bound by the laws of kinematics and therefore have a saturation limit which provides the possibility of increase intact spectrin despite activation of calpain.

This mechanism is considered is due to the heavy developmental role of GABA excitatory response detailed below.

As previously mentioned, GABA-mediated Ca^{2+} influx is a mechanism borrowed from early neuronal development [172, 177, 178]. This mechanism is heavily regarded as a means to facilitate neurite outgrowth and play a role in synaptogenesis following injury [173, 174, 177, 181]. And, PZ is known to exacerbate GABA levels [197, 198]. Therefore, it is not unreasonable to speculate that PZ is facilitating the “reconstruction” of the cytoskeletal matrix by increasing the degradation of spectrin. Our assay measures the extent of spectrin degradation as a percent of Sham animals, which does not assess the total amount of intact spectrin available in the cell. In other words, there may be more spectrin degradation in PZ-treated animals, but we have yet to assess if total intact spectrin is increased. This might explain why cortical tissue sparing can exist “without” a reduction of spectrin degradation which would be an observation first of its kind. Additionally, would call into question the validity of SBDP being a well-established surrogate for neuroprotection.

If PZ is increasing calcium buffering of mitochondria post-TBI then it is possible to observe decreased calcium buffering at later time points, when the mitochondria become overwhelmed. Other potential biases are explored in the next chapter that may account for the diminished ability of PZ to reduce spectrin degradation.

6.4.4 Some Calpain Inhibitors Fail to Prevent Spectrin Degradation but Increase Behavioral Recovery

Other reports have demonstrated a “counter-intuitive” relationship related to spectrin degradation as well. Calpain-mediated degradation does not always match the spatial and temporal characteristics of other axonal pathologies [150]. For instance, post-TBI neurological recovery was improved in the rat and mouse following treatment with the brain-penetrable calpain inhibitors E64 and SJA6017 but no reduction in cerebral spectrin degradation was found [34, 199]. On the other hand, another brain-penetrable calpain inhibitor MDL-28170 produced a significant reduction in early posttraumatic spectrin degradation, but did not increase sparing of cortical tissue [200]. Additionally, when FCCP was used to uncouple mitochondria, increased cortical tissue sparing was reported 18 days after injury [108]. However, FCCP should have theoretically increased cytosolic Ca^{2+} to the point of activating calpains that degrade spectrin and subsequently preempt the possibility of sparing tissue. Phenzazine may be among these compounds that show a dichotomy between increased tissue sparing and/or behavioral recovery improvement without any decrease in calpain-mediated spectrin degradation.

Chapter 7

Final Discussion

7.1 Brief Summary of Results

7.1.1 Summary of Aim 1 Ex Vivo Experiments

The material presented in **Chapter 4**, was a means to investigate a “proof of concept”. The aim of the conducted experiments was to “*assess the ability of the carbonyl scavenger PZ to protect uninjured, isolated rat brain mitochondria from ex vivo exposure to the deleterious, LP-derived reactive aldehydes 4-hydroxynonenal (4-HNE) and acrolein (ACR).*”

In order to test the concept that PZ can scavenge reactive carbonyls and provide protection, several key optimizations needed to first be made pertaining to the exogenous application of 4-HNE and ACR to isolated naïve mitochondria. The metrics of protection decided in these experiments were mitochondrial respiration and markers of oxidative damage. We chose these endpoints given the heavy involvement of mitochondrial dysfunction associated with TBI secondary injury mechanisms [56, 68, 99, 103, 110, 124, 160]. The sub-optimal dose (i.e. the dose that significantly decreased mitochondrial respiratory function without completely shutting it down) established in these experiments was found to be 30 μ M of 4-HNE and 3 μ M of ACR which was sufficient to significantly ($p < 0.05$) reduce mitochondrial respiration and to significantly ($p < 0.05$) increase 4-HNE and ACR markers of mitochondrial oxidative damage.

The concentrations of 30 μ M 4-HNE and 3 μ M ACR were used in the remainder of experiments, the purpose of which was to determine the concentration at which a PZ pretreatment that could scavenge reactive carbonyls (4-HNE and ACR). *Pre-treatments* of PZ were a necessary starting point for *ex vivo* experimentation and it was consistent with our previously published methods designed to explore optimal dosing paradigms [72, 144].

From these experiments, we determined that the optimal 5 minute pretreatment of 30 μ M PZ was able to significantly ($p < 0.05$) reduce mitochondrial markers of oxidative damage and significantly ($p < 0.05$) increase Complex I and Complex II-driven respiration. Substrates and inhibitors of Complex I and Complex II states of respiration are described in the **Introduction** and **Material and Methods**.

The 5 minute pretreatment PZ demonstrated the ability to protect mitochondrial function. However, the means by which PZ was able to do so was more appropriately examined in experiments that tested PZ against an analogous compound, pargyline (PG). PZ is a monoamine oxidase inhibitor (MAO-I) and speculation did exist on the mechanism of protection provided by PZ; MAO inhibition has been shown to be protective following neuronal injury [51, 168]. However, PG too is an MAO-I but it lacks the hydrazine moiety. The hydrazine moiety is the primary nucleophilic functional group responsible for the scavenging of neurotoxic aldehydes like 4-HNE and ACR [90, 116]. Accordingly, should PG provide the same type and extent of protection as PZ, then one could implicate that protection was due to the MAO activity. However, PG at an equimolar concentration was not able to reduce mitochondrial markers of oxidative damage nor was it able to improve respiratory function after 4-HNE or ACR insults.

Combined, the culmination of these experiments demonstrated that at least in *ex vivo* experimentation PZ could scavenge carbonyls to reduce mitochondrial markers of oxidative damage and protect mitochondria against 4-HNE and ACR-mediated respiratory insults. This provided incentive to test PZ's scavenging abilities *in vivo* following a severe TBI in the rat.

7.1.2 Summary of Aim 2 In Vivo Experiments

Given the efficacy of PZ to protect mitochondria *ex vivo* and reduce markers of oxidative damage, the aim of **Chapter 5** was to “*determine the ability of the carbonyl scavenger PZ to protect mitochondria after a controlled cortical impact induced traumatic brain injury in young, adult rats.*”

Previously our lab published that PZ (10 mg/kg s.c.) was able to protect mitochondrial respiration 3 hours after injury in the rat, and spare significant cortical tissue 2 weeks after injury [144]. In the current experiments, the dosing regimen of PZ was modified to include maintenance dosing of 5 mg/kg every 12 hours for 72 hours. This was based on published reports by the original manufacture Pfizer ©, indicating that the blood-serum half-life of PZ was 12 hours. Therefore, a maintenance dose of 5 mg/kg was injected s.c. every 12 hours to compensate for the approximated amount of PZ excreted. Despite the worst snowfall KY had seen in 15 years, the author of this dissertation ventured into the laboratory without fail to deliver injections to the brain-injured rats every 12 hours. The rationale to extend the dosing concentration over 72 hours was to match the duration

of posttraumatic 4-HNE accumulation [51] as an attempt to maximize the exposure of PZ to the reactive carbonyls 4-HNE and ACR.

In keeping with our *ex vivo* endpoints to measure mitochondrial function these experiments also investigated PZ's ability to protect respiration, mitigate oxidative damage markers, and increase calcium buffering.

Interestingly, PZ (10 mg/kg s.c.) injected 15 minutes after a severe controlled cortical impact (CCI) TBI, and (5 mg/kg s.c.) every 12 hours thereafter for 72 hours was able to significantly improve mitochondrial respiration when expressed as respiratory control ratio (RCR). However, when mitochondrial respiration data was expressed in terms of individual states of respiration, PZ significantly ($p < 0.05$) reduced the measured amount of oxygen consumed. In a similar dosing paradigm, when mitochondria were isolated from rats with a similar injury 72 hours after TBI mitochondria exhibited significantly less 4-HNE. When mitochondria were assessed with ACR by the same immunoblotting technique, the anti-body previously used to detect exogenous applications of ACR became ineffective in detecting ACR endogenously after TBI; even though, ACR after neuronal injury is present 40x more than 4-HNE [90, 201].

Another metric of mitochondrial function assessed was the ability of mitochondria to buffer calcium in the same injury and PZ dosing paradigm model. However, rats were euthanized 24 hours after injury to accommodate the therapeutic window determined by others [108]. Phenzine was able to significantly increase the capacity of mitochondrial Ca^{2+} buffering compared to untreated, injured mitochondria.

Although these experiments exhibited curious data in terms of PZ's ability to significantly improve RCR but significantly reduce individual states of respiration, PZ was able to significantly reduce mitochondrial markers of 4-HNE oxidative damage and significantly increase the ability of mitochondria to buffer calcium. Therefore, we concluded that PZ's was able to protect mitochondrial function by improving RCR. In order to determine if these findings would translate to neuroprotection we developed experiments to investigate spectrin degradation and cortical tissue sparing.

7.1.3 Summary of Aim 3 Neuroprotection Experiments

PZ exhibited mitochondrial protection *ex vivo* and *in vivo*. The ability of PZ to provide neuroprotection and the respective therapeutic window of neuroprotection were investigated in the following experiments. In **Chapter 6** our aim was to “*determine the extent to which PZ is able to provide neuroprotection in rats following CCI.*”

The original intent of the aim was to increasingly extend the treatment delay of PZ and assess for spectrin degradation. Spectrin degradation is a widely accepted marker of cytoskeletal integrity in neuronal injury models [33, 184, 189, 190, 202], and we had previously demonstrated that a single dose of PZ (10 mg/kg s.c.) following injury increases cortical sparing two weeks after injury [144]. At the time, it was an appropriate logical deduction to associate spectrin cytoskeletal degradation with histological cortical tissue sparing. Accordingly, we decided that we would use the new extended PZ dosing paradigm that spanned over 72 hours to examine the therapeutic window in regards to an anticipated protection against spectrin degradation.

We expected that the PZ extended dosing paradigm, referred to as PZ_m, would reduce spectrin degradation after TBI and that the therapeutic efficacy of PZ to afford this protection would then taper off as the delay of initial PZ administration increased after TBI. Again, we had previously published that PZ is capable of preserving cortical tissue sparing; a metric of neuronal protection that, in theory, is associated with the presence of the cytoskeletal network which spectrin functions to maintain.

Despite this flawless logic, PZ_m dosing paradigm was not able to significantly protect against spectrin degradation when delayed 15 minutes after injury or when delayed 3 hours after injury. We speculated about the dosing implications between PZ single dose (PZ_s) and PZ multiple dosing over 72 hours (PZ_m). The single dose was able to preserve cortical tissue after 2 weeks[144], but multiple doses of PZ had no effect on spectrin degradation. Accordingly, we sought to quantify the cortical tissue sparing of both the single PZ dose and a multiple PZ dosing paradigm at a common time point: 72 hours. 72 hours was chosen based on the time required to complete the multiple dosing paradigm.

In these cortical sparing experiments, we demonstrated that the PZ single dose did not significantly improve tissue sparing, although a trend may have been apparent. However, the PZ multiple dosing paradigm did significantly ($p < 0.05$) increase cortical tissue sparing at 72 hours post-TBI. These data implicate that the dose and frequency of PZ administration can play a pivotal role in carbonyl scavenging required to provide neuroprotection. We suspect that the higher dosing paradigm is able to spare cortical tissue because the duration of PZ treatment is increased and therefore the capacity to effectively scavenge deleterious reactive carbonyls over the entire 72 hours is increased relative to the

single PZ dose treatment whose effect would be drastically decreased during the first 24 hour after its administration.

However, there are gaps in the understanding of how PZ is able to improve so many components of mitochondrial function and provide cortical tissue sparing, but exhibit decreased individual states of mitochondrial respiration, while having essentially no protection against spectrin degradation. Mechanisms that could provide a theoretical accountability for these conundrums are discussed in the next sections.

7.2 Expansion of General Discussion

7.2.1 Mitochondrial Respiration

Three ideas may account for the discrepancy in PZ's ability to provide increased RCR but not increased oxygen consumption for individual states of respiration. The first of these which deals with PZ's effect to reduce the inherent use of oxygen when mitochondria are being assessed for respiration. Phenelzine is an MAO-I and reactions that catabolize monoamines utilize oxygen. Therefore, PZ-treated mitochondria may exhibit a higher rate of oxidative phosphorylation, while lacking the ability to consume oxygen in ancillary chemical pathways e.g. monoamine degradation. However, this is a less likely postulation given that the amount of neurotransmitters in isolated mitochondrial preparations is probably negligible. And, even if there were an abundance of neurotransmitters in the mitochondrial isolations, the sham animals given PZ exhibit no decrease in oxygen consumption when compared to Sham only animals.

Another idea to consider is that dopamine neurotoxicity could be responsible for the exacerbation of the injury effect in PZ-treated animals. Phenelzine, being an MAO-I, could theoretically increase dopamine transmitter levels within neuronal synapses thereby increasing levels of posttraumatic free radical production due to dopamine autoxidation. However, this contradicts our experimental observations in that PZ is able to at least reduce oxidative damage in mitochondria after TBI. If dopamine toxicity were responsible for decreased states of respiration, then markers of oxidative damage would likely increase, not decrease. Additionally, this idea draws little support in that the RCR would also likely decrease.

The other possibility is that PZ is exacerbating a known phenomenon to occur after neuronal injury: γ -aminobutyric acid (GABA) excitation [173]. GABA excitation is likely an aberrant developmental mechanism meant to facilitate growth cone modulation by allowing the efflux of chloride ions (Cl^-) which depolarize voltage-gated channels exacerbating the already excitotoxic calcium (Ca^{2+}) influx. [172, 176, 177, 180]. Phenelzine may indeed worsen this effect further through the inhibitory action of PZ metabolites which directly inhibit the primary means of GABA synaptic clearance: GABA-transaminase (GABA-T). Treatment with PZ would inhibit GABA-T, GABA levels would then rise to stimulate an excitation response e.g. an influx of Ca^{2+} . The additional influx of calcium would facilitate the decreased mitochondrial respiration which has been demonstrated in other published works by calcium's modulation of the membrane potential [73, 108].

Our previously and current data published manuscript seemingly contradicts this notion because mitochondria exhibit an increase of respiration (RCR) following a single

treatment of PZ. In the GABA hypothesis, we would expect a decrease in RCR. However, while it is true that PZ can inherently increase GABA levels [147, 197], low doses of PZ have been reported to inhibit MAO activity but not affect GABA levels [183]. This may explain why a single dose of PZ after TBI would increase respiration. It would also explain why in the current work, multiple doses would decrease individual states of respiration via GABA excitotoxicity.

This theory is also supported by our experiment evidence in **Chapter 5** which indicates that PZ significantly increases the capacity of mitochondria to buffer higher levels of calcium. The additional positive charges on Ca^{2+} influence many factors contributing to oxidative phosphorylation including but not limited to inactivation of matrix enzymes necessary for oxidative metabolism, altered local redox potentials for proton translocation, or even electron transfer mechanism interference [93]. In other words, PZ is allowing mitochondria to buffer calcium for a specified amount of time but the final result is decreased respiration.

7.2.2 Cortical Tissue Sparing without Protection from Spectrin Degradation

The ability of PZ to influence how the injured neuron handles Ca^{2+} accumulation might also explain why multiple doses of PZ can spare cortical tissue after injury, while a single dose may not. As previously mentioned a low dose of PZ will not affect significantly GABA levels. Under this premise one would expect that a single dose of PZ would be able to increase cortical tissue sparing as assessed 72 hours after injury because GABA excitotoxicity would not be a factor. On the contrary we demonstrate that multiple doses

of PZ are able to protect tissue sparing but not the single dose. Firstly, the single PZ dose may not entirely qualify as a “low dose” at 10 mg/kg and therefore some neurons would still exhibit GABA excitotoxicity. Secondly, higher doses of PZ that elicit tissue sparing may indicate that at 72 hours during the injury evolution, the ability to scavenge deleterious carbonyls is a far greater benefit than the deleterious effect of possibly stimulating spectrin degradation.

This notion though calls for the reappraisal, or at very least, a further investigation of the functionality of degraded spectrin. To use an analogy, if one’s home burns down then the appropriate means to repair the home would be to strip out all of the charred and damaged components of the house and frame. This may also hold true for synaptic plasticity that ensues after neuronal damage. GABA excitation already exists after neuronal injury to modulate neurite outgrowth, specifically by *causing* an influx of calcium that activates specific enzymes required for these remodeling processes. It is not beyond the realm of possibility that some of those intentionally activated enzymes would be calpains-- for the purpose of “remodeling” the cytoskeleton i.e. degrading spectrin just as one would be required to do in order to rebuild after a house fire.

In other words, PZ could exacerbate GABA excitation which increases calcium influx that leads to increases of calcium breakdown products. Counter-intuitively cell survival may be prompted by the benefit of reducing mitochondrial respiration in an uncoupled state (State IV), as well as the beneficial effect of PZ scavenging deleterious reactive aldehydes. This would require evidence that spectrin breakdown can exist with increased cell survival, which has currently not been demonstrated

7.3 Experimental Limitations

7.3.1 Synaptic Mitochondria vs. Non-Synaptic Mitochondria

We would be remiss not to have considered the implications of experimental limitations. For instance, one of the most noted and speculated limitation is in what type of mitochondria are benefiting from PZ exposure. Our isolation preparation consist of synaptic and non-synaptic mitochondria and therefore do not distinguish between mitochondria that exist within neurons and that of that other sources such as astrocytes, microglia, and vascular elements. At the very least if the mitochondria being protected after injury are indeed from non-neuronal sources—then salvaging this mitochondrial pool is still important since the brain’s astrocytic, microglial and vascular mitochondria are still important to protect along with the at risk neurons.

7.3.2 Phenzine Dose Response

An extensive dose response was performed *ex vivo* to establish the optimal dose required of PZ to protect against exogenously applied 4-HNE and ACR. However, both dosing paradigms that were used in **Chapter 5** were the result of indirect observations based upon our work and others’ [122, 144, 145]. The PZ single dose was a modification of previously published work, while the inclusion of multiple doses over 72 hours was based on the time course for 4-HNE and ACR and the desire to maximize PZ exposure to reactive aldehydes. The error in this logic is that this introduces the possibility to activate or inactivate cellular mechanisms not previously considered such as the likelihood of PZ

to exacerbate GABA excitotoxicity and possibly preempt spectrin degradation amelioration.

7.4 Technical Considerations

7.4.1 Previous Experiment Repeatability

Within this dissertation project we have investigated the ability of PZ to provide neuroprotection using histologic analysis of ipsilateral cortical tissue volume sparing and western blot cytoskeletal spectrin degradation assays. Although the intent of these experiments was to ascertain if PZ can spare cortical tissue after CCI-TBI in rats, the spared tissue is not necessarily comprised of *only* spared cortical neurons. Accordingly, important distinctions must be clarified when interpreting data based on a technical understanding of these experiments.

One fervent criticism to be addressed is repeatability of the current histological experiments with that of previously published work by our laboratory. It is absolutely necessary to recognize first that the current histology experiment of this dissertation is *not* a repeat experiment of the former published histological experiment: a single dose of PZ injected 15 minutes after injury and assessed 72 hours later is *not* a “recreation” of the previously published experiment wherein a single dose of PZ is injected 15 minutes after injury and then assessed 2 weeks later. The opposing critique implies that the current single PZ injection did not afford the same histological tissue sparing as we previously published and therefore have not provided repeated results. The nomenclature “opposing critique” is

used as because the single dose demonstrated the same percent of protection at 72 hours as the same does at 2 weeks although without reaching significance.

I am not so naïve as to disregard the diminished probability that brain tissue thought to be “lost” at a 72 hour time point would “regenerate” and then “exist” two weeks later. However, it is a blatant and cavalier assumption to assert that PZ does not at all possess the ability to decrease cortical cavitation over time, especially considering the experiment was not designed to investigate this possibility. Furthermore, PZ’s neuroprotective capabilities are hardly characterized and do not *necessarily* follow the same prototypical cortical cavitation evolution of a non-drug treated animal after TBI. Future exploration of PZ’s ability to mediate angiogenesis or enhance glial scar tissue formation within the cortical tissue previously thought to only exist as a cavity might better address the possibility that PZ is able to mediate such a response.

For argument’s sake, if PZ is not able to provide immediate tissue sparing at 72 hours but does increase tissue sparing at two weeks, some other underdeveloped biology could exist under the influence of PZ. To assert that tissue lost at 72 hours will never come back is an assumption; though it is one based on experience with the CCI model it is not a conclusion deduced from experimentation with PZ. PZ-induced tissue regeneration is a not an assumption but rather supposition that must be recognized as a possibility until it is definitely dismissed with evidence. Until that evidence is provided it would be inappropriate to anecdotally dismiss.

Additionally, my own technical capability to process histological sections have been regarded as “too delicate... [and] histological preparations would normally lose more

dead and dying tissue in the epicenter of the injury.” In other words, the single dose PZ treated animals would have more pronounced cavitation if I was not so careful as to preserve the tissue. To which I retort without hubris, my technique is the way it is for a reason. I aim to investigate the ability of PZ to spare cortical tissue, not only increase or maintain the neuronal population. If I lose tissue in processing, how would I be able to make conclusions?

Interestingly, further consideration of the data from the previous work and the current work are more similar than different and may even preempt the necessity for hypothetical cavitation recovery argued above. Regardless, my previous argument is not superfluous as it is imperative for a scientist to consider all possibilities and deduce from those that are most likely and pertinent.

For instance our previous publication had investigated the ability of PZ to spare cortical tissue after a CCI-TBI in the rat [50]. A single injection of PZ was given 15 minutes after injury and histological quantification of spared cortical tissue volume was performed 14 days after injury. As published, a statistically significant 96.8% (SD +/- 2.3, n =4) of ipsilateral cortical tissue in PZ treated animals was spared compared to contralateral cortical tissue. Our current work also investigated the ability of a single dose of PZ injected 15 minutes after injury but assessed for cortical tissue sparing 72 hours after injury. As submitted for publication, and presented in **Figure 6.3**, the mean ipsilateral cortical tissue spared was 96.4% (SD +/- 6.3, n =8). The reported means of cortical tissue sparing are both approximately 96%, however, the current experiment was not designed to exactly repeat the previous and included another group: the PZ multiple dosing paradigm cohort. Appropriately, when comparing multiple groups an ANOVA was used to

determine significance which is similar but different than the previous work reporting differences with a standard T-test. While it may seem appropriate to disregard the multiple dosing paradigm group and run another T-test, a Bonferroni correction is necessitated to account for multiple comparisons but would increase the chances of making a Type 1 error e.g. finding significance when there is none. Ironically, the Bonferroni correction reduces the chances of making a Type 1 error, but increases dramatically the chances of increasing a Type II error e.g. lose the power to detect true differences. The current experiment reports a higher variability (SD +/- 6.3, n =8), and Bonferroni correction is used the α increases and significance is lost between groups.

Even though the PZ single dose means that are reported from the current (96.4%) and previous work (96.8%) are indeed similar, the means for the vehicle-treated animals are not as near. The previous work reports vehicle-treated animals to have means of 85.9% (SD +/- 3.5, n =4) while the current work reports the vehicle treated means at 92.8% (SD +/- 2.7, n =8). See **Figure 7.1**. This is another important caveat that highlights that these two studies while related are not the same. One would reasonably expect more cortical tissue lesion volume in vehicle-treated animals as dead and dying tissue is cleared between 72 hours and 14 days. This would suggest that PZ in the previous work has a stronger effect as the lesion volume is larger than it is at 72 hours. This would mean that the effect of the drug might target neuron loss between 72 hours and 2 weeks more than 0-72 hours. However, this would require PZ to somehow target neuron loss between 72 hours and 2 weeks more than 0-72 hours, which is a concept that has yet to be explored as a viable possibility.

Figure 7.1 also demonstrates the PZ multiple and single dosing paradigm with the ability to increase cortical tissue sparing above 100%. Given that these measurements are made in comparison with the contralateral hemisphere, the PZ treated animals may be experiencing some localized swelling of the ipsilateral hemisphere. This could be from increased blood pooling or clotting as well as altering the nascent chemiosmotic environment of the injury to attract water molecules.

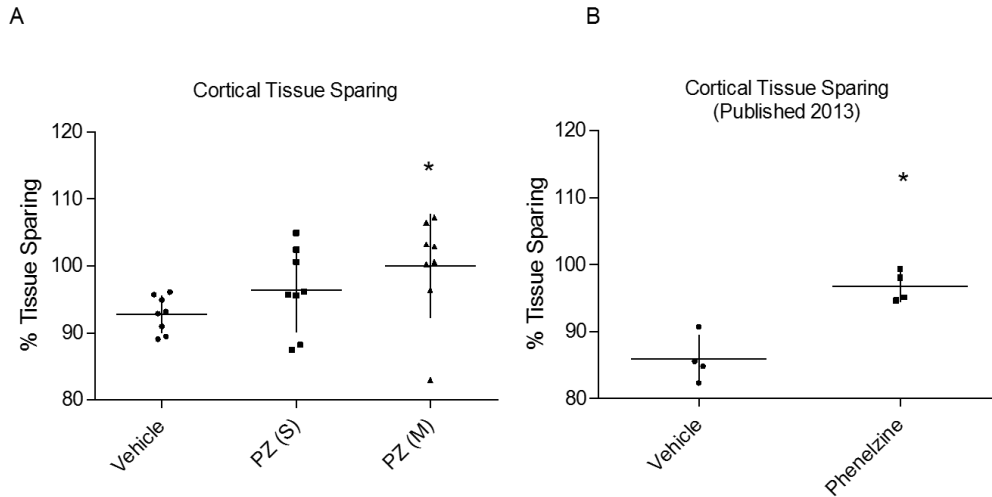


Figure 7.1 (A) Quantification of cortical tissue sparing as reported in Chapter 6. Rats were assessed 72 hours after severe CCI-TBI. Treatments consisted of either PZ_s or PZ_m. PZ_s group was given a single injection of PZ 15 minutes after injury. PZ_m group was given an injection of PZ 15 minutes after injury followed by a maintenance dose every 12 hours for 72 hours. ANOVA followed by Dunnett's post-hoc test. * = $p < 0.05$. Horizontal bars represent means. Error bars represent +/- SD; n = 8 rats per group.

(B) Quantification of cortical tissue sparing as previously published Student T-test. * = $p < 0.05$. Horizontal bars represent means. Error bars represent +/- SD; n = 4 rats per group. PZ_s demonstrates an increased variability that the previously published experiment did not.

With different surgeons come forth intrinsic differences in variability. And, gross anatomical investigation of our extracted rat brains compared to other labs' is also different. See **Figure 7.2**. We value the stochastic nature of the injury response and do not excessively wash or clean away the damaged tissue. This tissue may be of different origin e.g. infiltrating microglia or connective tissue supplied in the hematoma. This occurrence of tissue may or may not be classified as neuronal but it is tissue and it does exist where there was once a vacant lesion. We value the possibility of preserving the infrastructure for neurite outgrowth; rationalization afforded by experimentation with *in vitro* neuronal outgrowth. Neurons do like to grow where there exists no substrate.

One possible limitation is that the Vehicle-treated animals may still be losing tissue in the histological processing. When the gross anatomy of **Figure 7.2** is compared to that of the histological tissue sparing **Figure 6.3** the tissue in vehicle treated animals appears to have maybe more cavitation than that evident in coronal sections which suggest that tissue could be lost in the vehicle groups. The solution to rule out this possibility would be to use paraffin embedded histological processing to reduce further the chances of tissue being lost in free floating processing. However, our laboratory does utilize paraformaldehyde in our processing which is a polymer of regular formaldehyde that cross links amines at further distances for a more natural preservation. Formaldehyde only preparations can distort tissues by virtue of their inherently short length crosslinks and seem to have a more rigid quality susceptible to breakage.

It is important to note that while we value the measurements of all tissue within the cortical lesion, as do other labs [106, 123] this can introduce sampling bias in the

investigation of mitochondrial bioenergetics and spectrin degradation assays which will be considered in subsequent sections.

Of more pressing importance is the question of injury severity between different studies. The injuries in each of the studies were performed by different surgeons and as such variability would naturally exist between experiments. The severity of the injury can have a major effect on drug efficacy and may account for some experiment differences within in experiments. For instance, the lessened ability of PZ to provide tissue sparing with a single dose in the recent experiments maybe be due to PZ having to protect against a comparatively profound injury when compared to the original experiments performed in 2013.

Additionally, the means by which spared tissue is measure may inappropriately include narcotic tissue as the traces are made at 1.25X instead of higher magnification to circumvent dying tissue. Although the methods for measuring spared tissue were the same in both experiments, the recent experiments did use a computer device (free hand pen) with increased accuracy in tracing the outline of cortical spared tissue as opposed to a track-ball mouse. Taken together, different injury severities and intrinsic bias to count necrotic tissue are potentially significant sources of bias.

Extracted Rat Brains

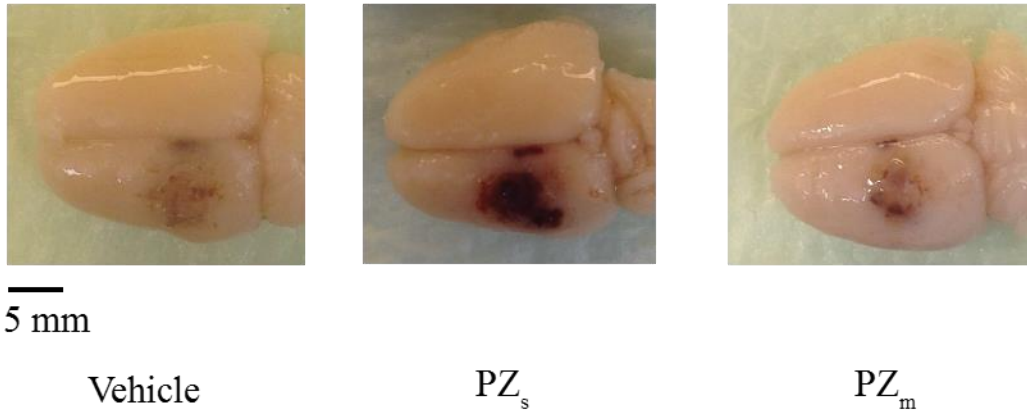


Figure 7.2 Macroscopic morphology of extracted brains and associated trauma. Animal brains were photographed after paraformaldehyde perfusion and glucose exposure gradients prior to histological processing and sectioning. Quantification of coronal sections was presented in **Figure 6.3**. The images above represent a single prototypical brain from each respective group (n =8).

7.4.2 Possibility of Mitochondrial Sampling Bias

The presence of mitochondria in vehicle treated animals is expected to decrease as the total amount of tissue is decreased. In other words, we would expect to see decreasing amounts of mitochondrial proteins in our vehicle-treated animals in our *in vivo* experiments. The logic is that the cavitation that exists 72 hours after injury is sufficient to reduce the quantity of mitochondria expected to be isolated in cortical tissue punches following experimental TBI.

What is observed, however, is similar amounts of mitochondrial protein isolated from each group save the PZ multiple dose group which is significantly elevated compared to sham. **Figure 7.3**

The elevated mitochondrial samples from the PZ treated groups can be supported with the preservation of cortical tissue sparing demonstrated in **Chapter 6**. Increased concentrations of mitochondria that are isolated from PZ treated rats, could be in part due to an uncharacterized ability of PZ to increase the amount of cells within the lesion e.g. microglia that could contribute to the mitochondria pool or increase proliferation of ancillary supportive tissue. A simple procedural intervention for future experiments would be to separate the mitochondrial pools and assess that which is only relative to neurons e.g. implement synaptic mitochondrial isolation protocols.

According to **Figure 7.3**, Vehicle-treated rats do not contribute less mitochondria despite having a pronounced lesion volume as evident by histology. As discussed previously, if the vehicle treated animals are losing tissue in the histological preparation then one could attribute the lack of mitochondrial deficit to the gross anatomical images

that do not appear to have such a pronounced lesion. Another possibility for finding equal concentrations of mitochondria in vehicle treated groups could be due to the increased presence of microglia and astrocytes which are facilitating the glia scar suspected in **Figure 7.4**, below.

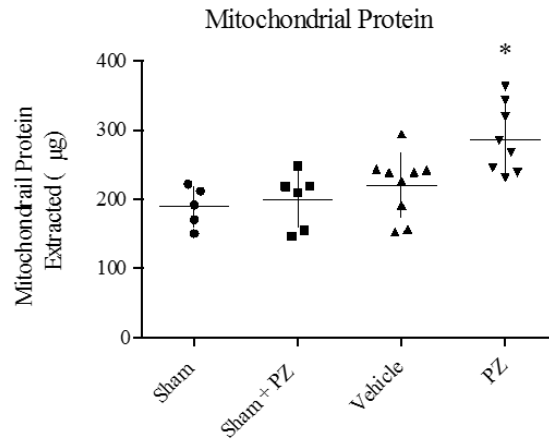


Figure 7.3 Quantification of rat cortical mitochondrial protein extracted from 8mm punch as measured by Bradford protein assay for mitochondrial bioenergetics studies reported in **Chapter 5**. ANOVA followed by Dunnet's post-hoc test. * = $p < 0.05$. Horizontal bars represent means. Error bars represent +/- SD; $n = 8/9$ rats per group except Sham and Sham + PZ where $n = 5/6$ rats per group.

High Magnification of Cortical Lesion

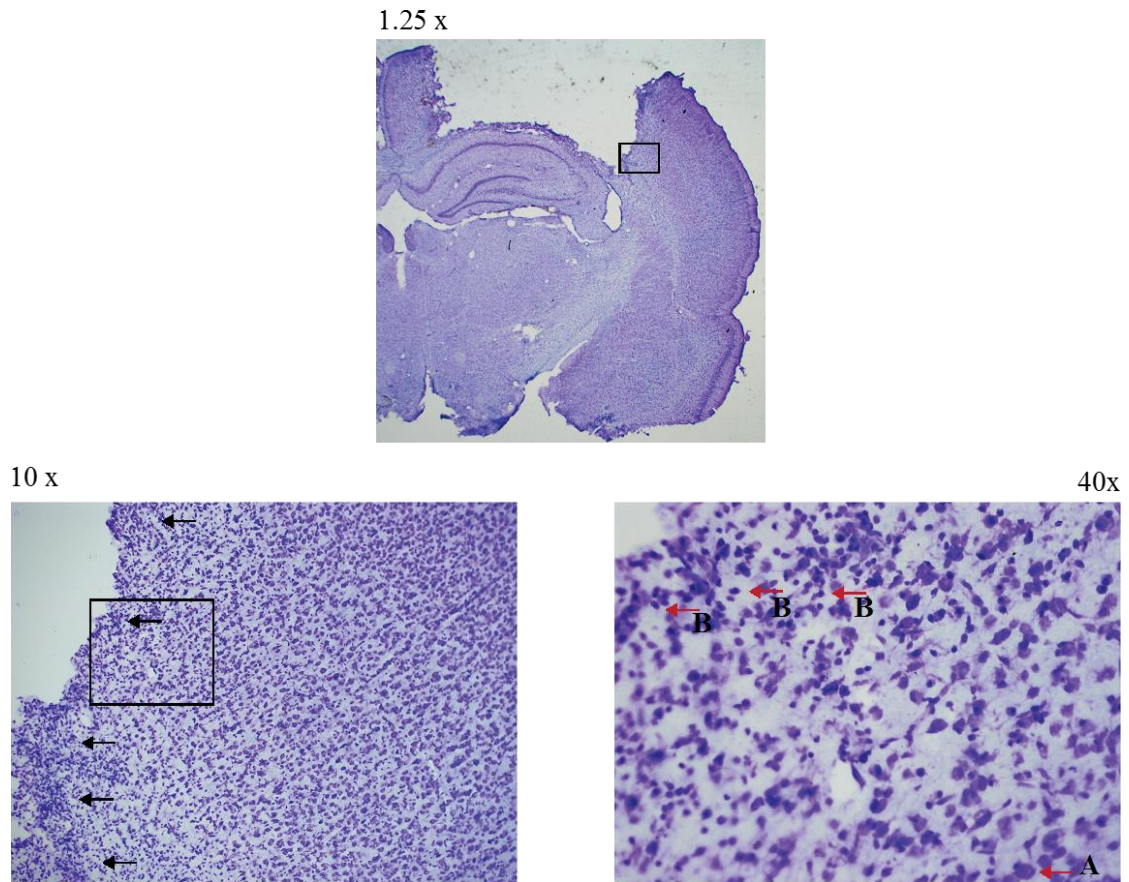


Figure 7.4 High magnification images of an intentionally chosen Vehicle treated rat following a severe TBI at 72 hours post injury. Sections were treated with cresyl violet (Nissl) staining. Low magnification image at 1.25x was included for frame of reference. Black box in 1.2x labeled image is the region identified in the 10x magnification image and so forth for the 40x image. The 10x magnification highlights with **black arrows** the abrupt cellular condensation of with glia morphology, indicative of the formation of the glia scar. Cortical neurons in the 40x magnification are identified by the letter **A** and **red arrow**. Morphology of glia tissue is exemplified in the 40x image labeled with the letter **B** and **red arrows**. Qualitatively, the images suggest that Vehicle treated animals can in some cases have no tissue in the approximately 5mm epicenter of the controlled cortical injury. However, the regions extracted by the cortical punch (8mm) would also sample surviving neurons as well as infiltrating microglia, monocytes, and microglia. The images chosen intentionally have a slightly more pronounced cavity lesion volume which seems to correlate with increased cellular condensation e.g. formation of glial scar.

There is theoretical merit in first preserving tissue, then preserving cortical neurons, then determining functionality of those neurons. This tiered approach may be a slightly more feasible means of providing neuroprotection as the former goals may facilitate the latter ones. For example, providing a matrix for astrocytic infiltration and proliferation may encourage the astrocytic Nrf2 antioxidant response to lessen ongoing free radical-mediated damage. Additional merit can be afforded in allowing glial scar tissue formation in an area that would not disrupt the function of surviving neurons. In other words, if glial scar formation disrupts normal neuronal circuitry then there may be benefit in facilitating scar tissue in the lesion cavity outside the presence of healthy neurons. While there is clinical merit in preserving any tissue, mechanistically the protection of mitochondria to afford neuroprotection may require additional experiments to investigate mitochondrial function from only neuronal origin and that of other populations.

7.4.3 Decreased Respiration of PZ-treated Mitochondria

Based upon the increased cortical tissue sparing, there is an expectation that PZ would increase mitochondrial respiration or at least preserve State III functionality. However, what is observed is a decrease in all states of respiration. The benefit of this is that mitochondria with decreased State IV respiration translates biologically to reduced respiration of mitochondria in an uncoupled state. This is apparent in the reported RCRs in **Chapter 5** wherein a decreased state IV increases the overall RCR. The Vehicle-treated mitochondria do not have a mean RCR that is below 5, what some consider the threshold

for healthy or non-healthy mitochondria. This may provide an alternative hypothesis as to why PZ is able to reduce all states of respiration aside from the GABA hypothesis discussed later.

If the effect of PZ is not apparent in the Sham treated animals, and the Vehicle-treated animals do not have dramatically (although significantly) reduced abilities to respire oxygen then one can reasonably argue that the sample of mitochondria from the Vehicle-treated groups might be exposed to sampling bias. If the histology of the Vehicle-treated animals is as pronounced as reported then the punch used to collect cortical tissue may only be sampling penumbral tissue that would survive regardless. In the vehicle treated groups, the presence of the lesion cavity implicates that no mitochondria are available e.g. there is no tissue in a cavity. Therefore the tissue in the difference of the approximate cavity size (5mm) and the cortical punch (8mm) samples tissue that has not only increase population of microglia with healthy mitochondria but also sample cortical neurons that are inherently healthier as they are more distal to the epicenter of injury. In other words, the Vehicle-treated animals have an increased occurrence of dead tissue and dead mitochondria that are removed in the isolation preparation. The effect is that the Vehicle-treated groups have an increased respiration at 72 hours. The treatment of PZ is seemingly obligating tissue that would otherwise die to instead remain and accordingly contribute more dysfunctional mitochondria to the respiration assay. Theoretically, merit can exist in increasing mitochondrial respiration of non-neuronal cells but, mechanistically future experiments should either reduce the severity of the injury i.e. reduce cavity formation or assess mitochondrial function at an earlier time point to be able to more definitively understand the influence of PZ on dysfunctional mitochondria.

7.4.4 Increased Spectrin Degradation and Increased Calcium Buffering Capacity

Phenelzine preserves ability of mitochondria to more effectively buffer increasing calcium concentrations after injury but simultaneously does not prevent the calcium-activated, calpain-mediated degradation of spectrin. The influx of calcium after injury may be sufficient enough to activate calpains and subsequently lead to increased cytoskeletal degradation. However, a technical limitation would be similar to that discussed earlier. The vehicle treated animals have a more pronounced lesion volume, because the cavity is void of dying tissue. Presumably, the tissue is already dead and cleared, then the amount of spectrin degradation in Vehicle-treated animals is reduced. If PZ is truly increasing spared tissue, this tissue could still be damaged, but managing to survive although somewhat dysfunctional. This could result in decreased degraded spectrin in Vehicle-treated tissue (as it is already cleared) and increased degraded spectrin in PZ-treated animals (as more damaged, but still surviving tissue is preserved). Future experiments will be needed to test this hypothesis by reducing the lesion cavitation by decreasing the severity of the injury or sampling cortical tissue earlier in the evolution of the cavity, for example at 24 hours.

7.4.5 Preserving Cortical Lesion Volume

As previously discussed, the effect of PZ does increase cortical tissue sparing significantly with a multiple dosing paradigm and to a lesser extent a single dose. An important caveat is that the intent is to preserve any cortical tissue beyond that of only cortical neurons. However, higher magnification of the peri-penumbral regions after PZ

treatments subsequent to TBI in the rat do qualitatively demonstrate a larger “transition” zone than Vehicle-treated animals. Qualitatively, Vehicle-treated animals have a more abrupt transition from typical “healthy” cortical neurons to that of cell morphologies that are indicative of glial scarring. In both PZ single and multiple treatment groups, the transition zones typified by the presence of glial cells and cortical neurons is seemingly larger. See **Figure 7.4**. Further quantification of this penumbral zone would help to directly implicate neuroprotection and not simply tissue sparing.

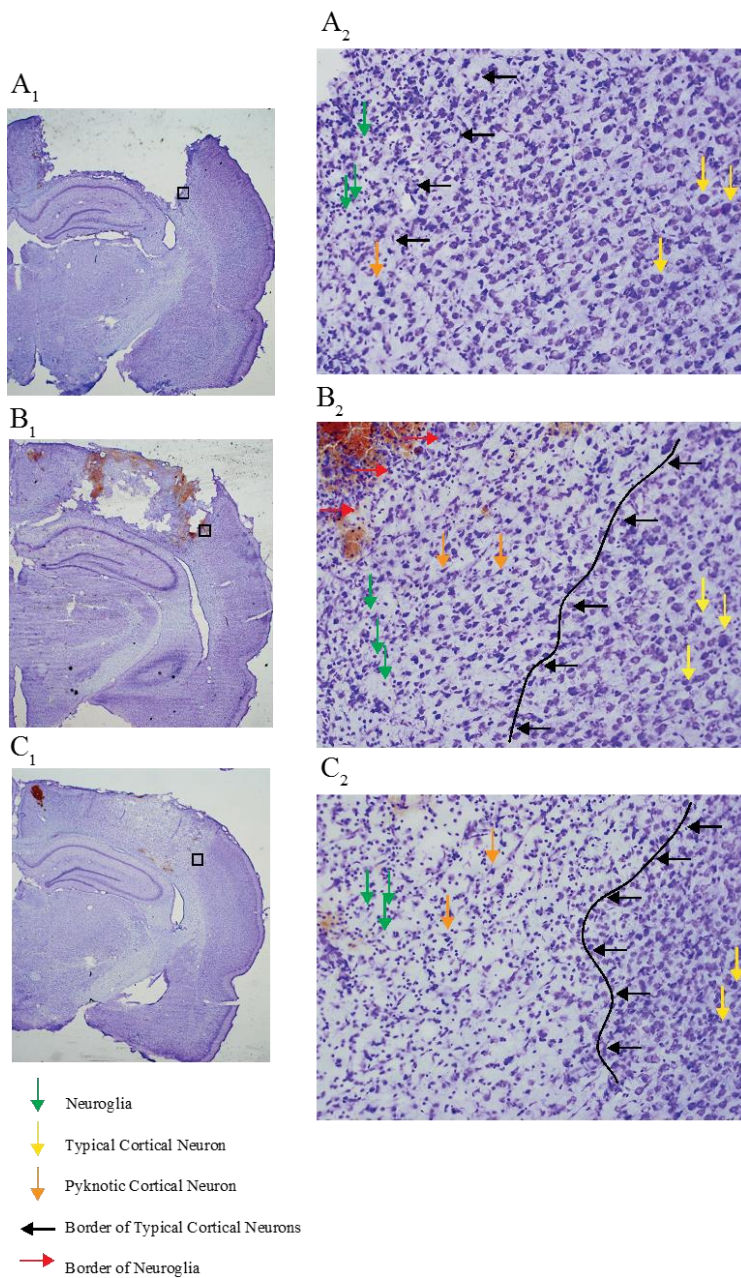


Figure 7.5 High 20x magnification images of Vehicle-treated rats (**A₁-A₂**), PZ_s (**B₁-B₂**), and PZ_m (**C₁-C₂**) processed for tissue sparing analysis in accordance with injury and dosing paradigms presented in **Chapter 6**. **A₁**, **B₁**, and **C₁** included for reference. Sections were treated with cresyl violet (Nissel) staining.

A2) Qualitative analysis of **A2** depicts sooner transition of cortical neurons **blue arrows** to cells consistent with microglial morphology **green arrows**.

B2) Cortical neurons represented by **blue arrows** appear to transition into pyknotic cortical neurons (**yellow arrows**) over a greater distance starting at the roughly drawn black line with **black arrows**. A larger zone of transition is evident compared to the Vehicle-treated animal. The transition zone, characterized by both pyknotic neurons and glial, tapers off dramatically at the edge of the preserved tissue wherein microglial become the predominant cell morphology **red arrows**.

C2) Cortical neurons **blue arrows** transition almost entirely through the epicenter (tissue directly under the point of impact). Pyknotic neurons are indicated by **yellow arrows**, while green arrows indicate cells of microglial morphology.

Collectively these images suggest that PZ is indeed sparing cortical tissue, and qualitatively appear to be increasing the extent of preserved cortical neurons by increasing the transition zone from the point of injury radially.

7.5 Ancillary considerations

7.5.1 Profiling

While the generalities of how 4-HNE and ACR are able to induce cytotoxicity for both the neuron and the mitochondria have been extensively discussed, the precise means of mitochondrial respiratory inhibition have yet to be determined. Further characterization of how 4-HNE and ACR specifically inhibit mitochondrial function or other cellular process could translate to a better drug design. For example, should reactive carbonyls be found to bind key enzymes within the mitochondrial matrix that are responsible for essential steps in substrate oxidation, future iterations of hydrazine-containing compounds could be designed with modified lipophilicity to penetrate with greater ease multiple lipid bilayers.

Other characterizations would be to further describe the extent of neuroprotection by examining protein crosslinking and PZ's ability to protect against it. Reactive carbonyls have the ability to facilitate protein cross-linking as is such with heat shock protein 90 (HSP 90) [119], which might have epitopes that current anti-bodies cannot detect due to protein complex steric hindrance.

7.5.2 Aberrant Scavenging and Metabolism

Additional considerations may be necessary to establish upper bounds of carbonyl scavenging after injury. There could exist a natural point at which the severity of the injury generates far too many reactive carbonyls that would require deleterious doses of PZ.

Subsequently these high doses of PZ may inappropriately scavenge endogenous useful carbonyls such a pyridoxal phosphate. Pyridoxal is a co-factor that does contain a carbonyl, however, the function of which is to potentiate the synthesis of vital neurotransmitters like dopamine, serotonin, and to make matters even more complex: GABA [141, 203].

Metabolic clearance may too be another eventual concern. The metabolism of excessively large protein complex that can form due to PZ conjugation may stress the metabolic clearance pathways. Typically, hydrazine-containing compounds that form conjugation products undergo degradation and clearance in the liver by glucuronidation, *N*-acetylation, and sulfonation [141]. However, metabolic clearance of super-complexes have not been investigate like the degradation of ACR *bis*-Michael additions. In this case, a single lysine residue would bind two ACR molecules rendering the protein dysfunctional but more deleteriously the protein is now capable of binding two more proteins (or PZs) through the remaining electrophilic centers on each of the bound ACRs [204].

These reactions, reported by the same authors, are the second most typical reactions formed by ACR when binding to lysine residues. Not only does this cause a concern for metabolic clearance as a complex formed to phenelzine, but also invites the potential to create neoantigens that could theoretically simulate drastic immune responses.

7.6 Concluding Remarks

Caution is always warranted when inviting a compound with rather complex pharmacology in to a biological system. Special attention should always be made for the

entire system and too much focus on pre-defined endpoints may demonstrate some miraculous recovery but compromise the integrity of the biological entity.

For, instance the introduction of PZ may indeed increase neuroprotection by increasing mitochondrial function but PZ could also derail a biologically self-limiting system. After TBI, reactive aldehydes like 4-HNE and ACR are produced in excess and bind to proteins with an affinity for *specific* protein residues to inhibit overall protein functionality. Separately, but concurrently with, the synthesis of 4-HNE and ACR is the activation of deleterious calpains and caspases. It is not irrational to speculate that the “intended” function of reactive aldehydes is to bind and inhibit deleterious calpains and caspases to prevent overall neuronal death. In this context, adding PZ to the system would scavenge most of the available reactive aldehydes that could theoretically be responsible for inactivating calpain-mediated spectrin degradation. Without further investigation, PZ could be *dis*-inhibiting natural self-limiting processes.

The role of phenelzine as a potential neuroprotective agent is certainly still in development and several key observations have communicated the complexity of its use *ex vivo* and *in vivo*. However, traumatic brain injury is *profoundly* complicated. The best solution will not be the easiest and low-hanging fruit is a farce. The complexity of the solution needs to match the complexity of the problem. And, so far PZ is pretty complex.

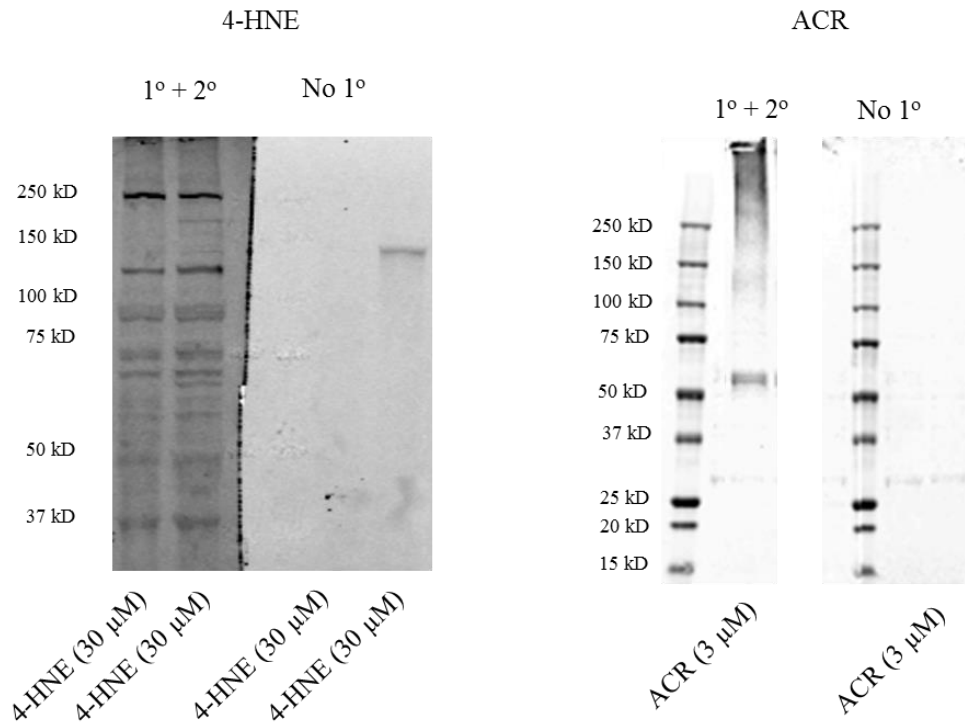
APPENDIX

Appendix A: List of Acronyms and Abbreviations

$\Delta\Psi_m$	Mitochondrial Membrane Potential
Δp	Proton Motive Force
3-NT	3-Nitrotyrosin
4-HNE	4-Hydroxynonenal
AA	Arachidonic Acid
ADP	Adenosine Diphosphate
ACR	Acrolein
ATP	Adenosine Triphosphate
ANOVA	Analysis of Variance
BBB	Blood-Brain Barrier
Ca ²⁺	Calcium Ion(s)
CaG5n	Ca ²⁺ -sensitive indicator Calcium Green 5 N
CCI	Controlled Cortical Impact
CDC	Center for Disease Control
CNS	Central Nervous System
CSF	Cerebrospinal Fluid
ER	Endoplasmic Reticulum
ETS	Electron Transport System
FAD	Flavin Adenine Dinucleotide
FCCP	p-trifluoromethoxy Carbonyl Cyanide Phenyl Hydrazone
FMNH ₂	Reduced Flavin Mononucleotide
GCS	Glasgow Coma Score
GABA	γ -Aminobutyric Acid
IMM	Inner Mitochondrial Membrane
IMS	Inner Mitochondrial Space
iNOS	Inducible Nitric Oxide Synthase
NO	Nitric Oxide
LP	Lipid Peroxidation
MAO	Monoamine Oxidase
MAOI	Monoamine Oxidase Inhibitory
MOS	Military Occupational Specialty
mPTP	Mitochondrial Permeability Transition Pore
mtNOS	Mitochondrial Nitric Oxide Synthase
NADPH	Nicotinamide Adenine Dinucleotide Phosphate-Oxidase
nNOS	Neuronal Nitric Oxide Synthase
NMDA	N-methyl-D-aspartate
OCR	Oxygen Consumption Rate
OMM	Outer Mitochondrial membrane

PBS	Phosphate Buffer Solution
PG	Pargyline
PM	Plasma Membrane
PUFA(s)	Polyunsaturated Fatty Acids
PZ	Phenelzine
PZ _m	Multiple Doses of Phenelzine
PZ _s	Single Dose of Phenelzine
RCR	Respiratory Control Ratio
RNS	Reactive Nitrogen Species
ROS	Reactive Oxygen Species
SBDP	Spectrin Breakdown Products
SCI	Spinal Cord Injury
SD	Sprague-Dawley
SOD	Super Oxide Dismutase
TBI	Traumatic brain injury
TBS	Tris-Buffered Saline
TCA	Tricarboxylic acid
VOC	Voltage-operated channels
UQ	Ubiquinone
UQ ^{•-}	Semiquinone Anion
UQH ₂	Ubiquinol

Appendix B: Immunoblotting, No Primary Controls



Appendix B: Naïve rat mitochondrial samples were exposed to a 10 minute incubation of 4-HNE (30 μ M) or ACR (3 μ M). 4-HNE and ACR were incubated consistent with previously described methods and concentrations. 4-HNE and ACR were also blotted without primary antibodies (right side of each western blot) to probe for non-specific binding. Non-specific binding was not present between 150 kD and 50 kD; the defined region of interest. Naïve rat mitochondrial samples assayed for 4-HNE adducts were separated on a precast gel (12% Bis-Tris w/v acrylamide; Criterion XT, Bio-Rad) with XT-MOPS buffer (Bio-Rad). Naïve rat mitochondrial samples assayed for ACR adducts were separated on precast gel (4-12% gradient Tris-Acetate gels) using MOPS buffer (BioRad). 4-HNE rabbit polyclonal primary antibody (Alpha Diagnostics) was diluted 1:2,000. ACR mouse monoclonal antibody (Abcam, United States) was diluted at 1:1,000. 4-HNE and ACR primary antibodies were detected via 2 hour incubation at room temperature with goat rabbit immunoglobulin G (IgG) or anti-mouse IgG secondary antibody conjugated to infrared dye (1:5000, IRdye-800CW, Rockland) in TBST.

REFERENCES

1. Summers, C.R., B. Ivins, and K.A. Schwab, *Traumatic brain injury in the United States: an epidemiologic overview*. Mt Sinai J Med, 2009. **76**(2): p. 105-10.
2. Thurman, D.J., et al., *Traumatic brain injury in the United States: A public health perspective*. J Head Trauma Rehabil, 1999. **14**(6): p. 602-15.
3. Communications, M.O.o.S., *DOD Numbers for Traumatic Brain Injury- Total Worldwide TBI Diagnoses*. 2013.
4. Control, N.C.f.I.P.a., *Report to Congress on Mild Traumatic Brain Injury in the United States: Steps to Prevent a Serious Public Health Problem*.
5. Maas, A.I., N. Stocchetti, and R. Bullock, *Moderate and severe traumatic brain injury in adults*. Lancet Neurol, 2008. **7**(8): p. 728-41.
6. LaPlaca, M.C., et al., *CNS injury biomechanics and experimental models*. Prog Brain Res, 2007. **161**: p. 13-26.
7. Sullivan, P.G., et al., *Dose-response curve and optimal dosing regimen of cyclosporin A after traumatic brain injury in rats*. Neuroscience, 2000. **101**(2): p. 289-295.
8. Narayan, R.K., et al., *Clinical trials in head injury*. J Neurotrauma, 2002. **19**(5): p. 503-57.
9. Sauaia, A., et al., *Epidemiology of trauma deaths: a reassessment*. J Trauma, 1995. **38**(2): p. 185-93.
10. Teasdale, G. and B. Jennett, *Assessment of coma and impaired consciousness. A practical scale*. Lancet, 1974. **2**(7872): p. 81-4.
11. Saatman, K.E., et al., *Classification of traumatic brain injury for targeted therapies*. J Neurotrauma, 2008. **25**(7): p. 719-38.
12. Lighthall, J.W., *Controlled cortical impact: a new experimental brain injury model*. J Neurotrauma, 1988. **5**(1): p. 1-15.
13. Hannay, H.J., et al., *Validation of a controlled cortical impact model of head injury in mice*. J Neurotrauma, 1999. **16**(11): p. 1103-14.
14. Smith, D.H., et al., *A model of parasagittal controlled cortical impact in the mouse: cognitive and histopathologic effects*. J Neurotrauma, 1995. **12**(2): p. 169-78.
15. Dixon, C.E., et al., *A controlled cortical impact model of traumatic brain injury in the rat*. J Neurosci Methods, 1991. **39**(3): p. 253-62.
16. Choi, D.W., *Ionic dependence of glutamate neurotoxicity*. J Neurosci, 1987. **7**(2): p. 369-79.
17. Tymianski, M., et al., *Cell-permeant Ca²⁺ chelators reduce early excitotoxic and ischemic neuronal injury in vitro and in vivo*. Neuron, 1993. **11**(2): p. 221-35.
18. Tymianski, M., et al., *Source specificity of early calcium neurotoxicity in cultured embryonic spinal neurons*. J Neurosci, 1993. **13**(5): p. 2085-104.
19. Alessandri, B. and R. Bullock, *Glutamate and its receptors in the pathophysiology of brain and spinal cord injuries*. Prog Brain Res, 1998. **116**: p. 303-30.
20. Arundine, M. and M. Tymianski, *Molecular mechanisms of calcium-dependent neurodegeneration in excitotoxicity*. Cell Calcium, 2003. **34**(4-5): p. 325-37.

21. Faden, A.I., et al., *The role of excitatory amino acids and NMDA receptors in traumatic brain injury*. Science, 1989. **244**(4906): p. 798-800.
22. Randall, R.D. and S.A. Thayer, *Glutamate-induced calcium transient triggers delayed calcium overload and neurotoxicity in rat hippocampal neurons*. J Neurosci, 1992. **12**(5): p. 1882-95.
23. LaPlaca, M.C. and L.E. Thibault, *Dynamic mechanical deformation of neurons triggers an acute calcium response and cell injury involving the N-methyl-D-aspartate glutamate receptor*. J Neurosci Res, 1998. **52**(2): p. 220-9.
24. Hanna, R.A., R.L. Campbell, and P.L. Davies, *Calcium-bound structure of calpain and its mechanism of inhibition by calpastatin*. Nature, 2008. **456**(7220): p. 409-12.
25. Cuerrier, D., T. Moldoveanu, and P.L. Davies, *Determination of peptide substrate specificity for mu-calpain by a peptide library-based approach: the importance of primed side interactions*. J Biol Chem, 2005. **280**(49): p. 40632-41.
26. Hyrc, K., et al., *Ionized intracellular calcium concentration predicts excitotoxic neuronal death: observations with low-affinity fluorescent calcium indicators*. J Neurosci, 1997. **17**(17): p. 6669-77.
27. Liu-Snyder, P., et al., *Acrolein-mediated mechanisms of neuronal death*. J Neurosci Res, 2006. **84**(1): p. 209-18.
28. Tompa, P., et al., *On the sequential determinants of calpain cleavage*. J Biol Chem, 2004. **279**(20): p. 20775-85.
29. Huh, G.Y., et al., *Calpain proteolysis of alpha II-spectrin in the normal adult human brain*. Neurosci Lett, 2001. **316**(1): p. 41-4.
30. Kilinc, D., G. Gallo, and K.A. Barbee, *Mechanical membrane injury induces axonal beading through localized activation of calpain*. Exp Neurol, 2009. **219**(2): p. 553-61.
31. Saatman, K.E., et al., *Traumatic axonal injury results in biphasic calpain activation and retrograde transport impairment in mice*. J Cereb Blood Flow Metab, 2003. **23**(1): p. 34-42.
32. Buki, A., et al., *Preinjury administration of the calpain inhibitor MDL-28170 attenuates traumatically induced axonal injury*. J Neurotrauma, 2003. **20**(3): p. 261-8.
33. Saatman, K.E., et al., *Prolonged calpain-mediated spectrin breakdown occurs regionally following experimental brain injury in the rat*. J Neuropathol Exp Neurol, 1996. **55**(7): p. 850-60.
34. Kupina, N.C., et al., *The novel calpain inhibitor SJA6017 improves functional outcome after delayed administration in a mouse model of diffuse brain injury*. J Neurotrauma, 2001. **18**(11): p. 1229-40.
35. Posmantur, R., et al., *A calpain inhibitor attenuates cortical cytoskeletal protein loss after experimental traumatic brain injury in the rat*. Neuroscience, 1997. **77**(3): p. 875-88.
36. Bains, M., et al., *Pharmacological analysis of the cortical neuronal cytoskeletal protective efficacy of the calpain inhibitor SNJ-1945 in a mouse traumatic brain injury model*. J Neurochem, 2012.

37. Saatman, K.E., et al., *Calpain inhibitor AK295 attenuates motor and cognitive deficits following experimental brain injury in the rat*. Proc Natl Acad Sci U S A, 1996. **93**(8): p. 3428-33.
38. Gutteridge, J.M. and B. Halliwell, *Comments on review of Free Radicals in Biology and Medicine, second edition, by Barry Halliwell and John M. C. Gutteridge*. Free Radic Biol Med, 1992. **12**(1): p. 93-5.
39. Valko, M., et al., *Free radicals, metals and antioxidants in oxidative stress-induced cancer*. Chem Biol Interact, 2006. **160**(1): p. 1-40.
40. Kovacic, P. and J.D. Jacintho, *Mechanisms of carcinogenesis: focus on oxidative stress and electron transfer*. Curr Med Chem, 2001. **8**(7): p. 773-96.
41. Cadenas, E. and H. Sies, *The lag phase*. Free Radic Res, 1998. **28**(6): p. 601-9.
42. Muller, F.L., Y. Liu, and H. Van Remmen, *Complex III releases superoxide to both sides of the inner mitochondrial membrane*. J Biol Chem, 2004. **279**(47): p. 49064-73.
43. Bianca, V.D., et al., *beta-amyloid activates the O-2 forming NADPH oxidase in microglia, monocytes, and neutrophils. A possible inflammatory mechanism of neuronal damage in Alzheimer's disease*. J Biol Chem, 1999. **274**(22): p. 15493-9.
44. Gao, H.M., et al., *Microglial activation-mediated delayed and progressive degeneration of rat nigral dopaminergic neurons: relevance to Parkinson's disease*. J Neurochem, 2002. **81**(6): p. 1285-97.
45. Hall, E.D., et al., *Lipid peroxidation in brain or spinal cord mitochondria after injury*. J Bioenerg Biomembr, 2015.
46. Adibhatla, R.M. and J.F. Hatcher, *Lipid oxidation and peroxidation in CNS health and disease: from molecular mechanisms to therapeutic opportunities*. Antioxid Redox Signal, 2010. **12**(1): p. 125-69.
47. Dohi, K., et al., *Gp91phox (NOX2) in classically activated microglia exacerbates traumatic brain injury*. J Neuroinflammation, 2010. **7**: p. 41.
48. McCord, J.M., *Oxygen-derived radicals: a link between reperfusion injury and inflammation*. Fed Proc, 1987. **46**(7): p. 2402-6.
49. Kontos, H.A. and J.T. Povlishock, *Oxygen radicals in brain injury*. Cent Nerv Syst Trauma, 1986. **3**(4): p. 257-63.
50. Singh, I.N., et al., *Phenelzine mitochondrial functional preservation and neuroprotection after traumatic brain injury related to scavenging of the lipid peroxidation-derived aldehyde 4-hydroxy-2-nonenal*. J Cereb Blood Flow Metab, 2013. **33**(4): p. 593-9.
51. Bains, M. and E.D. Hall, *Antioxidant therapies in traumatic brain and spinal cord injury*. Biochim Biophys Acta, 2012. **1822**(5): p. 675-84.
52. Beckman, J.S., *Oxidative damage and tyrosine nitration from peroxynitrite*. Chem Res Toxicol, 1996. **9**(5): p. 836-44.
53. Radi, R., *Peroxynitrite reactions and diffusion in biology*. Chem Res Toxicol, 1998. **11**(7): p. 720-1.
54. Hall, E.D., *Antioxidant therapies for acute spinal cord injury*. Neurotherapeutics, 2011. **8**(2): p. 152-67.
55. Hall, E.D., J.M. McCall, and E.D. Means, *Therapeutic potential of the lazaroids (21-aminosteroids) in acute central nervous system trauma, ischemia and subarachnoid hemorrhage*. Adv Pharmacol, 1994. **28**: p. 221-68.

56. Hall, E.D. and J.M. Braughler, *Free radicals in CNS injury*. Res Publ Assoc Res Nerv Ment Dis, 1993. **71**: p. 81-105.
57. Smith, S.L., et al., *Direct measurement of hydroxyl radicals, lipid peroxidation, and blood-brain barrier disruption following unilateral cortical impact head injury in the rat*. J Neurotrauma, 1994. **11**(4): p. 393-404.
58. Globus, M.Y., et al., *Glutamate release and free radical production following brain injury: effects of posttraumatic hypothermia*. J Neurochem, 1995. **65**(4): p. 1704-11.
59. Beckman, J.S., *The double-edged role of nitric oxide in brain function and superoxide-mediated injury*. J Dev Physiol, 1991. **15**(1): p. 53-9.
60. Radi, R., *Nitric oxide, oxidants, and protein tyrosine nitration*. Proc Natl Acad Sci U S A, 2004. **101**(12): p. 4003-8.
61. Alvarez, B. and R. Radi, *Peroxynitrite reactivity with amino acids and proteins*. Amino Acids, 2003. **25**(3-4): p. 295-311.
62. Beckman, J.S. and W.H. Koppenol, *Nitric oxide, superoxide, and peroxynitrite: the good, the bad, and ugly*. Am J Physiol, 1996. **271**(5 Pt 1): p. C1424-37.
63. Hall, E.D., et al., *Peroxynitrite-mediated protein nitration and lipid peroxidation in a mouse model of traumatic brain injury*. J Neurotrauma, 2004. **21**(1): p. 9-20.
64. Deng, Y., et al., *Temporal relationship of peroxynitrite-induced oxidative damage, calpain-mediated cytoskeletal degradation and neurodegeneration after traumatic brain injury*. Exp Neurol, 2007. **205**(1): p. 154-65.
65. Deng-Bryant, Y., et al., *Neuroprotective effects of tempol, a catalytic scavenger of peroxynitrite-derived free radicals, in a mouse traumatic brain injury model*. J Cereb Blood Flow Metab, 2008. **28**(6): p. 1114-26.
66. Kelly, K.A., et al., *Oxidative stress in toxicology: established mammalian and emerging piscine model systems*. Environ Health Perspect, 1998. **106**(7): p. 375-84.
67. Hall, E.D., R.A. Vaishnav, and A.G. Mustafa, *Antioxidant therapies for traumatic brain injury*. Neurotherapeutics : the journal of the American Society for Experimental NeuroTherapeutics, 2010. **7**(1): p. 51-61.
68. Hall, E.D., R.A. Vaishnav, and A.G. Mustafa, *Antioxidant therapies for traumatic brain injury*. Neurotherapeutics, 2010. **7**(1): p. 51-61.
69. Keller, J.N., et al., *4-Hydroxynonenal, an aldehydic product of membrane lipid peroxidation, impairs glutamate transport and mitochondrial function in synaptosomes*. Neuroscience, 1997. **80**(3): p. 685-96.
70. Hall, E.D., et al., *Effects of the 21-aminosteroid U74006F on experimental head injury in mice*. J Neurosurg, 1988. **68**(3): p. 456-61.
71. McIntosh, T.K., et al., *The novel 21-aminosteroid U74006F attenuates cerebral edema and improves survival after brain injury in the rat*. J Neurotrauma, 1992. **9**(1): p. 33-46.
72. Vaishnav, R.A., et al., *Lipid peroxidation-derived reactive aldehydes directly and differentially impair spinal cord and brain mitochondrial function*. J Neurotrauma, 2010. **27**(7): p. 1311-20.
73. Singh, I.N., et al., *Time course of post-traumatic mitochondrial oxidative damage and dysfunction in a mouse model of focal traumatic brain injury: implications*

- for neuroprotective therapy.* J Cereb Blood Flow Metab, 2006. **26**(11): p. 1407-18.
74. Hamann, K. and R. Shi, *Acrolein scavenging: a potential novel mechanism of attenuating oxidative stress following spinal cord injury.* J Neurochem, 2009. **111**(6): p. 1348-56.
 75. Petersen, D.R. and J.A. Doorn, *Reactions of 4-hydroxynonenal with proteins and cellular targets.* Free Radic Biol Med, 2004. **37**(7): p. 937-45.
 76. Stevens, J.F. and C.S. Maier, *Acrolein: sources, metabolism, and biomolecular interactions relevant to human health and disease.* Mol Nutr Food Res, 2008. **52**(1): p. 7-25.
 77. Catala, A., *Lipid peroxidation of membrane phospholipids generates hydroxy-alkenals and oxidized phospholipids active in physiological and/or pathological conditions.* Chem Phys Lipids, 2009. **157**(1): p. 1-11.
 78. Ansari, M.A., K.N. Roberts, and S.W. Scheff, *Oxidative stress and modification of synaptic proteins in hippocampus after traumatic brain injury.* Free Radic Biol Med, 2008. **45**(4): p. 443-52.
 79. Braughler, J.M. and E.D. Hall, *Involvement of lipid peroxidation in CNS injury.* J Neurotrauma, 1992. **9 Suppl 1**: p. S1-7.
 80. McCall, J.M., J.M. Braughler, and E.D. Hall, *Lipid peroxidation and the role of oxygen radicals in CNS injury.* Acta Anaesthesiol Belg, 1987. **38**(4): p. 373-9.
 81. Hall, E.D., *Free radicals and CNS injury.* Crit Care Clin, 1989. **5**(4): p. 793-805.
 82. Xiong, Y. and E.D. Hall, *Pharmacological evidence for a role of peroxynitrite in the pathophysiology of spinal cord injury.* Exp Neurol, 2009. **216**(1): p. 105-14.
 83. Lopachin, R.M. and A.P. Decaprio, *Protein adduct formation as a molecular mechanism in neurotoxicity.* Toxicol Sci, 2005. **86**(2): p. 214-25.
 84. Neely, M.D., et al., *The lipid peroxidation product 4-hydroxynonenal inhibits neurite outgrowth, disrupts neuronal microtubules, and modifies cellular tubulin.* J Neurochem, 1999. **72**(6): p. 2323-33.
 85. Zhu, Q., et al., *Natural Polyphenols as Direct Trapping Agents of Lipid Peroxidation-Derived Acrolein and 4-Hydroxy-trans-2-nonenal.* Chemical Research in Toxicology, 2009. **22**(10): p. 1721-1727.
 86. Ansari, M.A., K.N. Roberts, and S.W. Scheff, *A time course of contusion-induced oxidative stress and synaptic proteins in cortex in a rat model of TBI.* J Neurotrauma, 2008. **25**(5): p. 513-26.
 87. Uchida, K., *Current status of acrolein as a lipid peroxidation product.* Trends Cardiovasc Med, 1999. **9**(5): p. 109-13.
 88. Shi, R., J.C. Page, and M. Tully, *Molecular mechanisms of acrolein-mediated myelin destruction in CNS trauma and disease.* Free Radic Res, 2015: p. 1-8.
 89. Witz, G., *Biological interactions of alpha,beta-unsaturated aldehydes.* Free Radic Biol Med, 1989. **7**(3): p. 333-49.
 90. Esterbauer, H., R.J. Schaur, and H. Zollner, *Chemistry and biochemistry of 4-hydroxynonenal, malonaldehyde and related aldehydes.* Free Radic Biol Med, 1991. **11**(1): p. 81-128.
 91. Ghilarducci, D.P. and R.S. Tjeerdema, *Fate and effects of acrolein.* Rev Environ Contam Toxicol, 1995. **144**: p. 95-146.

92. Zick, M., R. Rabl, and A.S. Reichert, *Cristae formation-linking ultrastructure and function of mitochondria*. Biochim Biophys Acta, 2009. **1793**(1): p. 5-19.
93. Nicholls DG, F.S.B.S.D., Calif.: Academic Press. xviii, 297 p. p.
94. Chance, B. and G.R. Williams, *Respiratory enzymes in oxidative phosphorylation. III. The steady state*. J Biol Chem, 1955. **217**(1): p. 409-27.
95. Figueira, T.R., et al., *Mitochondria as a source of reactive oxygen and nitrogen species: from molecular mechanisms to human health*. Antioxid Redox Signal, 2013. **18**(16): p. 2029-74.
96. Quinlan, C.L., et al., *The 2-oxoacid dehydrogenase complexes in mitochondria can produce superoxide/hydrogen peroxide at much higher rates than complex I*. J Biol Chem, 2014. **289**(12): p. 8312-25.
97. Hall, E.D., J.A. Wang, and D.M. Miller, *Relationship of nitric oxide synthase induction to peroxynitrite-mediated oxidative damage during the first week after experimental traumatic brain injury*. Exp Neurol, 2012. **238**(2): p. 176-82.
98. Ichas, F. and J.P. Mazat, *From calcium signaling to cell death: two conformations for the mitochondrial permeability transition pore. Switching from low- to high-conductance state*. Biochim Biophys Acta, 1998. **1366**(1-2): p. 33-50.
99. Schinder, A.F., et al., *Mitochondrial dysfunction is a primary event in glutamate neurotoxicity*. J Neurosci, 1996. **16**(19): p. 6125-33.
100. Gunter, T.E. and K.K. Gunter, *Uptake of calcium by mitochondria: transport and possible function*. IUBMB Life, 2001. **52**(3-5): p. 197-204.
101. Stys, P.K., S.G. Waxman, and B.R. Ransom, *Ionic mechanisms of anoxic injury in mammalian CNS white matter: role of Na⁺ channels and Na⁽⁺⁾-Ca²⁺ exchanger*. J Neurosci, 1992. **12**(2): p. 430-9.
102. Crompton, M. and A. Costi, *A heart mitochondrial Ca²⁺(+)-dependent pore of possible relevance to re-perfusion-induced injury. Evidence that ADP facilitates pore interconversion between the closed and open states*. Biochem J, 1990. **266**(1): p. 33-9.
103. Nieminen, A.L., et al., *Mitochondrial permeability transition in hepatocytes induced by t-BuOOH: NAD(P)H and reactive oxygen species*. Am J Physiol, 1997. **272**(4 Pt 1): p. C1286-94.
104. Halestrap, A.P., *What is the mitochondrial permeability transition pore?* J Mol Cell Cardiol, 2009. **46**(6): p. 821-31.
105. Mazzeo, A.T., et al., *The role of mitochondrial transition pore, and its modulation, in traumatic brain injury and delayed neurodegeneration after TBI*. Exp Neurol, 2009. **218**(2): p. 363-70.
106. Sullivan, P.G., M.B. Thompson, and S.W. Scheff, *Cyclosporin A attenuates acute mitochondrial dysfunction following traumatic brain injury*. Exp Neurol, 1999. **160**(1): p. 226-34.
107. Scheff, S.W. and P.G. Sullivan, *Cyclosporin A significantly ameliorates cortical damage following experimental traumatic brain injury in rodents*. J Neurotrauma, 1999. **16**(9): p. 783-92.
108. Pandya, J.D., J.R. Pauly, and P.G. Sullivan, *The optimal dosage and window of opportunity to maintain mitochondrial homeostasis following traumatic brain injury using the uncoupler FCCP*. Exp Neurol, 2009. **218**(2): p. 381-9.

109. Singh, I.N., P.G. Sullivan, and E.D. Hall, *Peroxynitrite-mediated oxidative damage to brain mitochondria: Protective effects of peroxynitrite scavengers*. J Neurosci Res, 2007. **85**(10): p. 2216-23.
110. Sullivan, P.G., et al., *Mitochondrial permeability transition in CNS trauma: cause or effect of neuronal cell death?* J Neurosci Res, 2005. **79**(1-2): p. 231-9.
111. Sullivan, P.G., et al., *Traumatic brain injury alters synaptic homeostasis: implications for impaired mitochondrial and transport function*. J Neurotrauma, 1998. **15**(10): p. 789-98.
112. Hall, E.D. and J.E. Springer, *Neuroprotection and acute spinal cord injury: a reappraisal*. NeuroRx, 2004. **1**(1): p. 80-100.
113. Xiong, Y., A.G. Rabchevsky, and E.D. Hall, *Role of peroxynitrite in secondary oxidative damage after spinal cord injury*. J Neurochem, 2007. **100**(3): p. 639-49.
114. Luo, J., J.P. Robinson, and R. Shi, *Acrolein-induced cell death in PC12 cells: role of mitochondria-mediated oxidative stress*. Neurochem Int, 2005. **47**(7): p. 449-57.
115. Shapiro, H.K., *Carbonyl-trapping therapeutic strategies*. Am J Ther, 1998. **5**(5): p. 323-53.
116. Galvani, S., et al., *Carbonyl scavenger and antiatherogenic effects of hydrazine derivatives*. Free Radic Biol Med, 2008. **45**(10): p. 1457-67.
117. Hamann, K., et al., *Critical role of acrolein in secondary injury following ex vivo spinal cord trauma*. J Neurochem, 2008. **107**(3): p. 712-21.
118. Burcham, P.C. and S.M. Pyke, *Hydralazine inhibits rapid acrolein-induced protein oligomerization: role of aldehyde scavenging and adduct trapping in cross-link blocking and cytoprotection*. Mol Pharmacol, 2006. **69**(3): p. 1056-65.
119. Burcham, P.C., A. Raso, and L.M. Kaminskas, *Chaperone heat shock protein 90 mobilization and hydralazine cytoprotection against acrolein-induced carbonyl stress*. Mol Pharmacol, 2012. **82**(5): p. 876-86.
120. Reece, P.A., *Hydralazine and related compounds: chemistry, metabolism, and mode of action*. Med Res Rev, 1981. **1**(1): p. 73-96.
121. Aldini, G., M. Orioli, and M. Carini, *Protein modification by acrolein: relevance to pathological conditions and inhibition by aldehyde sequestering agents*. Mol Nutr Food Res, 2011. **55**(9): p. 1301-19.
122. Wood, P.L., et al., *Aldehyde load in ischemia-reperfusion brain injury: neuroprotection by neutralization of reactive aldehydes with phenelzine*. Brain Res, 2006. **1122**(1): p. 184-90.
123. Pandya, J.D., et al., *Post-Injury Administration of Mitochondrial Uncouplers Increases Tissue Sparing and Improves Behavioral Outcome following Traumatic Brain Injury in Rodents*. J Neurotrauma, 2007. **24**(5): p. 798-811.
124. Mustafa, A.G., et al., *Mitochondrial protection after traumatic brain injury by scavenging lipid peroxyl radicals*. J Neurochem, 2010. **114**(1): p. 271-80.
125. Lai, J.C. and J.B. Clark, *Preparation of synaptic and nonsynaptic mitochondria from mammalian brain*. Methods Enzymol, 1979. **55**: p. 51-60.
126. Sullivan, P.G., et al., *Mitochondrial uncoupling protein-2 protects the immature brain from excitotoxic neuronal death*. Ann Neurol, 2003. **53**(6): p. 711-7.

127. Sauerbeck, A., et al., *Analysis of regional brain mitochondrial bioenergetics and susceptibility to mitochondrial inhibition utilizing a microplate based system.* J Neurosci Methods, 2011. **198**(1): p. 36-43.
128. Dranka, B.P., et al., *Assessing bioenergetic function in response to oxidative stress by metabolic profiling.* Free Radic Biol Med, 2011. **51**(9): p. 1621-35.
129. Rogers, G.W., et al., *High throughput microplate respiratory measurements using minimal quantities of isolated mitochondria.* PLoS One, 2011. **6**(7): p. e21746.
130. Ferrick, D.A., A. Neilson, and C. Beeson, *Advances in measuring cellular bioenergetics using extracellular flux.* Drug Discov Today, 2008. **13**(5-6): p. 268-74.
131. Gerencser, A.A., et al., *Quantitative microplate-based respirometry with correction for oxygen diffusion.* Anal Chem, 2009. **81**(16): p. 6868-78.
132. Brown, M.R., P.G. Sullivan, and J.W. Geddes, *Synaptic mitochondria are more susceptible to Ca²⁺ overload than nonsynaptic mitochondria.* J Biol Chem, 2006. **281**(17): p. 11658-68.
133. Mbye, L.H., et al., *Attenuation of acute mitochondrial dysfunction after traumatic brain injury in mice by NIM811, a non-immunosuppressive cyclosporin A analog.* Exp Neurol, 2008. **209**(1): p. 243-53.
134. Mona Bains, J.E.C., Lesley K. Gilmer, Colleen C. Barnes, Stephanie N. Thompson and and E.D. Hall, *Pharmacological Analysis of the Cortical Neuronal Cytoskeletal Protective Efficacy of the Calpain Inhibitor SNJ-1945 in a Mouse Traumatic Brain Injury Model.* Journal of Neurochemistry, 2012.
135. Miller, D.M., et al., *Nrf2-ARE activator carnosic acid decreases mitochondrial dysfunction, oxidative damage and neuronal cytoskeletal degradation following traumatic brain injury in mice.* Exp Neurol, 2015. **264**: p. 103-10.
136. Billger, M., M. Wallin, and J.O. Karlsson, *Proteolysis of tubulin and microtubule-associated proteins 1 and 2 by calpain I and II. Difference in sensitivity of assembled and disassembled microtubules.* Cell Calcium, 1988. **9**(1): p. 33-44.
137. Bains, M., et al., *Pharmacological Analysis of the Cortical Neuronal Cytoskeletal Protective Efficacy of the Calpain Inhibitor SNJ-1945 in a Mouse Traumatic Brain Injury Model.* J Neurochem, 2012.
138. Michel, R.P. and L.M. Cruz-Orive, *Application of the Cavalieri principle and vertical sections method to lung: estimation of volume and pleural surface area.* J Microsc, 1988. **150**(Pt 2): p. 117-36.
139. Sullivan, P.G., A.H. Sebastian, and E.D. Hall, *Therapeutic window analysis of the neuroprotective effects of cyclosporine A after traumatic brain injury.* J Neurotrauma, 2011. **28**(2): p. 311-8.
140. Sheskin, D.J.H.o.P.a.N.S.P.r.e.B.R., FL: CRC Press. pp. 665–756. ISBN 1-584-88440-1.
141. Burcham, P.C., *Potentialities and pitfalls accompanying chemico-pharmacological strategies against endogenous electrophiles and carbonyl stress.* Chem Res Toxicol, 2008. **21**(4): p. 779-86.
142. Wondrak, G.T., et al., *Identification of α -dicarbonyl scavengers for cellular protection against carbonyl stress.* Biochemical Pharmacology, 2002. **63**(3): p. 361-373.

143. Burcham, P.C., et al., *Protein adduct-trapping by hydrazinophthalazine drugs: mechanisms of cytoprotection against acrolein-mediated toxicity*. Mol Pharmacol, 2004. **65**(3): p. 655-64.
144. Singh, I.N., et al., *Phenelzine mitochondrial functional preservation and neuroprotection after traumatic brain injury related to scavenging of the lipid peroxidation-derived aldehyde 4-hydroxy-2-nonenal*. J Cereb Blood Flow Metab, 2013.
145. Wooters, T.E. and M.T. Bardo, *The monoamine oxidase inhibitor phenelzine enhances the discriminative stimulus effect of nicotine in rats*. Behav Pharmacol, 2007. **18**(7): p. 601-8.
146. .
147. MacKenzie, E.M., et al., *Phenelzine causes an increase in brain ornithine that is prevented by prior monoamine oxidase inhibition*. Neurochem Res, 2008. **33**(3): p. 430-6.
148. Kampfl, A., et al., *mu-calpain activation and calpain-mediated cytoskeletal proteolysis following traumatic brain injury*. J Neurochem, 1996. **67**(4): p. 1575-83.
149. Thompson, S.N., et al., *Relationship of calpain-mediated proteolysis to the expression of axonal and synaptic plasticity markers following traumatic brain injury in mice*. Exp Neurol, 2006. **201**(1): p. 253-65.
150. Saatman, K.E., J. Creed, and R. Raghupathi, *Calpain as a therapeutic target in traumatic brain injury*. Neurotherapeutics, 2010. **7**(1): p. 31-42.
151. Burcham, P.C., et al., *Aldehyde-sequestering drugs: tools for studying protein damage by lipid peroxidation products*. Toxicology, 2002. **181-182**: p. 229-36.
152. Marshall, L.F., et al., *A multicenter trial on the efficacy of using tirilazad mesylate in cases of head injury*. J Neurosurg, 1998. **89**(4): p. 519-25.
153. LoPachin, R.M., et al., *Molecular Mechanisms of 4-Hydroxy-2-nonenal and Acrolein Toxicity: Nucleophilic Targets and Adduct Formation*. Chemical Research in Toxicology, 2009. **22**(9): p. 1499-1508.
154. Kroemer, G., B. Dallaporta, and M. Resche-Rigon, *The mitochondrial death/life regulator in apoptosis and necrosis*. Annu Rev Physiol, 1998. **60**: p. 619-42.
155. Toninello, A., et al., *Biogenic amines and apoptosis: minireview article*. Amino Acids, 2004. **26**(4): p. 339-43.
156. Gilmer, L.K., et al., *Age-related mitochondrial changes after traumatic brain injury*. J Neurotrauma, 2010. **27**(5): p. 939-50.
157. Gilmer, L.K., et al., *Early mitochondrial dysfunction after cortical contusion injury*. J Neurotrauma, 2009. **26**(8): p. 1271-80.
158. Hall, E.D., J.M. Braughler, and J.M. McCall, *Antioxidant effects in brain and spinal cord injury*. J Neurotrauma, 1992. **9 Suppl 1**: p. S165-72.
159. Azbill, R.D., et al., *Impaired mitochondrial function, oxidative stress and altered antioxidant enzyme activities following traumatic spinal cord injury*. Brain Research, 1997. **765**(2): p. 283-290.
160. Sullivan, P.G., et al., *Intrinsic differences in brain and spinal cord mitochondria: Implication for therapeutic interventions*. The Journal of Comparative Neurology, 2004. **474**(4): p. 524-534.

161. Giacomello, M., et al., *Mitochondrial Ca²⁺ as a key regulator of cell life and death*. Cell Death Differ, 2007. **14**(7): p. 1267-74.
162. Hinzman, J.M., et al., *Diffuse brain injury elevates tonic glutamate levels and potassium-evoked glutamate release in discrete brain regions at two days post-injury: an enzyme-based microelectrode array study*. J Neurotrauma, 2010. **27**(5): p. 889-99.
163. Castilho, R.F., et al., *Permeabilization of the inner mitochondrial membrane by Ca²⁺ ions is stimulated by t-butyl hydroperoxide and mediated by reactive oxygen species generated by mitochondria*. Free Radic Biol Med, 1995. **18**(3): p. 479-86.
164. Sullivan, P.G., et al., *Dietary supplement creatine protects against traumatic brain injury*. Ann Neurol, 2000. **48**(5): p. 723-9.
165. Lifshitz, J., et al., *Structural and functional damage sustained by mitochondria after traumatic brain injury in the rat: evidence for differentially sensitive populations in the cortex and hippocampus*. J Cereb Blood Flow Metab, 2003. **23**(2): p. 219-31.
166. Pike, B.R., et al., *Regional calpain and caspase-3 proteolysis of alpha-spectrin after traumatic brain injury*. Neuroreport, 1998. **9**(11): p. 2437-42.
167. Gnaiger, E., *Bioenergetics at low oxygen: dependence of respiration and phosphorylation on oxygen and adenosine diphosphate supply*. Respir Physiol, 2001. **128**(3): p. 277-97.
168. Cohen, G., R. Farooqui, and N. Kesler, *Parkinson disease: a new link between monoamine oxidase and mitochondrial electron flow*. Proc Natl Acad Sci U S A, 1997. **94**(10): p. 4890-4.
169. Fornstedt, B., E. Pileblad, and A. Carlsson, *In vivo autoxidation of dopamine in guinea pig striatum increases with age*. J Neurochem, 1990. **55**(2): p. 655-9.
170. Munoz, P., et al., *Dopamine oxidation and autophagy*. Parkinsons Dis, 2012. **2012**: p. 920953.
171. Zoccarato, F., M. Cappellotto, and A. Alexandre, *Clorgyline and other propargylamine derivatives as inhibitors of succinate-dependent H₂O₂ release at NADH:UBIQUINONE oxidoreductase (Complex I) in brain mitochondria*. J Bioenerg Biomembr, 2008. **40**(4): p. 289-96.
172. Obrietan, K. and A.N. van den Pol, *GABA neurotransmission in the hypothalamus: developmental reversal from Ca²⁺ elevating to depressing*. J Neurosci, 1995. **15**(7 Pt 1): p. 5065-77.
173. van den Pol, A.N., K. Obrietan, and G. Chen, *Excitatory actions of GABA after neuronal trauma*. J Neurosci, 1996. **16**(13): p. 4283-92.
174. Reichling, D.B., et al., *Mechanisms of GABA and glycine depolarization-induced calcium transients in rat dorsal horn neurons*. J Physiol, 1994. **476**(3): p. 411-21.
175. Ben-Ari, Y., et al., *Giant synaptic potentials in immature rat CA3 hippocampal neurones*. J Physiol, 1989. **416**: p. 303-25.
176. Cherubini, E., J.L. Gaiarsa, and Y. Ben-Ari, *GABA: an excitatory transmitter in early postnatal life*. Trends Neurosci, 1991. **14**(12): p. 515-9.
177. Obrietan, K. and A.N. van den Pol, *Growth cone calcium elevation by GABA*. J Comp Neurol, 1996. **372**(2): p. 167-75.

178. Spoerri, P.E., *Neurotrophic effects of GABA in cultures of embryonic chick brain and retina*. Synapse, 1988. **2**(1): p. 11-22.
179. Michler, A., *Involvement of GABA receptors in the regulation of neurite growth in cultured embryonic chick tectum*. Int J Dev Neurosci, 1990. **8**(4): p. 463-72.
180. Barbin, G., et al., *Involvement of GABAA receptors in the outgrowth of cultured hippocampal neurons*. Neurosci Lett, 1993. **152**(1-2): p. 150-4.
181. Staley, K.J., B.L. Soldo, and W.R. Proctor, *Ionic mechanisms of neuronal excitation by inhibitory GABAA receptors*. Science, 1995. **269**(5226): p. 977-81.
182. Tanay, V.A., et al., *Effects of the antidepressant/antipanic drug phenelzine on alanine and alanine transaminase in rat brain*. Cell Mol Neurobiol, 2001. **21**(4): p. 325-39.
183. Parent, M.B., M.K. Habib, and G.B. Baker, *Time-dependent changes in brain monoamine oxidase activity and in brain levels of monoamines and amino acids following acute administration of the antidepressant/antipanic drug phenelzine*. Biochem Pharmacol, 2000. **59**(10): p. 1253-63.
184. McIntosh, T.K., K.E. Saatman, and R. Raghupathi, *REVIEW ■ : Calcium and the Pathogenesis of Traumatic CNS Injury: Cellular and Molecular Mechanisms*. The Neuroscientist, 1997. **3**(3): p. 169-175.
185. Palmer, A.M., et al., *Traumatic brain injury-induced excitotoxicity assessed in a controlled cortical impact model*. J Neurochem, 1993. **61**(6): p. 2015-24.
186. Arundine, M. and M. Tymianski, *Molecular mechanisms of glutamate-dependent neurodegeneration in ischemia and traumatic brain injury*. Cell Mol Life Sci, 2004. **61**(6): p. 657-68.
187. McCracken, E., et al., *Calpain activation and cytoskeletal protein breakdown in the corpus callosum of head-injured patients*. J Neurotrauma, 1999. **16**(9): p. 749-61.
188. Kampfl, A., et al., *Mechanisms of calpain proteolysis following traumatic brain injury: implications for pathology and therapy: implications for pathology and therapy: a review and update*. J Neurotrauma, 1997. **14**(3): p. 121-34.
189. Buki, A., et al., *The role of calpain-mediated spectrin proteolysis in traumatically induced axonal injury*. J Neuropathol Exp Neurol, 1999. **58**(4): p. 365-75.
190. Wang, K.K.W., *Calpain and caspase: can you tell the difference?*, by Kevin K.W. Wang: Vol. 23, pp. 20–26. Trends in Neurosciences, 2000. **23**(2): p. 59.
191. Twiddy, D., et al., *Pro-apoptotic proteins released from the mitochondria regulate the protein composition and caspase-processing activity of the native Apaf-1/caspase-9 apoptosome complex*. J Biol Chem, 2004. **279**(19): p. 19665-82.
192. Mustafa, A.G., et al., *Pharmacological inhibition of lipid peroxidation attenuates calpain-mediated cytoskeletal degradation after traumatic brain injury*. J Neurochem, 2011. **117**(3): p. 579-88.
193. Mbye, L.H., et al., *Comparative neuroprotective effects of cyclosporin A and NIM811, a nonimmunosuppressive cyclosporin A analog, following traumatic brain injury*. J Cereb Blood Flow Metab, 2009. **29**(1): p. 87-97.
194. Newcomb, J.K., et al., *Immunohistochemical study of calpain-mediated breakdown products to alpha-spectrin following controlled cortical impact injury in the rat*. J Neurotrauma, 1997. **14**(6): p. 369-83.

195. McKenzie, R.C., T.S. Rafferty, and G.J. Beckett, *Selenium: an essential element for immune function*. Immunology today, 1998. **19**(8): p. 342-5.
196. Simpson, S.M., et al., *The antidepressant phenelzine enhances memory in the double Y-maze and increases GABA levels in the hippocampus and frontal cortex of rats*. Pharmacol Biochem Behav, 2012. **102**(1): p. 109-17.
197. McManus, D.J., et al., *Effects of the antidepressant/antipanic drug phenelzine on GABA concentrations and GABA-transaminase activity in rat brain*. Biochem Pharmacol, 1992. **43**(11): p. 2486-9.
198. McKenna, K.F., et al., *Chronic administration of the antidepressant phenelzine and its N-acetyl analogue: effects on GABAergic function*. J Neural Transm Suppl, 1994. **41**: p. 115-22.
199. Saatman, K.E., et al., *Behavioral efficacy of posttraumatic calpain inhibition is not accompanied by reduced spectrin proteolysis, cortical lesion, or apoptosis*. J Cereb Blood Flow Metab, 2000. **20**(1): p. 66-73.
200. Thompson, S.N., et al., *A pharmacological analysis of the neuroprotective efficacy of the brain- and cell-permeable calpain inhibitor MDL-28170 in the mouse controlled cortical impact traumatic brain injury model*. J Neurotrauma, 2010. **27**(12): p. 2233-43.
201. Kehrer, J.P. and S.S. Biswal, *The molecular effects of acrolein*. Toxicol Sci, 2000. **57**(1): p. 6-15.
202. Machnicka, B., et al., *Spectrins: a structural platform for stabilization and activation of membrane channels, receptors and transporters*. Biochim Biophys Acta, 2014. **1838**(2): p. 620-34.
203. Clayton, P.T., *B6-responsive disorders: a model of vitamin dependency*. J Inherit Metab Dis, 2006. **29**(2-3): p. 317-26.
204. Kaminskas, L.M., S.M. Pyke, and P.C. Burcham, *Michael addition of acrolein to lysinyl and N-terminal residues of a model peptide: targets for cytoprotective hydrazino drugs*. Rapid Commun Mass Spectrom, 2007. **21**(7): p. 1155-64.

VITA

John Eric Cebak	<ul style="list-style-type: none"> • PhD Candidate Spinal Cord & Brain Injury Research Center • 1LT (P), Brigade Medical Operations Officer HHB 138th Fires BDE
Citizenship: United States of America	

INSTITUTION AND LOCATION	DEGREE	YEAR(s)	FIELD OF STUDY
Academy of Health Sciences Ft. Sam Houston, TX	68W*	2003-2010	Combat Medic (Trauma Specialist)
U.S. Army Medical Department Center & School (AMEDD C & S)– Ft. Sam Houston, TX	License	2003- <i>Present</i>	Nationally Registered Emergency Medical Technician—Basic (EMT-B)
AMEDD C & S – Ft. Sam Houston, TX	Certification	2003-2010	Pre-Hospital Trauma Life Support
AMEDD C & S – Ft. Sam Houston, TX	Certification	2003- <i>Present</i>	Tactical Casualty Combat Care
AMEDD C & S – Ft. Sam Houston, TX	Certification	2003- <i>Present</i>	Basic Life Support
Non-Commissioned Officers Academy Camp Shelby, MI	Certification	2007-2007	Warrior Leadership Course <i>Former PLDC</i>
Kentucky Medical Command – Greenville, KY	Certification	2007-2007	Combat Medic Advanced Skills
Non-Commissioned Officers Academy Ft. Indiantown Gap, PA	Certification	2008-2008	Advanced Leadership Course <i>Former BNOC</i>
University of Kentucky – Lexington, KY	B.S.	2004-2009	Agricultural Biotechnology, <i>1st Degree</i>
University of Kentucky – Lexington, KY	B.S.	2004-2009	Biology, <i>2nd Degree</i>
AMEDD C & S – Ft. Sam Houston, TX	70B**	2010- <i>present</i>	Basic Officer Leadership Course (2012)
<i>University of Kentucky Lexington, KY</i>	<i>Ph.D.</i>	<i>2010- present</i>	<i>Neuroscience; Traumatic Brain Injury Anticipated: August 2015</i>
<i>Lincoln Memorial University, Lexington, KY</i>	<i>M.B.A</i>	<i>Starting 2015</i>	<u>Dual Degree Program:</u> <i>Masters of Business Admin. Anticipated: 2019</i>
<i>Lincoln Memorial University, DeBusk College of Osteopathic Medicine Lexington, KY</i>	<i>D.O.</i>	<i>Starting 2015</i>	<i>Doctor of Osteopathic Medicine Anticipated: 2019</i>

OCCUPATION	BEGIN DATE	END DATE	FIELD	INSTITUTION/COMPANY	SUPERVISOR/EMPLOYER
Track Commander	08/05	06/06	Combat Medicine	Army, Al Anabar Iraq	COL John Gronski
Medical Section Chief	01/08	04/11	Military Medicine	Army National Guard	COL Brian Wetzler
Teaching Assistant <i>ANA 209</i> <i>BIO 540</i>	08/12 01/09	<i>Present</i> 06/09	Anatomy Histology	Anatomy, Univ. KY Biology, Univ. KY	Guoying Bing, MD, PhD Philip Bonner, PhD
Graduate Student	08/10	<i>Present</i>	Neurotrauma	Neurobio., Univ. KY (SCoBIRC)	Edward Hall, PhD
Medical Operations Officer	09/11	<i>Present</i>	Military Medicine	KY, Army National Guard	COL Brian Wetzler
Scientific and Medical Advisory Board, Founding Member	03/15	<i>Present</i>	Military Medicine	Association of the United States Army	Llyod McMillian James Geddes, PhD
Board of Directors	01/11	<i>Present</i>	Community Association	Columbia Heights Neighborhood Association, KY	Janet Cowen, MS
Department Representative	01/12	06/12	Graduate Student Congress	University of KY	GCS Board
Military Consumer Reviewer	10/13 04/14 03/15	10/13 04/14 03/15	TBI/PTSD	Congressionally Directed Medical Research Program (CDMRP)	COL Wanda L. Salzer, M.D., Director

EDUCATION/TRAINING

Army Medical Department designation of Military Occupational Specialty (MOS)* and Area of Concentration (AOC).*

POSITIONS/ HONORS

Selected Academic and Professional Honors:

2005-2006 Combat Medical Badge (*Merit-based recognition*) – Al Anabar, Iraq*
2005-2006 Iraq Campaign Medal – Al Anabar, Iraq*
2005-2011 Army Commendation Medal x3
2007-2009 Horatio Alger Military Scholar: Association of Distinguished Americans (*Merit-based: \$5,000*) – University of Kentucky
2007 Warrior Leadership Course – Commandant’s List
2007 Dean’s List– University of Kentucky
2008-2011 “Among the Best” Non-Commissioned Officer Eval. Reports x3
2008 Basic Non-Commissioned Officers Course – Commandant’s List
2010-2013 Research Assistantship (\$23,500/year stipend) –U. of Kentucky
2013-*present* NIH Pre-doctoral Fellowship: Neurobiology Injury & Repair Training Grant (IT32 NS077889)

Membership in Professional Organizations:

2009-present Kentucky Academy of Science
2012-present National Guard Association, *National Member*
2012-present National Guard Association of Kentucky, *Lifetime Member*
2013-present National Neurotrauma Society

Communication:

Oral Presentation:

Massy Foundation TBI Summit, Center for Integrative Research in Critical Care— Ann Arbor, MI **Cebak JE**, Carbonyl scavenging following Traumatic Brain Injury. (UK, College of Medicine, Spinal Cord and Brain Injury Research Center, 2015)

LMU-DeBusk College of Osteopathic Medicine —Harrogate, TN. **Cebak JE**. Resiliency, Veterans Day Invited speaker. (November 11, 2014)

St. Jude's Children's Research Hospital—Memphis, TN. **Cebak JE**, Rucker E. Fluorescent-tagged UVRAG Autophagic Protein & Conditional Gene Knock Out (Dept. of Biology, UK 2010)

Abstract & Poster Presentation:

Symposium of Undergraduate Research Scholars—Lexington, KY. **Cebak JE**, Bonner P. Axon Regeneration Using Transplanted Notochord (Dept. of Biology, UK 2008)

29th Annual National Neurotrauma Symposium—Hollywood Beach, FL. Singh IN, **Cebak JE**, Hall ED. Protective Effects of Phenelzine as a Scavenger of Lipid Peroxidation-Derived 4-Hydroxynonenal, on Cerebral Mitochondria: an *in vitro* Study. SCoBIRC; Department of Anatomy & Neurobiology, 2011

Cebak, J.E., Singh, I.N., Miller, D.M., Wang, J.A. and Hall, E.D. Protective effects of Phenelzine against aldehyde-induced ex vivo oxidative damage to cortical mitochondria. SCoBIRC; Department of Anatomy & Neurobiology, 2014

Cebak, J.E., Singh, I.N., Miller, D.M., Wang, J.A. and Hall, E.D. An FDA-approved drug for the treatment of TBI. SCoBIRC; Department of Anatomy & Neurobiology, 2015

Published Manuscripts:

Bains M, **Cebak JE**, Gilmer LK, Barnes CC, Thompson SN, Geddes JW, Hall ED. Pharmacological analysis of the cortical neuronal cytoskeletal protective efficacy of the calpain inhibitor SNJ-1945 in a mouse traumatic brain injury model. J Neurochem. 2012 Dec 8. doi: 10.1111/jnc.12118. PMID: 23216523

Singh IN, Gilmer LK, Miller DM, **Cebak JE**, Wang JA, Hall ED. Phenelzine mitochondrial functional preservation and neuroprotection after traumatic brain injury related to scavenging of the lipid peroxidation-derived aldehyde 4-hydroxy-2-nonenal. J Cereb Blood Flow Metab. 2013 Jan 16. doi:10.1038/jcbfm.2012.211. PMID: 23321786

Bains M, **Cebak JE**, Mustafa A, Wang JA, Pleasant-Brelsfoard JM, Hall ED. Relationship of Neuroprotective Effects of Lipid Peroxyl Scavenger U-83836E to Early Motor Functional Recovery and Tissue Damage After Traumatic Brain Injury. *Manuscript in progress*

Cebak JE, Wang JA, Singh IN, Hall ED. Phenelzine protects brain mitochondrial respiratory function from oxidative damage by scavenging the lipid peroxidation-derived reactive carbonyls 4-hydroxynonenal and acrolein. *Manuscript under review in Journal of Free Radical Biology and Medicine*